



CZECH TECHNICAL UNIVERSITY IN PRAGUE  
FACULTY OF CIVIL ENGINEERING

Bridge Traffic Loads: Design and Assessment of  
Short-to-Medium Span Bridges

Dr.-Ing. Roman Lenner, PE

Habilitation

September 2023



---

**Abstract**

Infrastructure is one of the largest assets for a functioning economy, not only the initial investment, but also the overall life-cycle cost including maintenance and decommissioning. A limited part of the road infrastructure, yet perhaps critical, is the bridges. They present a high cost of investment and also potentially high cost of failure and are vital for a functioning network. This work summarizes the work so far performed by the author in the field of bridge traffic loading and that is development of load models based on data driven approach, application of the loading for the assessment of the existing structures and pointing out differences between general traffic and special, abnormal, traffic from the reliability perspective. The work is based on published book chapter and several scientific papers accepted in high ranking journals. It is shown however, that although lots of research has been performed in this field by the author and significantly more by others, it is still a field with open questions and demand for more work.

---

Chronological list of publications by the author used in this habilitation:

1. [Short-to-medium span bridges](#)  
C Caprani, R Lenner - Bridge Traffic Loading, 2021
2. [Dynamics of long multi-trailer heavy vehicles crossing short to medium span length bridges](#)  
MW Meyer, D Cantero, R Lenner - Engineering Structures, 2021
3. [Partial factors and reliability verification for the site load factor approach for the assessment of existing bridges](#)  
SP Sifre, R Lenner - Structures, 2021
4. [Reliability performance of bridges designed according to TMH7 NA load model](#)  
R Lenner, SE Basson, M Sýkora, PF Van der Spuy - J South African Inst Civ Eng, 2021
5. [Multiple lane reduction factors based on multiple lane weigh in motion data](#)  
P van der Spuy, R Lenner, T de Wet, C Caprani - Structures, 2019
6. [Towards a new bridge live load model for South Africa](#)  
P van der Spuy, R Lenner - Structural Engineering International, 2019
7. [Bridge assessment reduction factors based on Monte Carlo routine with copulas](#)  
SP Sifre, R Lenner - Engineering Structures, 2019
8. [Bridge loading and traffic characteristics in South Africa](#)  
R Lenner, DPG De Wet, C Viljoen - J South African Inst Civ Eng, 2017
9. [Partial factors for loads due to special vehicles on road bridges](#)  
R Lenner, M Sýkora - Engineering Structures, 2016

---

# Table of Contents

- 1 Introduction ..... 1**
  - 1.1 Motivation ..... 1
  - 1.2 Bridge Loading..... 1
  - 1.3 Goals..... 2
  - 1.4 Limitations ..... 2
  
- 2 Basic theory of data-oriented modelling..... 3**
  - 2.1.1 The Physical and Statistical Phenomenon..... 3
  - 2.1.2 Load Modelling Approaches ..... 4
  - 2.1.3 WIM-Based Load Modelling ..... 5
  - 2.2 Traffic Data ..... 7
    - 2.2.1 WIM Data and Recordings..... 7
    - 2.2.2 WIM filtration and cleaning ..... 8
    - 2.2.3 Measurement length ..... 9
    - 2.2.4 Overloaded vehicles ..... 10
  - 2.3 Loading Events..... 11
    - 2.3.1 Direct Use of Measured WIM Data..... 11
    - 2.3.2 Generation of Artificial Traffic Streams ..... 13
    - 2.3.3 Traffic Loading in Multiple Lanes ..... 18
    - 2.3.4 Multiple lane reduction factors..... 19
  - 2.4 Load Effects ..... 20
    - 2.4.1 Influence lines ..... 21
    - 2.4.2 Influence Surfaces ..... 23
    - 2.4.3 Load Movement ..... 24
  - 2.5 Dynamic Interaction ..... 26
  - 2.6 Statistical Prediction..... 27
    - 2.6.1 Prediction of extremes ..... 27
    - 2.6.2 Composite Distribution Statistics ..... 31
    - 2.6.3 Governing Form of Traffic ..... 32

---

2.7	Conclusions .....	34
<b>3</b>	<b>Considerations for developing a load model .....</b>	<b>37</b>
3.1	General Method for a single lane NML .....	37
3.1.1	Example application of NML .....	39
3.2	Multiple lane factors.....	43
3.2.1	Multiple lane factor independent of the structural solution.....	44
3.2.2	Example Application with WIM data from South Africa .....	47
<b>4</b>	<b>Special consideration for design and assessment.....</b>	<b>53</b>
4.1	Investigating partial factors for the assessment of existing reinforced concrete bridges .....	54
4.2	Adjustment of characteristic load value .....	57
4.2.1	Example application with WIM data from South Africa .....	57
4.2.2	Uncertainty and partial factors .....	61
4.2.3	Uncertainty in the determination of the characteristic load effects .....	65
4.2.4	Estimation of the traffic descriptors uncertainty .....	67
4.2.5	Reliability based partial factor.....	72
4.2.6	Model uncertainty partial factor .....	73
4.2.7	Final partial factors.....	73
4.2.8	Reliability verifications .....	73
4.3	Application of the site load factor approach with .....	77
4.4	Conclusions .....	79
<b>5</b>	<b>Example reliability assessment.....</b>	<b>81</b>
5.1	Reliability performance of bridges with WIM data from South Africa .....	81
5.1.1	Roosboom case study (RCS).....	82
5.1.2	Kilner Park case study (KPCS) .....	89
5.2	Discussion .....	97
5.3	Conclusions and recommendations .....	98
<b>6</b>	<b>Special loads on bridges .....</b>	<b>99</b>
6.1	Loads due to special vehicles .....	100
6.1.1	Load Combinations .....	101
6.1.2	Load effect of the special vehicle.....	102

---

6.2	Stochastic models for the load effects .....	103
6.3	Sensitivity factors and load ratio .....	107
6.4	Multiple crossings .....	109
6.5	Target reliability for crossing by special vehicles .....	111
6.6	Partial factors.....	111
<b>7</b>	<b>Summary and Conclusions .....</b>	<b>113</b>





## **1 Introduction**

### **1.1 Motivation**

Improved and maintained access to economic opportunities drives the facilitation of trade and movement of goods and people in any society. Hence a transport infrastructure is one of the largest assets for a functioning economy. This is crucial from the perspective of not only the initial investments, but also for the overall life-cycle cost including maintenance and decommissioning of the individual infrastructural components. Maintaining a functional network, managing the cost and securing serviceability is important for any developed and developing society.

Transport infrastructure can be fundamentally split in a set of facilities and systems that serve a region. If focused specifically on the road transport, then besides the extensive roadwork, bridges can be seen as the key components in securing a functional network. They also draw a high cost during the construction and through the life cycle, hence attracting a critical status. It is therefore pertinent to devote attention to the design of bridges, to the methods of construction and to the costs related to the life cycle. A bridge, in order to function, must reliably support the loads it is carrying over its entire service life.

### **1.2 Bridge Loading**

Bridge loads can be divided into permanent and variable actions. The permanent actions include self-weight of the structure itself and all components such as road surface, traffic barriers and utilities for road bridges, or rails, electrification, etc for rail bridges. Depending on the method of construction, the prestressing and secondary effects such as creep and shrinkage can be seen as further actions related to the permanent state. These are typically easily predicted and do not exhibit seasonal or daily variations.

Some of the variable actions stem from the environment and exposure conditions, where wind and temperature play the main role. This is particularly important for continuous structures as the restrained movement under the loading leads to a stress. However, for a typical bridge, the main variable action for consideration is the traffic load. Depending on the utilisation, the action might be contributed to the road, rail or mixed use. This load drives the final design of the structure – the bridge serves to carry the traffic, hence it must be designed and constructed in an appropriate way. Given the importance of the traffic action, this work aims to describe the contribution of the author to the field of traffic loading. The main topics discussed is the philosophy behind deriving a traffic load model and it continues with investigation of the individual components and extension the use of traffic load models beyond the design to the assessment of bridges. Many of the bridges service nowadays were constructed decades ago, thus it may be necessary to assess them in order to evaluate their performance. The traffic loading may be again a key component in assessing the reliability of the structure, especially with the consideration of densified and heavier traffic on the current road network.

### **1.3 Goals**

The overall goal of this work is to highlight the authors contribution to the field of traffic load modelling and assessment of structures. The aim is to discuss the modelling approaches, the philosophy behind load model specification, the individual components and model definition. More importantly, to showcase how these concepts were extended to the assessment of bridges, where a large gap remains if considering a code approach to the existing bridges. The goals are achieved in the following order:

- Chapter 2: Basic theory of data-oriented modelling
- Chapter 3: Consideration for developing a load model
- Chapter 4: Special considerations for design and assessment
- Chapter 5: Example reliability assessment
- Chapter 6: Consideration of special vehicles
- Chapter 7: Final conclusions

### **1.4 Limitations**

This work is related to short-to-medium span length bridges where the traffic load model is governed by individual or group of vehicles. Long span structures are out of the scope as the here presented fundamental derivation of load model and the derived parallels to the assessment would be invalid.

---

## 2 Basic theory of data-oriented modelling

The purpose of this chapter is to illustrate the own contribution to the basic understanding and formulating of theory for the development of a traffic load model considering data driven approach as presented by (Lenner & Caprani, 2021). The basic aim of the presented work is to summarize and to provide in an accessible format the developments in the field of road traffic load modelling and to share the basic theory. The audience of professional engineers and emerging researchers is provided with a compact summary of state-of-art practice in the field. To follow up in the succeeding chapters, authors own contribution to the specific parts of the traffic load modelling are highlighted.

### 2.1.1 The Physical and Statistical Phenomenon

Actual highway traffic loading on short to medium span bridges is characterized by the presence of uncertain single or multiple heavy vehicles on the bridge deck. The vertical static loading can be described in terms of the individual axle loads of each vehicle contributing to the total load effect, while interaction of the vibrating vehicle and bridge deck leads to the dynamic amplification of the static effect. This dynamic increase of the static load leads to higher load effects under free-flowing traffic. Congested, or stationary traffic, is slow moving, and so has little dynamic amplification. Consequently, it is a more critical loading situation for longer span lengths when multiple vehicles can be present. Within one lane in consideration, inter-vehicle gaps are crucial in determining whether single or multiple vehicles govern the extreme structural load effects (e.g., bending moment, shear force, etc.). For multiple lane bridges, the density and composition of traffic controls the probability of side-by-side truck occurrences. This in turn dictates the number of vehicles comprising a loading event, and hence the extreme load effects.

Identification of the extreme traffic loading events is made more complicated when the structural form of the bridge must be considered. Each bridge deck component has its own influence surface, and these may be highly peaked or quite flat, either longitudinally and/or transversely. The transverse bridge deck stiffness for the component of interest therefore controls the significance of vehicle loading across adjacent lanes. Similarly, the longitudinal shape of the influence lines for shear, bending or other load effects of interest is governed by the span count and connectivity type, whether a single simple span, two continuous spans, or multiple simple spans, for example.

Coupled with the vehicular arrangements and the structural system, engineering interest lies in some notion of an extreme loading situation, which reflects the underlying randomness of the phenomenon. Of interest though, is not a topological arrangement of some prescribed and certain real vehicles, but rather the value of the traffic action (or load effect) that has the prescribed probability of non-exceedance. Usually this is expressed in terms of some specified probability of non-exceedance or translated into a return period. It is important to recognize that the extreme loading events that can be

observed daily, or even monthly, may not be a good guide to identifying those rare forms of loading events that can govern the extreme load effects at the return period of interest.

The interplay between traffic characteristics, traffic lanes, truck fleet, bridge length and structural form, level of dynamic amplification, and statistical extrapolation, render the identification of the governing traffic loading for short-to-medium span bridges a challenging problem. There have been several paradigms of approaching this problem over the last century or so, but globally a data-driven approach has gained most traction in the last few decades. This chapter focuses on this approach, after some consideration of its historical development and some alternative approaches.

### **2.1.2 Load Modelling Approaches**

Historically, until the 1960s or so, load models were developed empirically to reflect the total weight of a typical vehicle using the bridge, mostly corresponding to a local standard load including some safety margin. In the simplest terms, it was the load effects due to a weight of a typical carriage multiplied by a factor deemed to give the required safety. As transport distances increased due to improved vehicle technology, the empirical method was expanded to national or regional levels by imposing limits on individual vehicle weights and/or axle loads in order to have a functional stock of bridges. As traffic volumes began to increase, and the vehicle stock diversified, there was an evident shift in the associated loading on a national level (Dawe, 2009). As a result, and simplistically stated, there was a demand for bridge design standards to introduce typical design loads for bridges.

Instead of standard formulas based on empirical estimates of weights and accompanying engineering judgment, methods based on actual traffic measurements started to emerge in the 1970s in Canada. This work was intended to reflect the frequency and variety of heavy trucks present in the traffic flow (Moses & Ghosn, 1985; Harman & Davenport, 1976; Hwang & Nowak, 1991). The inherent conservatism tied to the “traditional methods” specified by codes (e.g., AASHTO 1977 which applied in Canada at the time) was deemed as obscure, and a rationale for a limit state based design code with live loads based on traffic data was reasoned as necessary (Csagoly & Dorton, 1978). The Ontario Truck Survey of 1975 identified and weighed 9250 heavy trucks and formed the basis for the Ontario Highway Bridge Design Code load model (Nowak, 1994; Agarwal & Wolkowicz, 1976). In Europe, it wasn't until the 1980s that a concerted effort was made to measure truck traffic with the intention of deriving a bridge traffic load model (Calgaro & Sedlacek, 1992). The Eurocode traffic load model was initially based on a set of pavement Weigh-in-Motion (WIM) data from Auxerre, France, in 1986. After consideration of similar data from other countries, this site further proved to provide a high percentage of heavy vehicle in comparison to the others, although shortage of individual axle load distributions was noted (Hanswille & Sedlacek, 2007). The final load model was derived based on the statistical prediction of extremes corresponding to a return period of 975 years and 5% probability of exceedance in 50 years. This WIM-based load modelling paradigm of solving the traffic loading problem is now widespread and is considered in detail throughout this work.

---

An entirely different approach to traffic load model design was developed in Australia, where future load proofing of newly design bridges was the focus of the work. For the mentioned work, the maximum truck payload volume was determined from consideration of road geometry for turning circles, clearance heights, and lane widths. The resulting available volume is then the maximum possible available for the transport of goods. Consideration then turned to the relative frequency and density distributions of bulk and volumetric freight transports. This, coupled with economic analysis, led to a target freight density of 0.73 tons/m<sup>3</sup> from which the current SM1600 load is derived. This load model provides for the design of new bridges to withstand future possible increase of gross vehicle weights. This philosophy embraces the fact that it is more cost effective to provide for higher loads at the design stage instead of strengthening existing bridges in future to withstand increasing legal load intensities (Heywood et al., 2000).

Overall, the initial efforts of deriving load models based on actual traffic data all suffered from unavoidable limited information at the time. Inherent lack of data initiating from now deemed rudimentary surveys and short measurement periods was then compensated for by necessary assumptions. This was to overcome the issues resulting from the lack of a full description of loading, for example, regarding the gaps between vehicles, multiple presence of vehicles in individual and adjacent lanes, variability of gross vehicle weights from site to site, or the influence of truck survey length on the resulting load effects. Most of the early assumptions about traffic characteristics have now been either refined by newly available data or redefined as a result. This chapter provides a basic guidance on the development of traffic load models for short to medium span bridges using measured traffic weight data.

### **2.1.3 WIM-Based Load Modelling**

Generically, in the development of a load model for structural design, it is either necessary to employ pragmatism and engineering judgment, or a more scientific approach of utilising relevant available data. Given a history of recorded actions and the corresponding load effects, the prediction of a design load intensity for structures under similar loading is readily achieved through probability theory and statistical modelling. More recent decades have extended this concept to consider the distribution of resistances as well, so that the overall level of structural safety can be determined and managed.

The modelling of structural behaviour has improved since the advent of the finite element method, so that the calculated load effects under a given load are taken to be very close to those of the real structure. For traffic loading on bridges, this means that the main uncertainty comes from the traffic itself, and so its measurement is the main input to the scientific approach developing a load model. The static response of the structure under load can be represented through influence lines and surfaces for the load effect of interest. When coupled with the measured traffic, this forms the basis of modern WIM-based traffic load modelling. The detailed process is summarized in Figure 1, including the statistical modelling to determine the extreme load effect and the subsequent design of a notional load model where required.

The input data is cleaned and calibrated in Step 1 to produce a suitable database of measured vehicles, containing axle weights, numbers of axles, and inter-axle spacings. A train of this data, including inter-vehicle spacings, is established in Step 2. There are some studies where a ‘train’ of vehicles can be simulated but if a sufficient quantity of WIM data is available, this is not necessary (Fu & You, 2010); there are also intermediate bootstrapping approaches that can be adopted (Melhem et al., 2020). The bridge response to the train of vehicles (either recorder or simulated) is calculated in Step 3 to give a history of load effects (LEs) on the bridge. Generally, this LE data is fitted to a suitable statistical distribution is fitted to this LE data in Step 4 and the characteristic maximum value is found in Step 5. However, if a sufficient quantity of artificial LE data can be generated, then fitting to a distribution may not be necessary and the value corresponding to the desired probability of non-exceedance may be obtained directly (Enright & O’Brien, 2013) – Step 4B. Lastly, for where it is required, a notional load model is developed in Step 6 to represent the characteristic loading due to traffic but through a simplified representation of the loading (e.g. uniformly distributed load and axle-bogey or design truck). All steps are discussed in detail further.

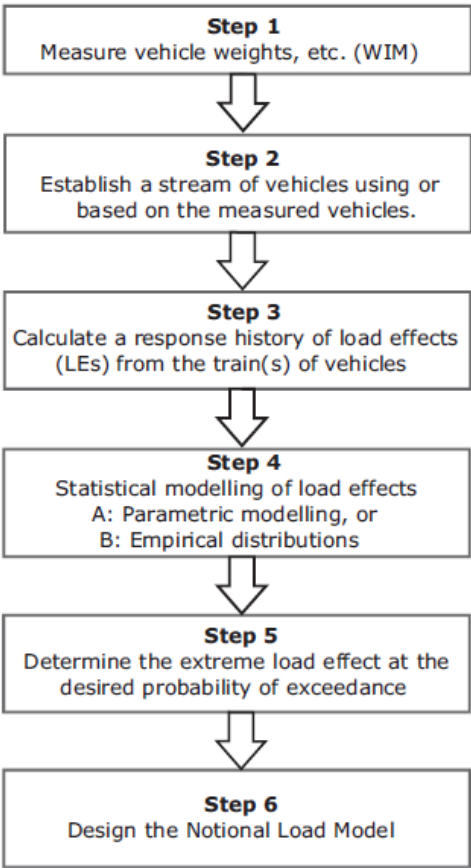


Figure 1: Flowchart of the main steps in WIM-based development of a notional load model (Lenner & Caprani, 2021)

---

## 2.2 Traffic Data

### 2.2.1 WIM Data and Recordings

WIM systems are widely used to measure dynamic axle loads at free-flow speeds on the road surface. The axle loading data are most commonly used in pavement management systems for planning purposes and for timeous scheduling of pavement maintenance actions. They are also used as screeners in conjunction with load control centres for preselection of potentially overloaded vehicles for accurate weighing, and prosecution if necessary. Lastly, they are used for intensive monitoring of overloading. A commonly used WIM technology is bending plates or piezoelectric sensors that are embedded in the road surface, mostly in the path of either left or right wheel only to save the cost of installation and maintenance. To note, the above is typically not at a bridge site but rather a level, straight segment of a selected road providing information about the traffic there. An alternative method of collecting required data is a Bridge WIM (BWIM) system, where axle detectors at the approach of the bridge are coupled with, for example, strain gauges attached at different positions of the superstructure. Axle loads are then determined numerically from the known geometry of the truck and the measured response of a bridge to that load.

The WIM system measurements are typically continuous for each of the discussed system and therefore provide a continuous record of all traffic passing by the station or bridge. The main purpose is to record or calculate by the system a wheel (axle) load and a time it occurred. It is further possible to obtain the axle spacing, or in another words a truck geometry. With further refinement, it can be distinguished between recorded individual vehicles and their respective geometry. A typical WIM station data line record therefore shows:

- date of record
- time of vehicle arrival
- vehicle speed
- vehicular configuration (type)
- gross vehicle mass
- individual axle loads
- axle spacings

The WIM accuracy requirements are based measuring 95% of Gross Vehicle Mass (GVM) within a certain error margin. Typical requirement would be that 95% of vehicles GVW is measured accurately to within 10% to 15%. COST 323 (1998) indicates various percentages for different classes ranging from A(5) of 5% to Class B(10), C(15), D(25) and E which are within 10%, 15%, 25% or more respectively. The exact requirement is still being debated as an extensive history of WIM performance typically achieves the required accuracy. It is noted by (O'Connor & O'Brien, 2005) that specific error margin and sensitivity of bridge loading to WIM accuracy is not critical for development of load models

up to 50m, and any WIM data of Class C or better is therefore sufficient for this purpose. Nevertheless, the collected data should be properly cleaned and calibrated.

Table 1: Tolerances according to COST 323 (1998)

Type of measurement	Domain of use	Accuracy Classes: Confidence interval width $\delta$ (%)					
		A(5)	B+(7)	B(10)	C(15)	D(25)	E
1. Gross weight	Gross weight > 3.5 t	5	7	10	15	25	>25
Axle load:	Axle load > 1 t						
2. Group of axles		7	10	13	18	28	>28
3. Single axle		8	11	15	20	30	>30
4. Axle of a group		10	15	20	25	35	>35

Agencies and WIM vendors across the world are still experimenting with variations (and often simplifications) of the two most respected WIM guidelines for calibration, such the American ASTM E1318 Standard and the COST 323 European Specification (Table 1). Enhancements contributed by researchers are often highly complex and consequently under-utilized in practice (Lenner et al., 2017). The calibration procedures are typically developed based on measurements of known static weight of a specified truck (either a 2-axle and or a 5-axle for E1318 and a 3-axle for COST 323).

A post-calibration method for longer vehicles based on for 6- and 7-axle vehicles called The Truck Tractor method (TT method) was developed by (de Wet, 2010) in South Africa. It allows for the suppression of a systematic error associated of each station after the data collection. While single calibration factor is generally applied to all axle load measurements, some methods have been developed internationally where the systematic error is removed based on different factors, such as speed (Papagiannakis et al., 1996); for further techniques refer to (Enright & O'Brien, 2011).

It is important to note that, while the WIM technology is used to estimate static loads, the WIM-measured data contain a dynamic component. This is not to be confused with dynamic amplification of static loads due to vehicles on bridges and the interaction with the bridge deck. The estimation of static weight is optimized by using good-quality WIM technology installed in pavements with suitable stiffness and riding quality, and utmost care is taken to install bending plates as flush with the road surface as possible. Alternatively, for bridge WIM systems, careful calibration of the influence lines is required, and suitable bridges must be used. Notwithstanding these efforts, loading distributions from WIM data will always be more dispersed than the true static distributions, owing to dynamic effects.

### 2.2.2 WIM filtration and cleaning

Once the required, calibrated, WIM data are obtained, it is necessary to apply a basic filtration in order to remove potentially incorrect values that could disrupt the results. The exact cleaning rules depend on national specification or the type of vehicles on the roads, there will be differences globally as for example European standard 5-axle truck is different to the trucks in USA or Australia. In the absence of



---

national specifications for minimum rejection criteria, the following is suggested to be applied to remove invalid records:

- Truck travelling at less than 5 km/h or more than 150 km/h. While to note, Enright & O'Brien (2011) suggest an interval of 60 to 120 km/h.
- Truck length less than 4 m or greater than 26 m.
- Truck with fewer than 2 axles.
- Truck with GVW less than 3.5 t.
- Truck with any individual axle heavier than 16 t.
- Truck with any axle spacing shorter than 0.4 m or larger than 10 m.
- Recorded number of axle spacings must equal to recorded number of axles plus one.
- Day and time attached to all truck records must be chronologically sorted.

The cleaning must conform to the national regulations in terms of allowable axle loads, typical lengths of trucks or number of axles per vehicle. Any other criteria can be further established, depending on the format and ability of the specific WIM station in use, whether is using high speed or low speed measurements.

The accuracy, or resolution in form of a time stamp of a WIM station is an important aspect for the development of load models. It is essentially the information about the arrival of vehicles at the station and the resolution can range anywhere, depending on the equipment used, from 0.001 s to 1 s. It is recommended to use station with at least a 0.01 s, as anything above will prove difficult for modelling of inter-vehicle gaps (Enright & O'Brien, 2011). Furthermore, when multiple lanes are measured at the site, high resolution is required in order to obtain the correct spatial distribution of all trucks occupying all lanes. The accurate relative position of the vehicles is an important aspect not only from the gap perspective, but also for to simultaneous loading due to adjacent vehicles on the bridge deck. This is an essential issue when considering the loading model beyond the slow lane. At the same time, short to medium span bridges are not as sensitive to multiple vehicles in a single lane, as single vehicle events tend to govern the response there. The accurate time stamp enables to build convoys or scenarios of multiple truck groups which is a recommended practice.

### **2.2.3 Measurement length**

The available length of measurement is an additional key aspect in determining which method can be used to establish the desired load effects. As the development of the load model is based on the statistical procedures, either direct extrapolation or numerical simulations, it is required to obtain a sufficient length of data. The longer the measurement period is, a more representative description is obtained, and variations of the traffic flow and its characteristics can be observed. These variations can be contributed to local laws regarding truck traffic over weekends, or to periods associated with school holidays. Also, a seasonal variation in the truck traffic can significantly influence the development of a load model.

With that in mind, it is suggested to obtain at least a month of WIM data. This is however not ideal for direct statistical extrapolation since a month of data results in small blocks (in this case a daily maximum is chosen as the block size) and the assumption of independent and identically distributed (*iid*) loading events may be violated. As the blocks become larger – a week, or a month, the *iid* assumptions become valid (Basson & Lenner, 2019). It is thus the best to use longer periods of measurements to remove the effect of variation and to obtain large blocks of data falling under the *iid* assumption. A month of available data is also not ideal in the case of numerical simulation methods (such as Monte Carlo), as the underlying distributions required for the sampling may not exhibit the correct tail behavior and it is difficult to assign the most fitting statistical distribution. It can be therefore deducted that long periods of measurements are desirable, and anything more than couple years may result in a load model better representing the traffic loads. In the absence of long periods of measurements, advanced modelling techniques can be applied.

To overcome the issue of traffic variation, it is necessary, beyond seasonal flows, to investigate different locations in the region as well. Traffic in this sense is not completely random and different stations will measure different loadings that can be contributed to the location – either an important national road, or proximity of industrial sites, or a location near a commercial port, etc. Some stations attract a bias in measurement and will exhibit for instance high average daily truck traffic (ADTT), while others will experience higher gross vehicle weight (GVW) in comparison. A crucial question is the geographical domain over which the load model should be representative – this requires the representative WIM data.

It is a custom, albeit in some instances questionable, to select the station exhibiting the highest intensity of heavy vehicles in terms of both the flow and the loading (Sedlacek et al., 2008) as this should result in a conservative load model for the region in question. Aggregating multiple WIM stations would be in this case beneficial, and especially in the cases of shorter available WIM measurements, as this results in more complete description of the traffic, possibly more blocks, or a better description of the tail. Alternatively, multiple WIM stations should be investigated separately at the same time and resulting load effects compared. This enables to calibrate the load model based on a distribution of load effects and not incomplete information and assumptions such as number of heavy vehicles at a site, high percentage of heavy vehicles, etc.

#### **2.2.4 Overloaded vehicles**

The development of a load model and assessment of extreme events is related to normal traffic observed on the roads, while permit trucks should be treated separately. However, it is very difficult to distinguish between illegal overloaded trucks forming a fleet of normal vehicles and special, permit, vehicles by looking at the GVW only. Here, a typical example facing the analyst is illustrated using data recorded at Roosboom station in South Africa. Figure 2 shows the overall site histogram of GVW, along with that of each vehicle type, as identified through the number of axles. At this site, 56 t is the legal limit and there are clearly 7-axle vehicles operating at weights beyond the legal load. The bi-modal shape of

the GVW distribution is typical and corresponds to the loaded and the unloaded vehicles. The second peak at approximately of 53 t is characteristic of freight operators staying below the legal limit while maximizing transportation efficiency.

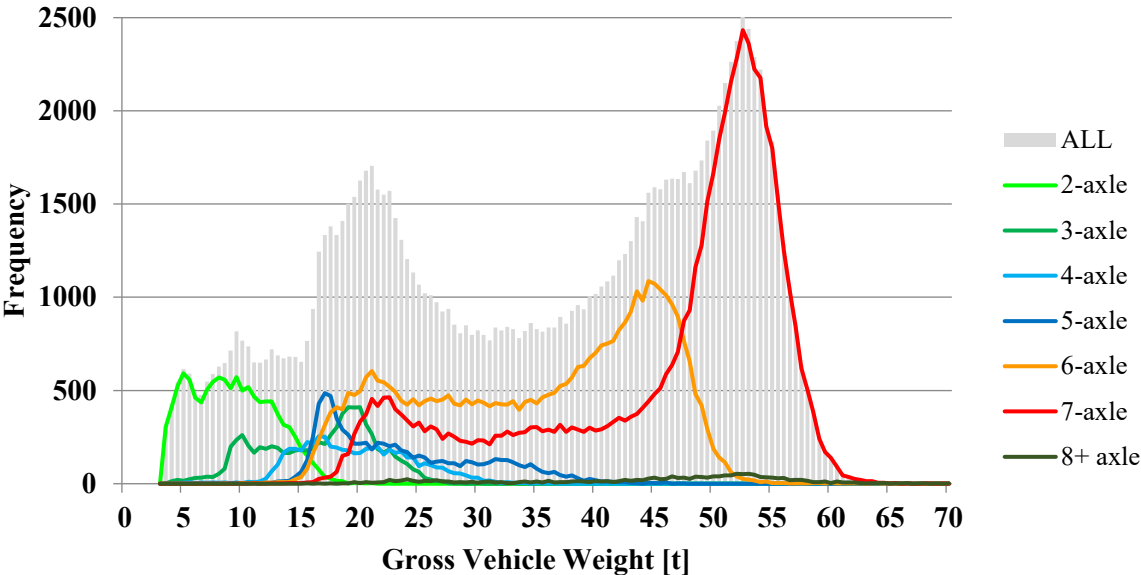


Figure 2: GVW frequency distribution per vehicle type at Roosboom (Lenner et al., 2017)

It is virtually impossible to distinguish between illegally overloaded vehicles and permit vehicles from only WIM data such as that shown in Figure 2. Hence the permit vehicles cannot be filtered out, unless there are known parameters such as a quad axle on a nine-axle vehicle. Identifications at the WIM site can be improved through video surveillance, or ideally automatic number-plate recognition. For the development of ‘normal’ traffic load models it is desirable to filter the permit vehicles, as these are typically captured under an ‘abnormal’ traffic load model. Nevertheless, the illegally overloaded vehicles do form part of the population of normal traffic and must be accounted for in its statistical description.

**2.3 Loading Events**

The data collected at WIM stations does not directly provide information about the loading a bridge might experience. Rather, it can be rather utilized in static calculations of load effects. Typically, this is done by passing individual axle loads forming a vehicle over corresponding influence lines for computational efficiency. These axle loads may be those directly measured, or they can be simulated based on the measurements using Monte Carlo or bootstrapping methods. Either way, the aim is to obtain bending moments and shear forces representative of those experienced by a bridge as if it was at that site.

**2.3.1 Direct Use of Measured WIM Data**

Should there be a sufficiently long record of WIM data available, it could be used directly to obtain the desired bridge load effects. The main benefit of this approach is that any statistical relationships between

the variables comprising the truck fleet and traffic are implicitly captured in the resulting load effects. For example, there is correlation between the vehicle weight, number of axles, axle weights, and vehicle lengths, which can be difficult to otherwise model, as explained later. A drawback of using WIM data directly, is that alternative situations cannot be examined; for example, hypothesized traffic growth or modal shifts cannot be studied.

A vehicle in free-flowing traffic travels at around 25 m/s and therefore crosses a short to medium length bridge in one or two seconds. As gaps between vehicles are generally greater than one second, the number of occurrences of multiple following vehicles on a short-to-medium length bridge tends to be small. Even where it does occur, the second vehicle is often only partially on the bridge when the first is at a critical location and is sometimes presumed to contribute little to the load effect. However, the contribution of course, depends on the shape of the influence line or surface. In any case, for single lanes, some researchers consider only single vehicle loading events in the calculation of characteristic loads. This approach is especially suitable for shorter bridges. However, it is not difficult to consider the possibility of multiple in-lane vehicle presence when processing WIM data as weights, speeds and relative positions (arrival times) are known for all vehicles and can be taken directly from the data. Consequently, a long convoy of vehicles can be built from the underlying WIM data. The same is true for two-lane bidirectional bridges, where the train of vehicles in each direction are considered (usually independently). The case of multi-lane same-direction traffic is more complex and is discussed in Section 2.3.4 and 3.2.

When considering multiple in-lane vehicles, it is important to prevent unrealistic overlapping of vehicles during the bridge traverse. While this can be avoided by modelling driver behaviour, including acceleration and deceleration (as is done for long-span bridges), the computational effort involved is unwarranted for the short durations involved. Nevertheless, any overlapping must be prevented. One approach is to take the times of arrivals as being those at the detector, and to impose a constant velocity on all vehicles. In most cases, where speeds do not vary much, taking the average velocity of the stream, and imposing it on all vehicles, is adequate. However, in non-stationary conditions, such as transitions from free-flow to congested flow, which may exist in the measurements, speeds can fluctuate significantly. In these cases, if the selected constant velocity is higher than the actual velocity of several adjacent vehicles then the space headways will be overestimated leading to underestimated load effects. In contrast, for brief periods of velocities higher than the set constant velocity, the problem is reversed.

Another means of preventing overlapping is to consider each successive arrival in turn, adjusting the velocity of the following vehicle as necessary. Key dimensions of the vehicles for this situation are illustrated in Figure 3 and the times of arrivals are based on the successive arrivals of the front axles (thereby including the length of the lead vehicle). In particular, the velocity of the following vehicle is adjusted to ensure that a target time gap to the vehicle in front is ensured at the end of the traverse. In the following, subscripts  $f$  and  $r$  refer to the front and rear vehicles, and  $L$  and  $v$  to their lengths and

velocities respectably. Of course, when  $v_r \leq v_f$  there is no risk of overlapping on the bridge, and so what follows applies when the rear vehicles are catching up,  $v_r > v_f$ . At the end of the traverse, the target minimum time gap (headway) to the vehicle in front can be written as:

$$\Delta T_{\min} = \frac{L_f + b_s}{v_r} + b_T \quad \text{Equation 1}$$

where  $b_s$  is a physical space buffer (e.g., wheel diameter, say 1.0 m) and  $b_T$  is a time buffer (e.g., extreme minimum feasible time gap between vehicles, e.g., 0.1 s conservatively). These buffers can be further adjusted depending on whether or not the WIM data contains the front and rear overhangs (Figure 3). If the headway between the vehicle arrivals at the start of the bridge of length  $L_B$  is  $\Delta t$  (i.e., the time gaps in the WIM record), then this minimum time gap at the end of the bridge will not be achieved when:

$$\Delta t + \frac{L_B}{v_r} - \frac{L_B}{v_f} < \Delta T_{\min} \quad v_f \geq v_r \quad \text{Equation 2}$$

When this is the case, to achieve the target minimum time gap, the speed of the rear vehicle must therefore be adjusted to

$$v_r^* = \frac{L_B}{L_B/v_f + \Delta T_{\min} - \Delta t} \geq v_f \quad \text{Equation 3}$$

but is bounded to the speed of the front vehicle. In considering relationships like this, it is beneficial to draw the space-time plot of vehicle movements (straight lines for constant velocity) on the bridge deck.

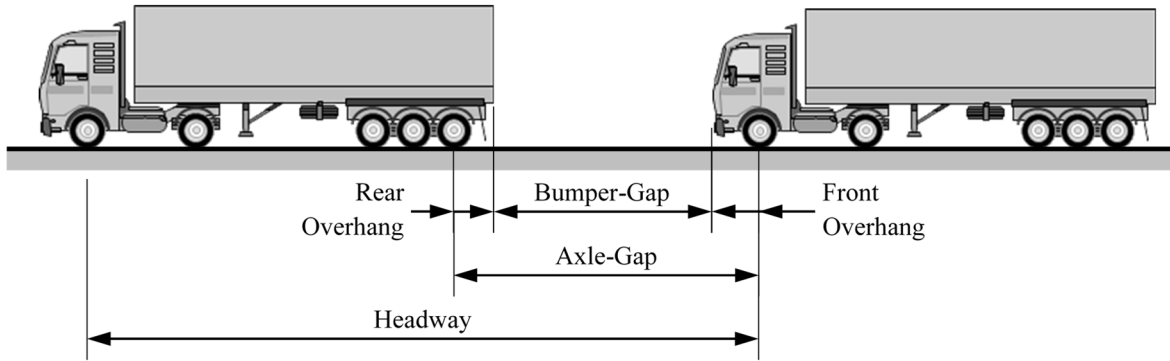


Figure 3: Key physical parameters of the spacing of vehicles (Lenner & Caprani, 2021).

### 2.3.2 Generation of Artificial Traffic Streams

Where there is insufficient WIM data to obtain sufficiently long periods of load effects, the generation of artificial streams of vehicles can be used. A benefit of this approach is that different scenarios of traffic flow and composition can be studied, including potentially traffic growth. However, the main challenge is the accurate modelling of the complex relationships that exist within the vehicle and traffic flow parameters.

The important parameters of traffic for bridge loading can be classified as:

1. the physical parameters of the vehicles, and
2. the parameters of the traffic flow.

With this classification, it is useful at times to think of a ‘garage’ of vehicles that are inserted into defined traffic streams. The physical parameters of the vehicles include the number of axles, the axle spacings and weights, and the gross vehicle weight, amongst others. The parameters of the traffic flow include the hourly flow in each lane, the distribution of vehicle types between lanes, and the headway or gaps between successive vehicles. For short-to-medium span bridges, it is reasonable to neglect the possibility of lane changes on the bridge, and so the measured traffic properties in each lane at the site of interest, is sufficient. Consequently, statistical independence of traffic between lanes is commonly assumed in literature and is a reasonable assumption for traffic in opposing directions. However, it is known to be somewhat inappropriate for same-direction traffic (O’Brien & Enright, 2011). Where there are multiple same-direction lanes, light trucks often overtake heavier ones resulting in correlated weights. Truck presence is also correlated – the presence of a truck in the overtaking lane is almost always associated with a vehicle in the slower lane. The composition of the traffic stream is usually determined from the measured proportions of the different vehicle classes, however defined. Monte Carlo simulation is used to generate the class of the ‘next’ vehicle in the stream using an appropriate model. Typically, independence of vehicle class arrivals is assumed, but autocorrelations of vehicle class within the stream can be modelled where necessary.

Considering the ‘garage’ of measured vehicles, each vehicle classification has its own statistical model developed for the generation of vehicles representative of that type. The classifications can be quite simple, such as the number of axles, or more complex (e.g., formal FHWA, Euro13, or AustRoads Classifications). A problem with this, is that only classifications with enough samples in the WIM data are modelled, thereby artificially limiting the vehicle types in the stream. Notably (Enright, 2010a) overcomes this problem and provides a means of generating vehicles with more axles than those observed in the traffic stream. However, this method does require considerable traffic data (e.g., 1 year) to be reasonably robust. Vehicle articulation can also be used to distinguish vehicle classes for statistical modelling. For example, (Bailey, 1996) uses 14 classes of vehicles, but only considers vehicles with up to five axles, the remainder being made up of tractor-trailer combinations.

### *Monte Carlo simulation*

Harman & Davenport (1976) were among the first to propose Monte Carlo simulation of vehicles and headways to generate load effects for further statistical analysis. Monte Carlo simulation is a process that generates ‘typical’ data, consistent with a specified statistical distribution. Monte Carlo simulation can be based on fitted parametric (e.g., normal), or non-parametric (e.g., cumulative frequency) distributions. For example, if vehicle gross weight is known to be Normally distributed with mean of 50

t and standard deviation of 5 t, repeated application of this formula will generate numbers that are mostly between 40 and 60 t, with a concentration around the mean of 50 t. The benefit of parametric modelling is that samples beyond the WIM data can be generated, but still reflective of the population. In contrast, when adopting non-parametric modelling, no sample beyond that already observed can be generated. Consequently, non-parametric modelling can be suitable for axle spacings and axle weights as a proportion of GVW, but at least for the extreme upper tails of GVW, parametric modelling allows samples beyond the measured data.

### *Modelling Vehicles*

A basic set of statistical models of the relevant vehicle properties summarized in Table 2. More advanced models for some of these properties are reported in the literature, and some of these are summarized further.

Table 2: Statistical models of vehicle and flow characteristics (Caprani, 2005)

<b>Traffic Characteristic</b>	<b>Statistical Model</b>
Gross Vehicle Weight (GVW)	Tri-modal Normal distribution
Axle spacings	Uni- or bi-modal Normal distributions, as appropriate
Axle weights for 2- & 3-axle trucks	Tri- or bi-modal Normal distributions, as appropriate
Axle weights for 4- & 5-axle trucks	Expressed as a percentage of GVW for the first and second axles and for the remaining tandem group. In each case, the percentage is modelled as a Normal distribution
Composition	Measured percentage of 2-, 3-, 4- and 5-axle trucks
Speed	Normal distribution – considered independent of truck type and uncorrelated with GVW
Flow rates	For each hour of the day, the average flow rate (ignoring weekend days and public holidays) was used for all the days available
Headway	Modelled with a number of distributions dependent on flow and gap, as described in

For Gross Vehicle Weight, (Harman & Davenport, 1976) were the first to use a linear combination of three Normal distributions – the tri-modal Normal distribution, given by:

$$f_X(x) = \sum_{i=1}^3 \rho_i \varphi(x; \mu_i, \sigma_i) \quad \text{Equation 4}$$

in which  $i$  is the mode,  $\rho_i$  is the weighting, and  $\varphi(x; \mu_i, \sigma_i)$  is the probability density function for a Normal distribution with mean,  $\mu_i$  and standard deviation,  $\sigma_i$ . This model has been widely adopted. The fitting of bi-modal and tri-modal Normal distributions is a flexible tool for modelling a range of properties including gross-vehicle weight, axle spacings, and axle weight.

Bailey (1996) used the Beta distribution for each of the traffic characteristics. This is a suitable distribution as it is very flexible and has upper and lower limits, which can be used to impose physically realistic values. Bailey considered axles within groups as having equal weight, since the weight is evenly distributed between closely spaced axles. There is no physical reasoning for axles within the same group (a tandem for example) to exhibit significantly different loads. A generalized bi-modal Beta distribution was used to fit the observed axle group weights and correlation of this weight with the GVW is also considered.

To better simulate individual axle loads, Crespo-Minguillón & Casas (1997) allocated axle weights and GVW based on their measured correlations. Geometries in their work are based on measured correlation coefficients for axle spacings. The GVW and axle weight distributions are defined numerically from measured cumulative distribution functions derived from the histograms of WIM data (i.e., a non-parametric approach). Srinivas et al. (2006) used copulas to accurately model the dependence structure between multi-modal distributions of axle weights. In a simplified manner, (Pérez Sifre & Lenner, 2019) used bivariate copulas to establish a relationship between the GVW and individual axle loads for up to 7-axle vehicles that can be further utilized in the non-parametric approach of simulations.

Enright et al. (2015) developed a semi-parametric approach for modelling some vehicle parameters. Up to a certain GVW threshold, where there is sufficient data, a measured bivariate histogram is used to generate GVW and the number of axles. The frequency threshold is selected as that level for which the bin count exceeds 16 observations, using a bin size of 1 t. Beyond this point, a parametric fit is used, in this case the upper tail of a Normal distribution. This semi-parametric approach means that average vehicle properties are exactly represented while ensuring that extreme weights can be generated beyond anything recorded in the database. For axle spacings, Enright et al. (2015) use empirical distributions of the ordered axle spacings and their positions in the vehicle; an approach which gives the axle layout for any vehicle and allows the generation of vehicle classes beyond the observations. For standard vehicles (e.g., 5-axle semi-trailer), this approach gives a similar accuracy to past approaches in which axle spacings are modelled based on position only. However, for heavier and less common vehicles (e.g., cranes, low-loaders, permit vehicles), Enright's approach is superior.

### *Generating Gaps*

Probably the most important parameter in the generation of artificial traffic stream for short-to-medium length bridges is the headway, Figure 3, as it controls the number of axles loads that can simultaneously exist on the bridge (O'Brien & Caprani, 2005). Headway is related to the physical gap by the vehicle



length and overhangs and can be measured either in time or distance. WIM measurements typically contain headway in units of time and so many models represent it in this manner. The most basic vehicle arrival model is based on the assumption that vehicle arrivals are Poisson-distributed, resulting in a negative exponential distribution for headway. Allowing for vehicle length, this becomes the shifted negative exponential distribution with cumulative distribution function:

$$F(\Delta t) = 1 - \exp[-\gamma(\Delta t - \Delta t_{\min})] \quad \text{Equation 5}$$

where  $\gamma = Q/(Q\Delta t_{\min} - 1)$  and  $Q$  is the flow (vehicles/hour). The minimum headway,  $\Delta t_{\min}$  in this model, is determined by a nominal vehicle length and speed. There is criticism that applies to the choice of these nominal parameters, and so an alternative model often used to avoid these problems is the Gamma distribution. However, this distribution gives a high probability to small headways. Interestingly, (Crespo-Minguillón & Casas, 1997; Grave, 2001) find that the distribution of “normalized headway”, defined as the headway divided by the mean headway per hour, is consistent regardless of flow. The cumulative distribution function for headway,  $\Delta t$ , is therefore given by:

$$F(\Delta t) = \frac{Q_T}{3600} [1 - e^{-\lambda \Delta t}] \quad \text{Equation 6}$$

where  $\lambda$  is the mean normalized headway and  $Q_T$  is the truck flow (trucks/hour). Using this model for headways over 4 s, (O’Brien & Caprani, 2005) propose polynomial fits to the measured WIM data for the flow-dependent cumulative distribution function of headways less than 4 s. Enright (2010) also adopts this approach but instead of headway uses the axle-gap as the parameter being modelled. This is useful because it avoids the potential for vehicle overlap on the bridge. Finally, the traffic flow rate is a particularly significant parameter as flow tends to vary through the day and clearly has a significant influence on gaps. To allow for this, it is essential that each hour of the day is simulated separately.

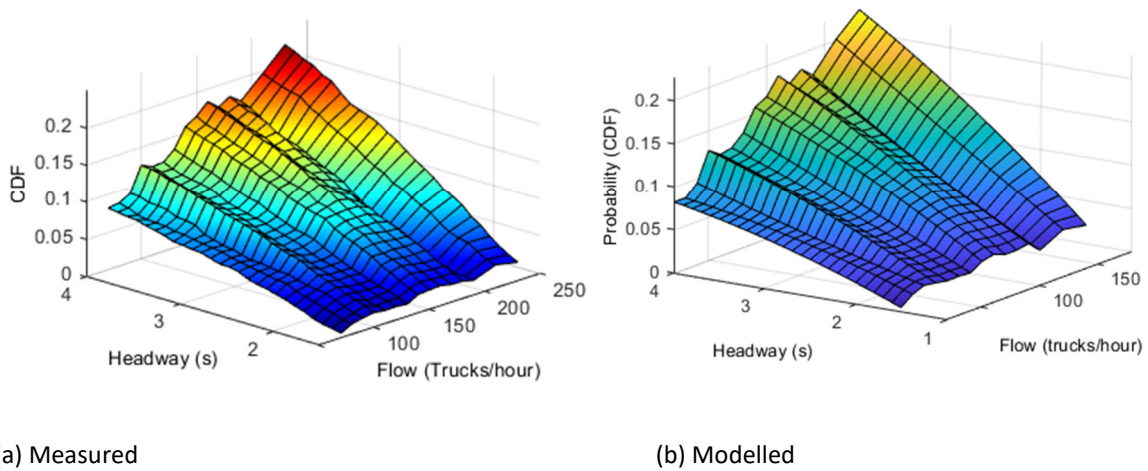


Figure 4: Cumulative distribution functions for truck flows between 1.5 s and 4 s (O’Brien & Caprani, 2005)

When generating headways (and not axle-gaps) for successive arrivals the minimum gap at the end of the traverse, shown in Equation 7, should be met to avoid inappropriate overlapping. Considering that the vehicle properties are already defined, including velocities, when the following truck is moving slower than the front truck ( $v_r \leq v_f$ ), the minimum required headway upon arrival at the bridge is just this target gap  $\Delta t_{\min} = \Delta T_{\min}$ . However, when the following truck is catching up on the lead truck, using the notation from earlier, the minimum headway upon arrival at the bridge must be:

$$\Delta t_{\min} = \frac{\Delta T_{\min} v_r + L_B}{v_f} - \frac{L_B}{v_r} \geq b_T \quad \text{Equation 7}$$

Upon generation of the random headway according to the adopted headway model, the requirement of Equation 7 should be checked and imposed if necessary. For bi-directional bridges, the above formulation represents a “mixed-datum” case in which the arrival datum is at one end of the bridge for the lanes in one direction, and at the other end, for the other traffic direction. Caprani (2005) considers the minimum gap requirements for the single-datum case, where the vehicle arrival datum for both directions is located at one end of the bridge. While this is a more faithful representation of the single point of measurement of a WIM station, the additional complexity is rarely warranted for short-to-medium span bridges for which traffic parameters can be considered as a statistically stationary process over this short distance.

### 2.3.3 Traffic Loading in Multiple Lanes

When considering more than one traffic lane, the analysis and modelling varies depending on whether the lanes are assumed with traffic running in the same or opposing directions. Studies consider more than two lanes rarely for two reasons: (i) for most short/medium-span bridges, the transverse stiffness is such that traffic in a lane rarely has a significant influence on lanes that are not immediately adjacent and (ii) trucks are often restricted from travelling in more than two lanes.

#### *Opposing-direction traffic*

Two lane bi-directional traffic is the most basic two-lane bridge to study. This is because the properties of vehicles traveling in opposite directions can be assumed to be statistically independent – there is no reason to expect the weights of two vehicles meeting on a bridge to be correlated (as the event is arbitrarily placed relative to the road network). Hence, for this case, the generation of the traffic streams in each direction reduces to the generation of two independent lanes of traffic. While each direction may have its own vehicle characteristics, it is more common to consider just differences in flow and composition. For bi-directional bridges with more than one lane in one or both directions, the assumption of independence in direction usually remains valid, and then the problem reduces to consideration of two same-direction multi-lane models.

---

### *Same-direction traffic*

Two or more lanes of same direction traffic are best examined considering just two lanes initially. In countries with asymmetric passing rules (e.g. Europe), experience suggests that the vehicles driving in the overtaking lane tend to be lighter and faster than those in the driving or slow-lane. Consequently, in these situations, there are statistical relationships between lanes that should be captured for accurate representation of traffic loading. For countries with symmetric passing rules (e.g., the United States), it may be feasible to consider each lane as independent for some suitable sites.

O'Brien & Enright (2011) reviewed early work on same-direction multiple-lane bridge traffic loading. With little or no available data, early work was based on subjective assumptions. As an example, (Nowak, 1993) assumed that one in 15 heavy trucks is part of an overtaking event. For these overtaking events, he further anticipated that the truck weights are fully correlated in one of 30 cases. Kulicki et al. (2007) acknowledged the lack of sufficient data and that their assumptions are based on limited observations. For weight correlation, their assumptions were based entirely on judgment and proposed multiple vehicle presence probabilities that are a function of average daily truck traffic as clearly heavier traffic results in more overtaking events. They use subjective field observations to find conservative values. Soriano et al. (2017) however treat the simultaneous loading and side-by-side effects based on WIM instead of the early assumptions. Multiple WIM sites from NYC are used to predict the effect of two combined lanes using a convolution based on the WIM recordings showing no correlation between trucks in the same or adjacent lanes.

#### **2.3.4 Multiple lane reduction factors**

A similar approach is used by (van der Spuy et al., 2019) where multiple lane recordings of both same and opposite direction traffic can serve for the prediction of combined load effects in any number of lanes, given that multiple lane data is available, a detailed example is offered in Section 3.3. Interestingly, for the Eurocode load model, each lane was simulated independently based on both direct use of the WIM data and Monte Carlo generation of artificial traffic streams (Bruls, Croce, & Sanpaolesi, 1996; Dawe, 2009). Consequently, there was no explicit consideration of the relative positions of vehicles in adjacent lanes.

For load models that are based on the probability of side-by-side truck occurrences, as in the United States, a precise definition of by “side-by-side” is warranted. In a parametric study (Board et al., 2007) defined a side-by-side event as one where adjacent trucks have a headway difference of less than 18.3 m (60 ft): a typical tractor-semi-trailer in the United States is 70 to 80 ft. This approach is subsequently refined with a description of side-by-side, staggered, following and other multiple-presence events (Sivakumar et al., 2008). They use WIM data to estimate the frequency of these event types for different truck traffic volumes and bridge lengths. They also calculate multiple-presence probabilities either directly from WIM data or estimate them from traffic volumes.

*Scenario Modeling*

O’Brien & Enright (2011) propose the concept of “scenario modeling” that addresses most of the challenges posed by multiple lanes of same-direction traffic. Based on the recorded data, they show that there are correlations between vehicle weights, speeds and inter-vehicle gaps. In a study of data from two European sites it is found that for nearly 75% of fast lane trucks there is an associated truck within 2 seconds of it in the slow lane, i.e., most fast lane trucks are overtaking a slow lane truck. This phenomenon increases the probability of multiple-truck presence on a bridge over any simulation that treats the lanes as independent. Due to the difficulty in simultaneously modelling all the interdependencies in a traffic scenario, they propose to use the measured scenario as the basis for simulation.

An example of a traffic scenario taken directly from measured WIM data is shown in Figure 5. This traffic scenario has 21 parameters – the GVWs and speeds of seven trucks, six gap values and a flow rate. The correlations and relationships between these parameters are implicit within each scenario, as they are taken directly from the measured WIM data. To allow for the possibility of loading scenarios other than those in the database, O’Brien & Enright (2011) ‘perturb’ the scenarios identified from the WIM data before finalizing them, i.e., they make small changes to the key parameters by adding statistical ‘noise’. They argue that these random perturbations do not significantly damage the integrity of the relationships between the parameters yet allows for unforeseen and unrecorded combinations of vehicles. Notably, in a subsequent study, (O’Brien et al., 2015) validate the process by comparing it with a reference dataset generated by micro-simulation.

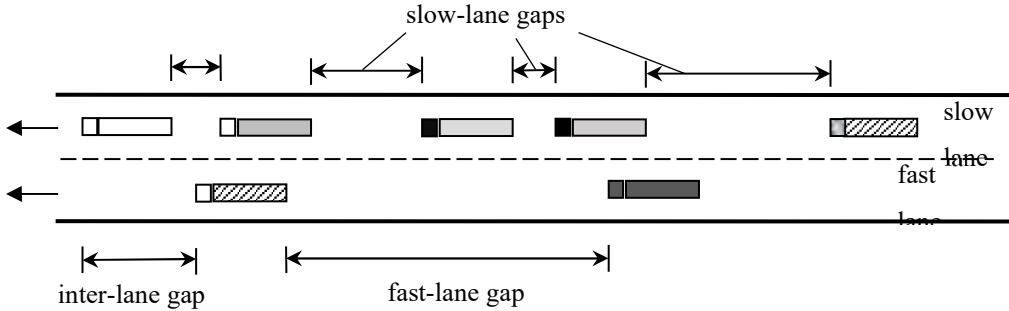


Figure 5: Traffic scenario (O’Brien & Enright, 2011).

**2.4 Load Effects**



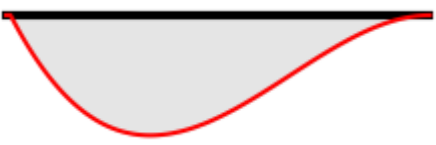


Given a stream of vehicles, the induced structural effects due to this loading are of course the main goal of the computation. There are a wide range of methods for calculating these load effects, ranging from influence lines, to influence surfaces, to grillage models, to elaborate finite element models. Due to the typical need for many vehicle crossing events to be evaluated, expensive structural analysis methods that require much computation at each time step (e.g., matrix inversion) are not preferred (though


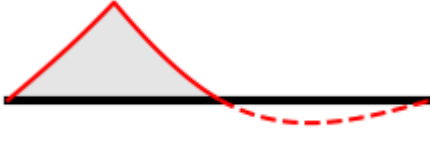
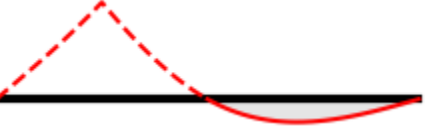
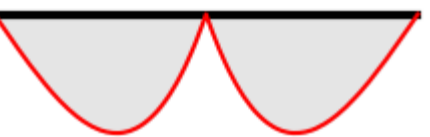
possible). Consequently, a consensus has emerged around the use of influence lines, surfaces, and lane weights, that minimizes computation wherever possible, allowing very long simulations of traffic streams (e.g., 10,000 years) to be feasible with modern desktop computers. Thus, the static load effects due to traffic on a bridge deck are typically obtained from a series of simple (static) analyses of the different static systems. In this section, these methods are outlined, and recommendations given to ensure accurate evaluations.

**2.4.1 Influence lines**

Influence lines are frequently used in traffic loading studies. They give reasonably good estimation of the longitudinal global load effects, and can be adopted, as explained later, to account for lateral distribution of load. Typical representative load effects of interest include maximum positive bending moment in a simply supported bridge, shear force at the support or negative support moment at the center of a 2-span bridge. An important suite of influence lines typical of those used in traffic load effect studies is given in Table 3. As indicated, influence lines with positive and negative lobes can be truncated so that only the relevant loaded length is considered; that is, the maximum positive or negative effect. This is typically done for the development of a load model – Section 3.1 – but for determining the actual effects the complete influence line should be used (Guo & Caprani, 2019).

Table 3: Influence lines used in background studies to the Eurocode (Lenner & Caprani, 2021).

Ref.	Description of the influence line	Shape of the Influence Line
I1	Maximum bending moment at mid-span of a simply supported beam.	
I2	Maximum bending moment at mid-span of a double fixed beam with an inertia that strongly varies between mid-span and the ends.	
I3	Maximum bending moment on support of the former double fixed beam.	
I4	Minimum shear force at mid-span of a simply supported beam.	
I5	Maximum shear force at mid-span of a simply supported beam.	

Ref.	Description of the influence line	Shape of the Influence Line
I6	Total load.	
I7	Minimum bending moment at mid-span of the first of the two spans of a continuous beam (the second span only is loaded).	
I8	Maximum bending moment at mid-span of the first span of the former continuous beam.	
I9	Bending moment on central support of the former continuous beam.	

In the calculation, the train of vehicles represented by point loads is passed over the one-dimensional bridge in small steps, e.g., 0.5 m or 0.2 m. Figure 6 shows the load effect calculation for a given arrangement of vehicle (or vehicles) on the bridge in a given step. The load effects due to each axle are calculated and combined by means of a superposition to give the total effect. The procedure for calculating the load effects due to a train of vehicles is the same as for a single vehicle. The axle weights are applied as point loads on the influence line. Moving the vehicle(s) to the next position in predefined increments, creates the load effect history.

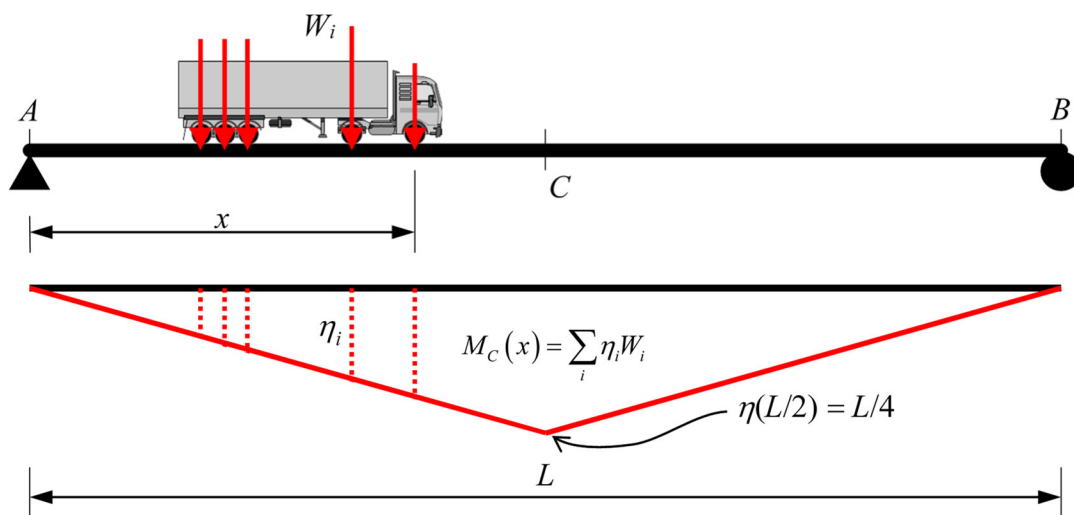


Figure 6: Calculation of mid-span bending moment,  $M_c$  in a simply supported beam under a truck load using its influence line.  $\eta_i$  is the influence line ordinate corresponding to the  $i^{\text{th}}$  axle (Lenner & Caprani, 2021).

---

### 2.4.2 Influence Surfaces

Influence lines (e.g.) give load effect as a function of load's longitudinal position along the length of the bridge. By only considering longitudinal position, these functions do not take account of the vehicle's transverse position. Extending the influence line concept into the transverse direction as well, gives the influence surface, which provides the load effect at a point as a function of both longitudinal and transverse position of the applied load. With an influence surface, a vehicle can be positioned at any point on the bridge, and the load effect resulting from each individual wheel load can be found and added. This approach is applicable where transverse positioning of vehicles within their lanes is critical for obtaining accurate results. An influence surface rarely has a closed-form expression, and linear or quadratic interpolation between adjacent points (where the surface is defined) is required to determine influence ordinates for arbitrary positions of wheel loads. Because of this need for interpolation, it is best to use as few points to describe the influence surface as possible, to reduce look-up computational time, but without compromising the accuracy. For example, planar portions of influences surfaces can be described using only four points, regardless of the dimension. Figure 7 shows a typical influence surface that is obtained from a grillage model and so is only defined at discrete points on the bridge deck, provoking the need for interpolation for intermediate positions of axles.

A second approach, that has lower fidelity but less computation, is to use slices or cross-sections through the influence surface corresponding to the wheel lines of the vehicles. If the vehicles run perfectly along the center line of the lane, and reasonably assuming that wheel loads are equal, then the mean of the influence ordinates for the two-wheel lines through the influence surface, produces an influence line representing the lane. Referring to Figure 7 this lane 'mean' influence line can be seen along the center line of the lane and is the average of the two influence lines of the wheel paths. It is important to note that the mean slice is not necessarily the same as a slice through the influence surface at the center of the lane, since the influence surface may have a highly nonlinear shape transversely. For each lane on the bridge, this process is followed, and the total load effect can then be summed over all lane influence lines to obtain the total load effect at the point of interest. Typically, for this method, the lane influence line is only determined numerically (e.g., Caprani et al., 2012), and an interpolation between adjacent node points is needed for arbitrary positions of load, which again suggests the use of as few points as possible to reduce look-up times in the vector of influence ordinates.

A third approach for accommodating transverse load distribution is far less computationally demanding and is sufficiently accurate where the influence surface is approximately linear in the transverse direction. In this case, the influence surface is represented by a single influence line shape, but with a weighting factor for each lane for scaling. Again, the total component load effect is found by summing the effects over all such lane-weighted influence lines. Although this approach assumes a linear transverse variation of the influence surface for the component of interest, this is quite reasonable for many situations. A further benefit of this method is that the influence lines can often be expressed as a closed-form expression, negating the need for additional interpolation computation.

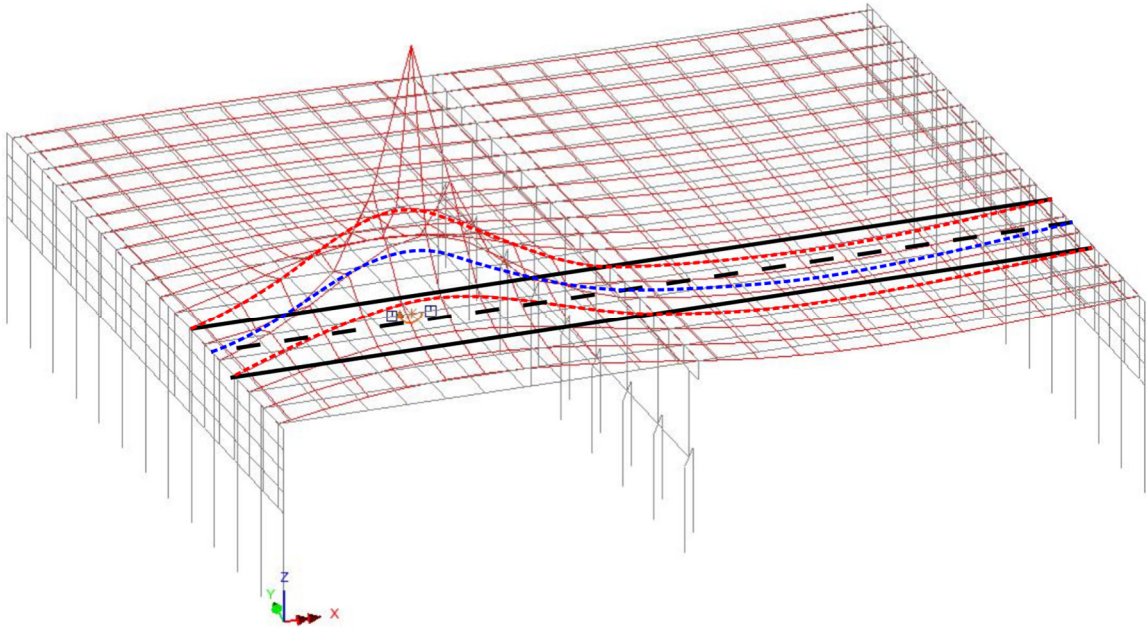


Figure 7: An influence surface for mid-span bending moment in a girder of a two-span integral bridge showing wheel paths as slices and a ‘mean’ lane influence lane (Lenner & Caprani, 2021).

**2.4.3 Load Movement**

For accurate results, an important setting in the calculation of load effects is the step or increment size,  $\delta x$ , by which the vehicle is moved across the bridge. Moreover, consider when there are multiple vehicles with differing speeds: in this case, vehicles are not incremented through a position change, but through a time step,  $\delta t$ , from which the increment in the vehicles’ positions are determined from each vehicle’s speed,  $v_i$ , as  $\delta x_i = v_i \delta t$ . It can be seen from Table 3 that the peaks of influence lines around the maxima are smoother in some cases than others. This gives an indication of the sensitivity of the calculated maximum response to the step size. Sharp peaks in the influence line manifest themselves in peaks in the responses as can be seen in Figure 8. In particular, the accurate determination of the maximum shear (or reaction) is clearly strongly dependent on the step size adopted, due to jumps in the response as axles enter the bridge.

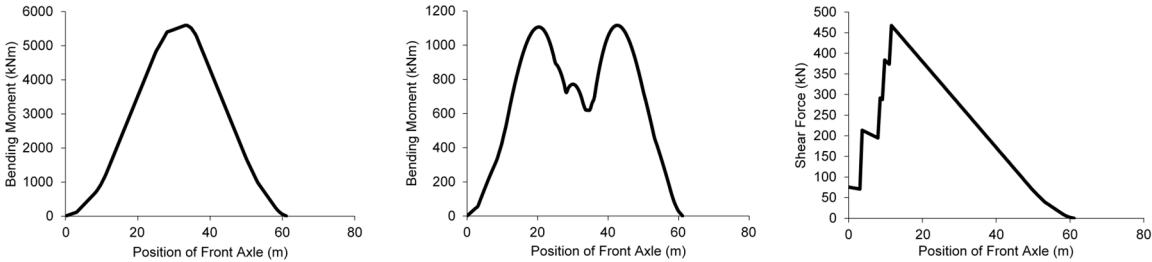


Figure 8: Responses of a 50 m long bridge to a single 5-axle truck for (left-to-right): mid-span bending moment of a simply-supported bridge; hogging moment at the central support of a two-span bridge; left hand shear force of a simply supported bridge (Lenner & Caprani, 2021)..



Other load effects can also exhibit this phenomenon (e.g., torsion at mid-span of a box-girder). The obvious solution is to use a very small step size, but this increases the computational effort. A further consideration is that quite usually, there is more than one load effect (influence line) being simultaneously calculated for the given traffic topology. Therefore, it is recommended to undertake an initial sensitivity study of the results to the chosen step size for the particular influence lines under consideration.

As an example, a sequence of vehicles on a 50 m long, two-lane bi-directional traffic bridge, is simulated using a range of time steps, for the three load effects of Figure 8. The results are shown in Figure 9. For the load effects with influence lines that are continuous (and have no discontinuities), the responses are smooth and not very sensitive to the time step. For the influence line with a jump discontinuity (Load Effect 3), the response is seen to be sensitive to the time step adopted. For this example, Load Effect 3 is underestimated nearly 2% for the 0.05 s time step and by nearly 10% for the 0.2 s time step (Figure 10). The other load effects are not significantly affected.

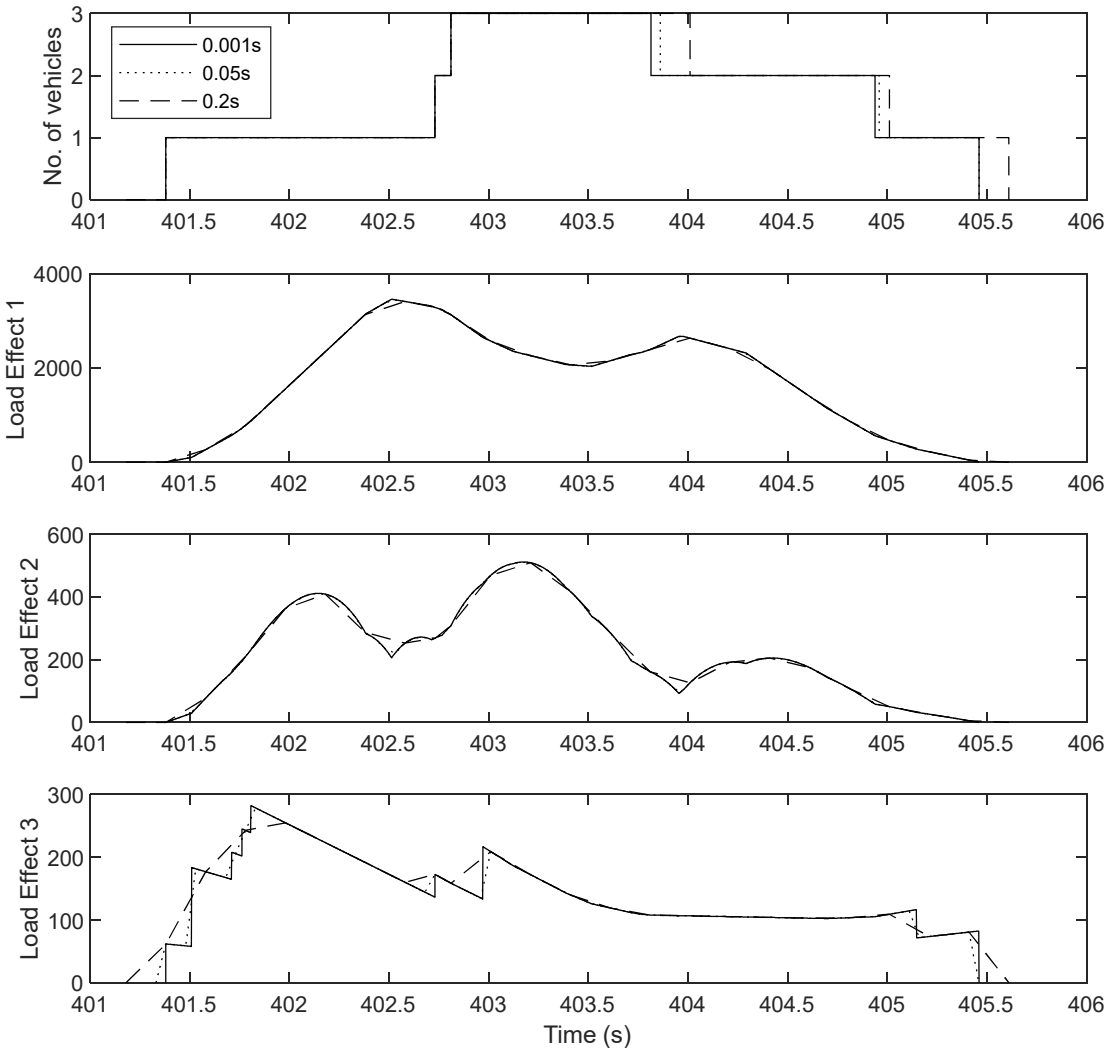


Figure 9: Static responses for three load effects using a range of time steps on a 50 m long bridge (Lenner & Caprani, 2021).

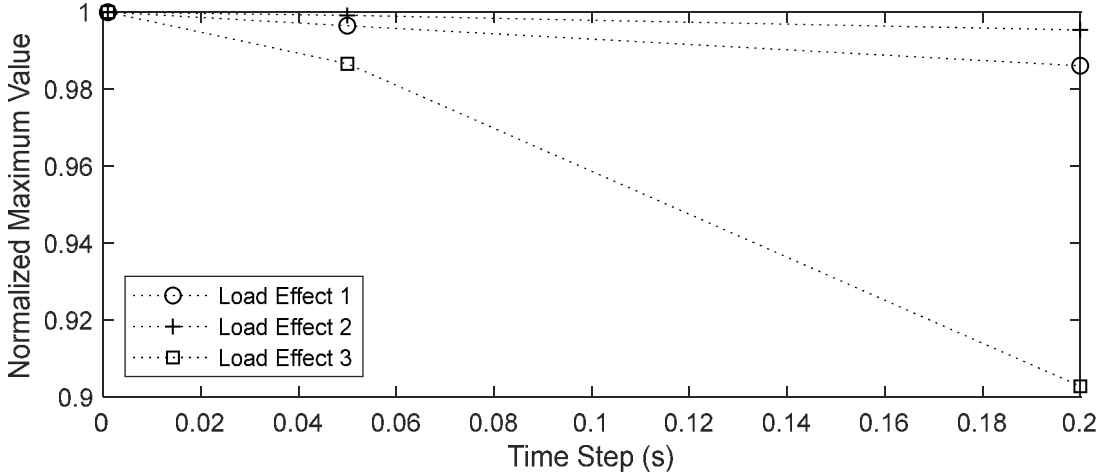


Figure 10: Error in static maximum response due to time step (Lenner & Caprani, 2021).

**2.5 Dynamic Interaction**

The preceding analysis has entailed solely static calculations. Factors that consider the vehicle-bridge dynamic interaction are particularly significant for the extreme loading effects on short-to-medium span bridges. It is common practice that these static load effects are amplified to account for vibration effects. This is straightforward to do, and to accommodate in the statistical prediction analysis that is to follow. However, in recent years an alternative refined treatment of dynamic effects has emerged which can be incorporated into the extrapolation of load effect.

Firstly, it is mostly well established that for typical highway vehicles the dynamic increment reduces with increasing static load effect; essentially, heavy trucks do not “bounce around” as much as lighter trucks, even though the total stress is greater. In single degree of freedom systems, as the mass increases, the amplitude and frequency of the response decreases. This is however to large extent dependent on the loading frequency of the vehicles in the relation to the natural frequencies of the bridge as shown by (Mei et al., 2023; Meyer et al., 2021) . Secondly, the dynamic amplification of static load effects under multiple trucks is even lower (Caprani, 2005; Caprani et al., 2012; González, OBrien, et al., 2010). Indeed, this is reasonable considering the destructive interference that occurs between the multiple vehicle dynamic systems and the bridge system. Together these vibratory effects mean that at increasing static values of load effect, and thus reduced probability of occurrence, the dynamic allowance reduces. A final complexity of the dynamic effect is its intrinsic uncertainty: even for the same vehicle(s) and bridge, the system is sufficiently complex that it is not deterministic. Thus, this uncertainty exists alongside the reducing dynamic increment with reducing probability of occurrence and both can be captured through a probability distribution of dynamic effect.

---

## 2.6 Statistical Prediction

### 2.6.1 Prediction of extremes

Extreme low probabilities of exceedance are often expressed in terms of the average recurrence interval, more commonly known in engineering terms as the return period. Codes of practice often express design loading through statements or definitions such as that with a probability of exceedance of 10% in 100 years. The return period,  $R$ , is related to a design life,  $T$ , and a probability of exceedance,  $p$ , as follows (Ang & Tang, 1975):

$$R = \frac{1}{1 - (1 - p)^{1/T}} \approx \frac{T}{p} \quad \text{Equation 8}$$

The load effect at the return period  $R$ , can be referred to as the return level or characteristic maximum load. It is important to note that the return period,  $R$ , should not be confused with the design life,  $T$ . In Europe for instance, bridges are designed for a service life of 100 years with the capacity to resist load effects corresponding to a return period of approximately 975 years. Thus, they are designed to carry a characteristic load that would be expected to occur in only approximately 10% of bridges just once in their lifetimes. These values coupled with appropriate partial factors based on relevant target reliability indices  $\beta_t$  then correspond to the design point (ISO 2394, 2015).

The artificial simulation of traffic and load effects can in principle be engaged so it produces load effects for any period required (Enright & O'Brien, 2013). Of course, the results are only as good as the assumptions inherent in the vehicle simulations, but this approach has the advantage that the statistical distribution of the LE does not have to be assumed. In the absence of such extensive simulations, it is necessary to employ statistical techniques to predict the load effects at the specified return periods at the basis of recorded traffic load effects of limited lengths.

A train of vehicles generates a response history of LE as discussed in Section 2.3. This includes the responses due to single or multiple vehicles and load gaps in the history between when there is no vehicle on the bridge. Since we are typically interested in the largest (or smallest, which is easily dealt with as the largest negative of small data), to obtain the load effect at specified return period is necessary to consider the distribution of maxima  $F_N(x)$ :

$$F_N(x) = F^N(x) \quad \text{Equation 9}$$

where  $N$  is related to the number of events in the required return period and  $F(x)$  is a distribution of the observed load effects (all data). This form of extrapolation dramatically amplifies minor errors or poor fitting in the upper tail of the distribution (Caprani, 2005). It is therefore more appropriate to utilize asymptotic models and estimate approximate distributions based on extreme data only (Coles, 2001). In practice this means that extrapolations should not be based on the distribution of all load effects, but on the distribution of maximum load effects in a specified block of time. Distributions of maximum-per-

day, maximum-per-working-day, maximum-per-month and maximum-per-year have all been used in relevant kinds of studies, depending on the quantity of data available (Bailey, 1996; Zhou, 2013; Zhou et al., 2012).

The time blocks used as a basis for extrapolation should be statistically similar. The block size should be large enough to accommodate any minimum variations, and the measurement or simulation period should be extended enough to capture long term variations. Flows vary yearly, seasonally, daily, and hourly. Respectively, these variations are governed by economic activity, seasonal production, demands, and holiday periods, working days and weekends, and the daily cycles of traffic, such as peaks hours and nighttime. Against this background, a common assumption has been to represent ‘economic days’ as those relevant for bridge loading. This is why weekend days and holidays are often separated from working days. If working with daily maxima, there are then around 250 economic days per year (5 working days for 52 weeks in a year, minus about 10 for public holidays). This however depends on the national regulations, as in some countries, heavy traffic is permitted on the weekends and public holidays which effectively results in longer periods; care must be taken here with respect to the local conditions. As an example, South Africa has no imposed restrictions on heavy traffic operation and therefore the full 365 days are utilized in the preliminary development of the load model (van der Spuy & Lenner, 2019). Finally, given the variation in traffic flow during a day in most sites, it is not recommended to use a block size of less than one day.

While there are many approaches to extrapolation, here the focus is on a basic extrapolation using the block maximum extreme value theory. Given a dataset of (say) for example daily maximum bending moments, with perhaps 250 samples (one economic year), it is of interest to determine the bending moment corresponding to a 100-year return period, as may be typical of a reliability analysis for extending the life of an existing bridge. There are three classes of extreme value distributions that are relevant to this data set, the Gumbel (Type I), Fréchet (Type II), and Weibull (Type III) distributions. To avoid the need to decide between these, it is easier to fit the Generalized Extreme Value (GEV) distribution which incorporates all three. The cumulative distribution function of the GEV distribution is (Coles, 2001):

$$G(z; \theta) = \exp \left\{ - \left[ 1 + \xi \left( \frac{z - \mu}{\sigma} \right) \right]_+^{-1/\xi} \right\} \quad \text{Equation 10}$$

where  $[h]_+ = \max(h, 0)$  and the parameter vector is  $\theta = (\mu, \sigma, \xi)$  – the location, scale and shape parameters respectively. The shape parameter distinguishes to which of the classes of extreme value distribution the GEV corresponds, namely: Gumbel, Fréchet, and Weibull. Note that some publications express Equation 10 differently, changing the meaning of the shape parameter sign. The shape parameter has significance because the Weibull distribution is bounded (has an upper limit), while the Gumbel and Fréchet distributions are unbounded (the Fréchet is a heavy tailed distribution). Figure 11 illustrates the

three upper tail behaviours of the GEV distribution for a standardized load effect (i.e., location shifted to zero and width scaled to unity). The probability density and cumulative density plots are quite familiar. The Gumbel probability paper plot is frequently used in extreme value statistics, as it emphasizes very small changes in probability near 1.0 in the upper tail. The ordinate is a rescaling of the cumulative probability, referred to as the Standard Extremal Variate (SEV), as follows:

$$SEV(z) = -\log[-\log(G(z))] \quad \text{Equation 11}$$

This rescaling of the vertical axis means that Gumbel distributions appear as straight lines, and so it is referred to as Gumbel Probability Paper (Ang & Tang, 1975). Probability papers for other distributions are also sometimes used (e.g., Normal). However, it is recommended to prefer one form, so that the meaning and locations of curves in the plots of data become known with experience.

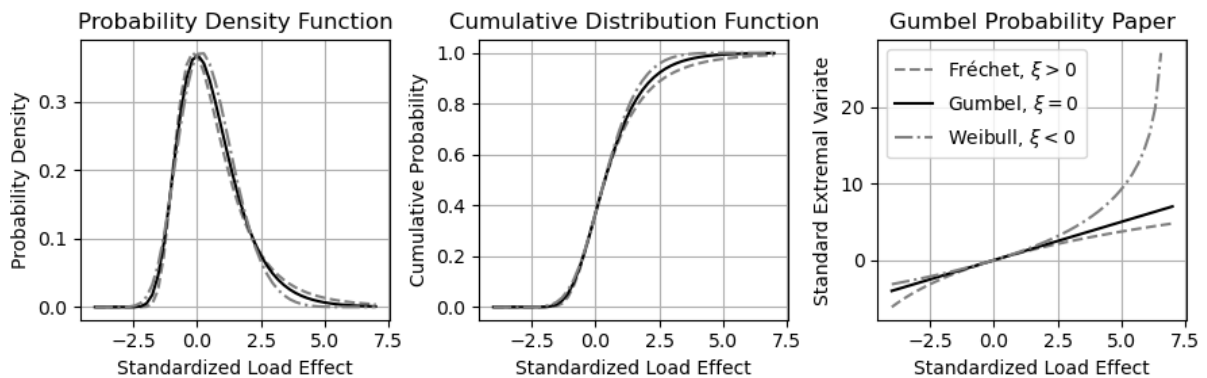


Figure 11: The three forms of GEV distribution (location = 0, scale = 1) with shape parameters of -0.15 (Weibull), 0 (Gumbel), and 0.15 (Fréchet), shown on three common forms of plots (Lenner & Caprani, 2021).

Noting the tail behaviors in Figure 11, it is frequently argued that bridge traffic loading is a Weibull-distributed process, or Gumbel at worst (Bailey, 1996; O’Brien, Schmidt, et al., 2015). This is logical given that the Weibull distribution is bounded, i.e., it applies to data with a finite upper limit. It is reasonable to believe that traffic loading must have a physical upper bound corresponding to the maximum mass of manufactured vehicle types that can fit on a bridge. The Fréchet distribution is an unbounded distribution and bridge traffic load effects should not fall within this distribution type. It is possible for bridge LEs to approach a Gumbel distribution and several authors have applied it for this purpose. Yet, though the approach with Weibull seems to be favored, research by (Hwang & Nowak, 1991; Soriano et al., 2017) shows that fitting to a Normal distribution may work as well, but this has an unbounded tail like the Gumbel distribution.

Bridge traffic loading is a complex statistical process, with many sub-populations of randomness. For example, bending moment under 2-axle trucks will be distributed differently to those under 5-axle semi-trailers; single truck loading events are similarly differently distributed to events comprised of multiple trucks. These mixtures of data generating processes mean that the use of a single probability distribution can frequently prove incapable of properly modelling the entire population of data. To deal with this

added complexity, two approaches have emerged: (1) fitting the single distribution to the tail of the data only; (2) fitting multiple distributions to each separated sub-population and recombining.

For fitting single distributions to mixed data, the mixtures around the middle of the data are to be avoided, and the upper tail data is assumed to be comprised of a single generating mechanism representative of extreme load effects. The challenge then is the selection of an appropriate tail length as this may have a significant influence on the extrapolated value, especially when the fitted data is due to a mixture of events. Various tail thresholds have been investigated in previous studies, including the upper  $\sqrt{n}$ ,  $2\sqrt{n}$ ,  $3\sqrt{n}$  and upper 5% and 30% of values (Castillo et al., 1996; Crespo-Minguillón & Casas, 1997; Soriano et al., 2017; Zhou et al., 2012) with many authors favoring the length  $2\sqrt{n}$  as initially proposed by (Castillo, 1988). In using a tail-fitting approach, judgement needs to be used to identify a tail that represents a reasonable quantity of data, but where there is a clear and consistent trend. This is consistent with (O'Brien, et al., 2015) who concluded that the distribution chosen is less important than the quality of the fit in the tail.

To complete this basic introduction to prediction, a simple extrapolation is illustrated by example. Consider that a client wishes to keep an existing bridge operational for another 10 years without major refurbishment. A characteristic load effect is required for the assessment with a here considered 100-year return period, corresponding to a probability of exceedance of approximately 10% for the next 10 years. The bridge is located at a site for which 3 months of traffic data was collected. The traffic data was used to compute daily maximum load effects for 5 economic days per week, for 12 weeks, giving  $n = 60$  daily maxima samples. The data,  $z_i$ , is sorted in ascending order,  $i = 1, \dots, n$ , and the empirical probability of each data point is found from:

$$\hat{G}(z_i) = \frac{i}{n+1} \quad \text{Equation 12}$$

Using this along with Equation 11, the plotting position (ordinate) of each data point on Gumbel probability paper can be found. Prior to the widespread usage of desktop computers, a Gumbel distribution could then be fitted through these points as a straight line, and its parameters found (Ang & Tang, 1975). Nowadays, statistical computation methods that do not rely on empirical formulas for ordinates are preferred, such as maximum likelihood estimation. These yield the parameter estimates for the GEV distribution that best describes the data,  $\hat{\theta} = (\hat{\mu}, \hat{\sigma}, \hat{\xi})$ . Figure 12 shows the GEV distribution fitted to the data on Gumbel paper. Since we are looking for the largest load effect that can occur in 250 economic days per year over the 100-year return period while working with underlying daily maxima load effects, the probability that all load effects are less than this (i.e. the probability of non-exceedance) is:

$$p_{RL} = 1 - \frac{1}{250 \times 100} = 0.99996 \quad \text{Equation 13}$$

Using this, and given the parameter estimates, the return level at the 100-year return period is found from the inverse cumulative density function of the GEV, giving:

$$z_{R=100\text{yrs}} = G^{-1}(p_{RL}; \hat{\theta}) = 13860.1 \quad \text{Equation 14}$$

Also shown in Figure 12 is the return level SEV value, found from:

$$SEV_{R=100\text{yrs}} = -\log[-\log(p_{RL})] = 10.127 \quad \text{Equation 15}$$

and this provides a useful visual aid on the extrapolation ‘distance’. Furthermore, it is at the intersection of this line, with the fitted distribution, that the return level is found, as shown.

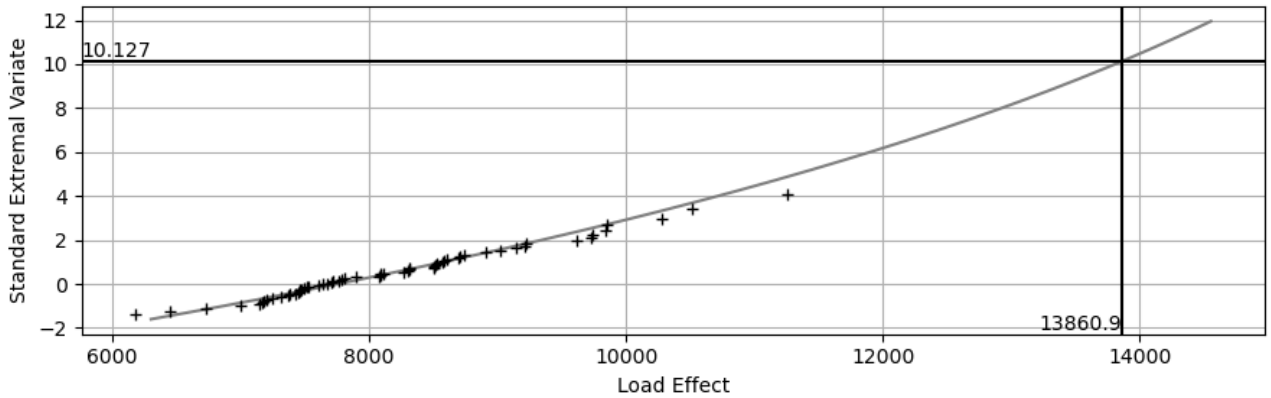


Figure 12: Example fit to sample data generated from a GEV (8000, 850, -0.15) distribution – 60 data points (daily maxima for 3 months) extrapolated to 100 year return period at 250 days per year (Lenner & Caprani, 2021).

## 2.6.2 Composite Distribution Statistics

In the previous section, it is noted that highway bridge loading events are known to arise from a mixed population (e.g., 1-truck, 2-truck loading events), and that this causes challenges with extrapolation. Caprani et al. (2008) introduced Composite Distribution Statistics (CDS) to account for the mixed population. CDS includes the relative contributions of different types of loading event to the overall probability of a specified level of LE not being exceeded – the non-exceedance probability. This is an interesting alternative to the conventional approach of tail-fitting a single distribution, as it provides an insight into the types of loading events that govern the (unobserved) extreme values of LE. CDS takes each distribution separately and combines the results by calculating the probability of non-exceedance of a specified LE level as the product of the component non-exceedance probabilities. The total probability of non-exceedance is the probability of not being exceeded by 1-truck loading events, and not being exceeded by 2-truck loading events, and so on. As the event types are independent, these component probabilities are multiplied, and the composite distribution of non-exceedance is:

$$G_C(x) = \prod_{i=1}^N G_i(x) \quad \text{Equation 16}$$

where  $G_i(\cdot)$  is the cumulative distribution function for the  $i$ -truck loading event of the  $N$  loading event types.

Figure 13 illustrates an example of the CDS method on Gumbel probability paper. Noting that the increasing ordinate corresponds to increasing rarity, it can be seen that 2-truck loading events appear as the critical form of loading up to a LE level of around 4400 kNm, where 3-truck loading events become more critical. The total probability of LE exceeding a specified level includes all the component probabilities. Really interesting is that short periods of observation (months), corresponding to lower values of SEV, suggest that 2-truck events are critical, whereas longer observations (many years) actually reveal that the rarer 3-truck events are more critical (at SEV around 8). For example, at the 4400 kNm level, the contributions from 1-truck and 5-truck loading events are negligible. At a LE value of around 4800 kNm, the 3-truck event curve merges with the composite distribution, showing that all other event types have become negligible. This is despite the clear governance of 2-truck events around the mean (ordinate value 0.36; LE value around 3400 kNm). Indeed, this is quite typical: the ‘average’ block-maximum loading events are not necessarily reflective of the composition of the extreme loading events.

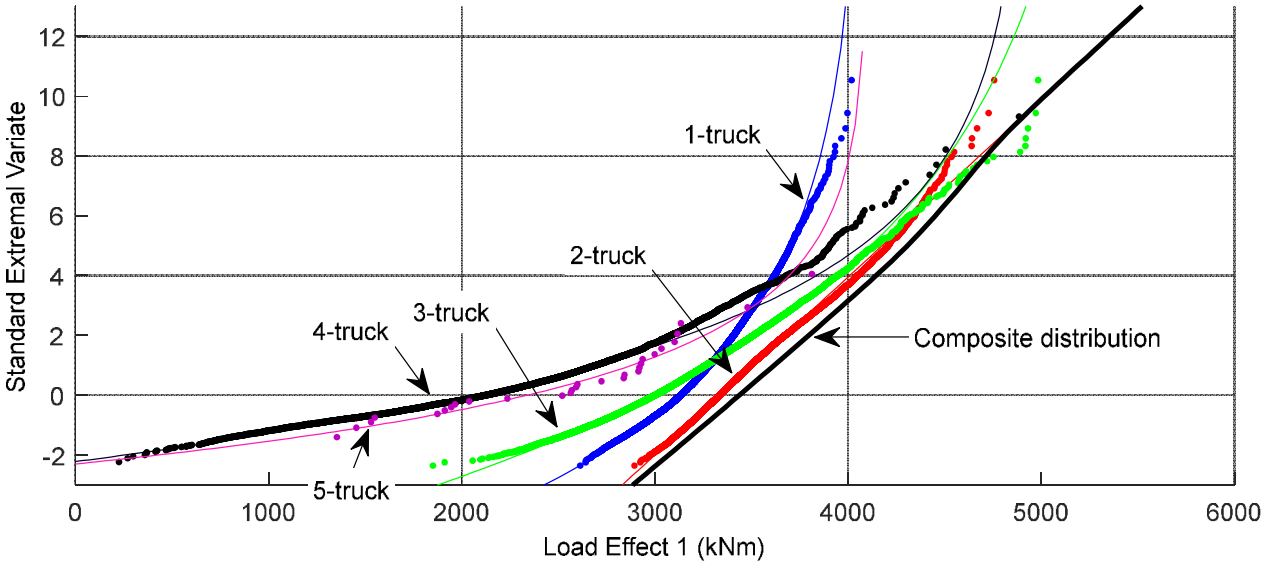


Figure 13: Daily-maximum LE distribution fits for  $i$ -truck free-flow traffic loading events and the overall composite distribution for mid-span moment in a 40-m simply supported bridge (Lenner & Caprani, 2021).

**2.6.3 Governing Form of Traffic**

The governing forms of loading are generally considered to be a function of loaded length – the adverse portion of the influence line for the LE of interest. An indicative summary is given in Table 4. Beyond a certain loaded length, usually taken to be around 40-45 m, congested traffic is commonly thought to govern over free-flowing traffic. This 40-45 m length appears to have arisen based upon the values of dynamic amplification that have been so-far included in codes of practice. Vehicles traveling in free flow at full highway speed are typically more than 25 m apart. Vehicles in stopped traffic can be as little



as 2 m apart. Hence, although no dynamic allowance applies, LEs from congested traffic tend to be greater on longer loaded lengths in comparison to the free-flowing traffic with a dynamic allowance. In the past few decades, a number of factors have emerged to challenge the perception that congested takes over from free-flowing traffic at around 40 m, exposing a deeper complexity to this issue. A study by (Meyer et al., 2021) exposes the dynamic amplification factor for multi-axle vehicles and points to the fact that the commonly accepted reverse relationship between dynamic amplification and gross vehicle weight is not necessarily true, as the axle group configuration plays a significant role. It can be however safely assumed that the value taken for the dynamic amplification of static LEs is the key consideration. While values of 1.2 and 1.4 have been used in the derivation of the Eurocode load model, lower values have been suggested in more recent studies, as the one by (Meyer et al., 2021). When the allowance for dynamics is indeed less than previously used, then the LEs due to congested loading become critical at much lower loaded lengths.

Table 4: Governing forms of loading for different (approximate) loaded lengths. \* The point where congested traffic becomes more onerous than free flowing is a subject of much debate.

<i>Approximate loaded length</i>	<i>Governing Case</i>	<i>Traffic</i>
Point locations (e.g., expansion joints), or lengths < ~1.0 m	Single axles	Free flowing
Less than ~8.0 m	Axle groups (tandem, tridem, etc.)	Free flowing
~8.0 to ~20.0 m	Single vehicle per lane	Free flowing
~20.0 to ~40.0 m*:	Multiple vehicles per lane	Free flowing
> ~40 m*	Multiple vehicles per lane	Congested

Using CDS, Caprani (2012) proposes a statistical model to capture the preceding complexities, and gives the total distribution of load effect as being made up of dynamic, free-flow, and congested components:

$$G_T(z) = [D(\cdot) G_C^{FF}(z)] G_C^{CF}(z) \quad \text{Equation 17}$$

In this formulation, the composite distributions of free-flow (“FF”) and congested flow (“CF”) are found using the usual traffic streams, load effect calculations, and statistical estimation methods that have been described already. To account for dynamic effects, Equation 17 includes a purposefully vaguely defined “dynamic function”,  $D(\cdot)$ . This dynamic function is defined by the user, and can arise from site measurements, a code of practice, or advanced dynamic and probabilistic modelling. It could be a constant (e.g., 1.3z as defined in Australia), or reduce with increasing load effect,  $z$ , or even depend on the probability of the load effect  $z$ .

A nuance of combining traffic states is that the relative periods of congested and free-flow at the site should be considered. For example, if it is considered that the site will experience 2 hours of congestion per day, then 200 hours of simulated congested traffic and 2200 hours of free-flowing traffic will

correspond to 100 days; the daily maxima for free-flow and congestion is then taken as the maxima of the blocks of 22 and 2 hours respectively.

(Caprani, 2012) illustrates an example of this approach in a probability paper plot, reproduced here as Figure 14. At the return level, no single form of traffic governs, but a mixture of both free flow (including dynamics) and congestion actually governs. Analysis using this total site load effect framework suggests that, for loaded lengths where neither free flow nor congested traffic dominate, both ought to be considered. The frequency of occurrence of each traffic type is also significant. However, what is clear from the results of this approach so far, is that congested traffic governs at much shorter spans than previously considered. A side effect of this is that bridge lengths and load effects previously thought to be governed by free-flow traffic plus dynamics, could be found to be governed by congested traffic, at a slightly lower level of characteristic load effect.

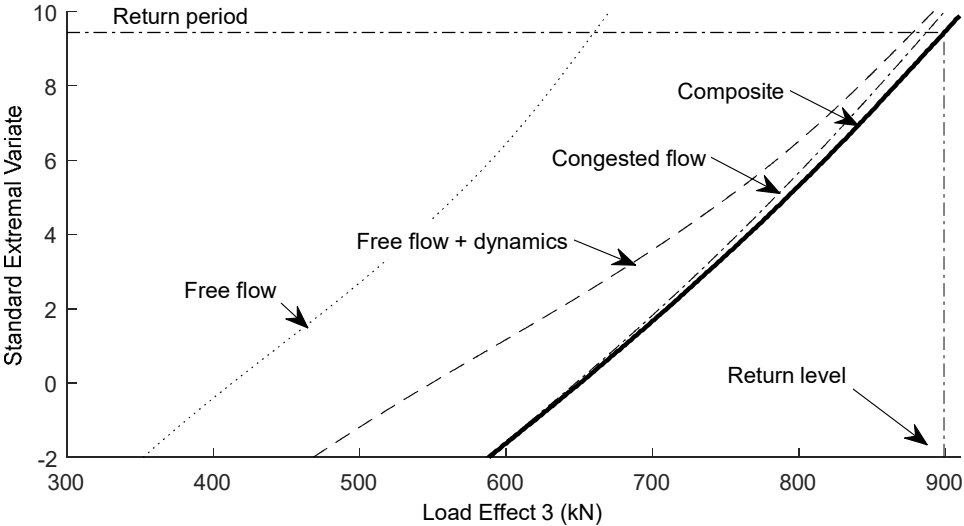


Figure 14: Extrapolation for total site load effect (shear on a simply supported 40 m span) distributions of free-flow, free-flow plus dynamics, congested flow, and the composite, or overall, distribution, for a site with 0% cars using the AASHTO LRFD DAF model (Lenner & Caprani, 2021).

**2.7 Conclusions**

Modelling of traffic for short-to-medium span lengths bridges can be summarized by some distinctive points. It is first necessary to establish the composition and statistical description of the traffic currently operating on the roads, where the most important parameters include the frequency distribution of gross vehicle weights, axle loads, truck geometry and spacings between individual vehicles. Typical means of collecting the required input is the data from WIM systems. An alternative approach is the identification of a governing event in form of a critical truck crossing during the proposed service life of a bridge – then the critical truck then represents a vehicle with a geometry and loads to cause a critical loading in the considered period. Most codes are however currently reliant on the collected WIM data which is subsequently rigorously cleaned and calibrated.

---

As the obtained data contains information the truck geometry and individual axle loads, this enables beyond direct calculation of load effect also a sampling and generation of artificial traffic events at long periods that can possibly equal to the specified return period. The often-highlighted advantage of this approach coupled perhaps with scenario simulation is the generation of non-observed events at the data collecting station. From either measured or artificial traffic, load effects can be calculated using the influence lines or surfaces for different the bridge types under consideration. Subsequent fitting of appropriate statistical distribution functions, often from the extreme value family, and following the statistical extrapolation of obtained load effects to the required return period, provides characteristic values representative for the chosen time frame. There is currently no consensus about the appropriate return period of the return values and in absence of such, it is suggested to rely on nationally or internationally specified target reliability values that essentially specify the probability of non-exceedance that can be then tied to both design and characteristic values.

Key parameters to be observed in either technique are the inter-vehicle gap modelling and the governing type of traffic loading, where the type is largely driven by the selected dynamic amplification model. The importance of vehicle spacing dwells in correctly capturing the events that can be contributed to multiple vehicles present in each of the individual lane considered; multiple vehicles in single and adjacent lanes causing a critical loading and maximizing the load effect are therefore captured. The simplest form of capturing side-by-side events for the derivation of a load model is the consideration of two-lane opposite direction traffic. At the same time, the transition from free-flow to congested traffic, with congestion defined by the slow speed and reduced gaps between vehicles, coupled with the appropriate dynamic amplification of the free flow determines the governing form of traffic on the considered bridges. Short spans are governed by single vehicle events and the dynamic amplification is dominant there, but medium span length bridges receive a mix of vehicle events along with reduced dynamic interaction and therefore care is warranted in deciding on scenarios driving the development of the load model. The composite distribution approach along with the highlighted suggestions in previous sections point towards a careful consideration of the governing form of traffic by a cautious evaluation of both gaps and dynamic effects.



---

### 3 Considerations for developing a load model

It is clear from Chapter 2 that a traffic load model is data driven, especially when considering an approach based on measured WIM data. It should also be evident from the described approach of obtaining load effects, that there will be a variety of results depending on the source of the data. The source in this case is a measuring station that is providing very localised information about a traffic flow at a discrete point in the road network. This naturally can carry a bias and it is often unknown how well the measured data at a certain location compares to the overall situation. Depending on the number of WIM stations in a given network complex approaches can be developed for the quantification of the statistical build-up of the traffic (Morales-Napoles & Steenbergen, 2014). Given the fact that widespread WIM stations are still not available this work concentrates on the situation with a few stations available and discusses the development of a load model based on a localized source, yet covering a region.

#### 3.1 General Method for a single lane NML

A traffic load in the design norms that adopted the semi-probabilistic approach is a stand-alone model, that represents the extreme action due to the passing vehicles. Hence, this model, often called a Notional Load Model (NML) is a set of loads that replicate the extreme load effects of based on real traffic streams when applied to a structural model. A well-developed NML balances the need for simplicity with an attempt to provide close approximations of target characteristic load effects for the range of spans and influence lines considered – hence covering a various structure for the future design stages. The load model should perform well at a critical scenario – meaning at a scenario where for instance the bending moment at a certain span length needs to be match for the stock of typical bridges. Even though the load model might perform well at the single occurrence, it may result in excess safety for other situations – meaning other load effects and other span lengths. Important to note is, that since the WIM data are mostly collected at a single lane, the NML then also aims initially to replicate the extremes for a single lane on the bridge, the extrapolation of such model is to multiple lanes is discussed in Section 3.2 as it is not a trivial scaling exercise. At the same time opposite to the notion of a load model fitting a bridge stock, NMLs can be developed for a single bridge and a single measured traffic stream – sometimes known as a Bridge Specific Allowable Load Limit (BSALL) – then the data and structural system will be those for that bridge, but more commonly are developed to apply to a larger number of bridges across a region or specific road network for which is relevant data available.

While there is an inevitable conservatism tied to this pragmatism of selecting a NML for the critical scenario of a bridge stock, at the design stage, the cost of the initial investment is easily offset by the gained additional safety margin for the rest of the situations. Meaning that even though load model is conservative for other load effects and span lengths, it is calibrated to perform well at the critical point hence the remainder of scenarios gains an increases safety margin. In contrast to design, for the assessment of existing structures, knowledge of the actual traffic loads should be exploited wherever possible, and the conservatism should be offset by actual available data, discussed in Chapter 5 and 6.

To start, the target values of characteristic load effect that the NML should replicate must be determined. To do this, the range of applicability of the model should be defined. This will determine the traffic data that is required, and influence lines for which the characteristic load effects should be determined. Commonly, the NML is aimed at all of the bridges over a large geographic region, a suite of influence lines, span lengths, and the most onerous traffic data coming from a critical WIM station for that region should be determined. Critical station is judged by the number of recorded heavy vehicles, that is an absolute number or frequency of recorded gross vehicle weights. For example, in the development of the Eurocode, the model was based on 1986 traffic data from the Auxerre site in France, which had exhibited the highest frequency of heavy loads in comparison to the other European stations (Hanswille & Sedlacek, 2007). The span lengths of  $L = \{5, 10, 20, 50, 100, 200\}$  m were considered for each of the influence lines given in Table 3 (Bruls et al., 1996). Single station was considered as a simplification and to overcome the difficulties with the computational power at the time. Yet, more prudent approach is the evaluation of actual load effects from a multiple WIM station in the region, should they be available. It is difficult to judge whether a chosen station is critical based on solely GVW frequency or maximum recorded weight as there is no direct link between the vehicle weight and extrapolated load effects. Multiple WIM stations will enable to provide an envelope of load effects representative for the region for a range of load effects and a range of span lengths. To summarize, with the available data and following the computational and statistical procedures outlined in the previous sections, the target characteristic values of load effects are then found for each necessary scenario.

Hence, the typical Notional Load Models are defined to replicate the target characteristic values of load effect across all span lengths and influence lines considered. Almost all NMLs world-wide use a combination of:

- Point loads
- Uniformly distributed loading

It is in fact necessary to combine the two different types of loads, as it is illustrated in the further Section 3.2 in order to capture the different internal forces. The point loads are primarily needed to replicate the shear force occurring due to heavy axles of vehicles, but it is complemented by the uniform load to capture the bending moments correctly. It is an optimization exercise where many possible combinations exist, and the choice is between simplicity of the adopted model and the ability to replicate the extreme load effects across various scenarios. Therefore, when selecting the point loads of the NML, the primary purpose of a NML is not to represent a typical vehicle in the region, but to replicate the characteristic load effects for a wide range of bridge lengths and influence lines. Many code developers do use realistic vehicle silhouettes (e.g. The US's HL-93, Australia's SM1600, China's D60). Since, of course, the NML will prescribe very high values of loading, it can be argued that realistic vehicle silhouettes can mislead road freight operators in the allowable forms of truck traffic on the road network. More abstract NMLs, such as the Eurocode's two-axle bogey or the older BS5400 single-axle knife-edge load, do not have

this risk of misleading road freight operators. However, a controlling factor in the selection of the number and distribution of the point loads can be the historical legacy of previous design codes and what practitioners in the region are familiar with.

The uniformly distributed load part of the load model is often found to reduce in required intensity with increasing span. This is because the probability of multiple trucks exceeding a specified weight simultaneously in the same lane reduces as the number of trucks increases with the increased span length. Hence, for long convoys of trucks, the average weight of each truck tends to reduce with the increasing convoy length. Some standards allow for this with a uniform loading of variable intensity. For example, the intensity of the uniform loading in the South African TMH-7 NA load model is illustrated in Figure 15. While such specification of loading is more accurate for longer loaded lengths, it is more complex to use (Lenner et al., 2017). As a result, most standards, such as AASHTO and the Eurocode, use a uniform loading of fixed intensity which tend to be conservative for longer spans, but have the advantage of simplified application.

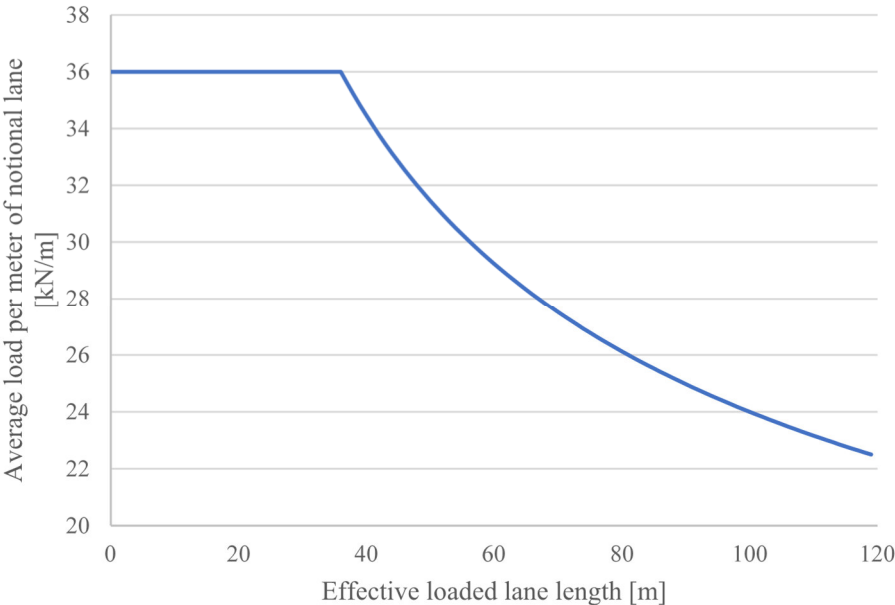


Figure 15: UDL as a function of loaded lane length (Committee of State Road Authorities (CSRA), 1991).

For sites with multiple lanes, it is typical to initially develop the NML for the lane corresponding to the heaviest traffic (Bruls et al., 1996). For the remaining lanes, the NML point load and UDL values tend to be reduced with increasing number of lanes due to the reduced probability of multiple heavy vehicles simultaneously occupying adjacent lanes (van der Spuy et al., 2019), refer further to Section 3.3.

### 3.1.1 Example application of NML

To illustrate in a simplified form why the two forms of loading are necessary and also to showcase the decision for setting appropriate values, this section refers to a work summarized by a paper (van der

Spuy & Lenner, 2019) and to the doctoral thesis of (van der Spuy, 2020) accomplished under the supervision of the author.

The Roosboom WIM station has been utilized in this research as it was previously identified as a heavy station (Lenner et al., 2017) and WIM data were readily available. In fact, the station is in operation from 2000 producing reliable data. For the study showcased here by (van der Spuy & Lenner, 2019) seven years of combined traffic from 2010 to 2016 were utilized, totaling of 12.5 million vehicles in both slow lane directions combined. Following already highlighted procedures for cleaning, filtering, and calibrating data along with static calculations, load effects were obtained as per Chapter 2. Weibull distribution with the upper bound was initially examined to arrive at extreme values corresponding to 5% exceedance in 50 years for sagging, hogging and shear effect as summarized in Table 5. This assumption made during writing this particular paper was later superseded by a more appropriate fit of a censored GEV distribution (van der Spuy, 2020). This generalised distribution of extreme values fits the tail of the calculated load effects regardless of the family and results in slightly different values, refer to Section 3.3.

Table 5: Weibull extrapolated load effects from Roosboom station 2010-2016 (van der Spuy & Lenner, 2019)

<b>Span Length (m)</b>	<b>Hogging (kNm)</b>	<b>Sagging (kNm)</b>	<b>Shear (kN)</b>
5	239	370	337
10	738	1110	466
15	1521	1861	530
20	2096	2805	630
25	2472	3899	718
30	2931	5056	785
35	3650	6305	836
40	4271	7644	876
45	5197	9042	907
50	6391	10,476	933

With the identified span lengths from 5m to 50m and extrapolated internal forces, the ground was set to propose a NML that would represent these effects. To further simplify the situation in arriving in a preliminary load model, it was decided to directly extrapolate the measured axle loads to represent a unique value of a point load, or point loads, that would be complemented by the UDL. This decision enabled to some extent replicate extreme axle loads on the roads, but mainly allowed simplification of the optimisation problem where both point loads and uniformly distributed loads are unknown and theoretically any combination of the two can lead to the representative extreme load effect. Hence in the



published paper, measured axles loads at the Roosboom station were extrapolated to 5% exceedance in 50 years assuming a Weibull distribution and produced a 158 kN axle load.

The decision that remained was about the actual configuration of the load model. This is usually done through ad hoc and iterative approaches, and commonly considers the pre-existing load model configuration in the jurisdiction. Should the load model should be composed of a single knife edge load such as current TMH-7 in South Africa, or a double axle such as LM1 per EN1991-2 or perhaps a silhouette of a vehicle such as HL-93 in AASHTO was in question. To answer that, the decision was to select a suit of point loads that would be matched by a constant UDL and be as close as possible to the extreme values.

The axle spacings parameters according to the normal distribution as evaluated by (Lenner et al., 2017) at the Roosboom station show that for both vehicle types, the multi-axle single trailer, and multi-axle multi-trailer the mean value is at minimum 1.34m and 1.35m respectively. This closely resembles the value adopted in EN LM1, which is 1.20m between the tandems.

Table 6: Axle spacing at Roosboom 2010-2016 – normal distribution parameters in [m] (Lenner et al., 2017)

Type	Axle 1-2		Axle 2-3		Axle 3-4		Axle 4-5		Axle 5-6		Axle 6-7	
	$\mu$	$\sigma$	$\mu$	$\sigma$	$\mu$	$\sigma$	$\mu$	$\sigma$	$\mu$	$\sigma$	$\mu$	$\sigma$
Multi-axle single trailer	3.48	0.87	2.22	2.24	6.63	2.02	1.41	0.58	1.34	0.06	--	--
Multi-axle multi trailer	3.26	0.83	1.48	0.85	5.86	1.15	1.51	0.98	5.48	1.35	1.46	0.60

Considering the extrapolated 160 kN axle load and the limiting EN axle spacing value of 1.2m, the configurations of axle groups chosen for the derivation of UDL are shown in Figure 16.

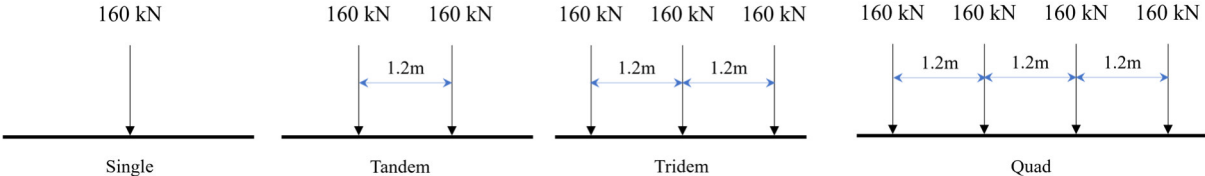


Figure 16: Single, tandem, tridem and quad axle groups, each with 160 kN axle weight

The final step was then the selection of an appropriate uniform load intensity, that if combined with any of the axle configuration from Figure 16, would reflect the necessary extrapolated load effect values provided in Table 5. To illustrate the decision-making process, necessary magnitude of UDL is plotted for bending moments and shears as a function of span length in Figure 17.

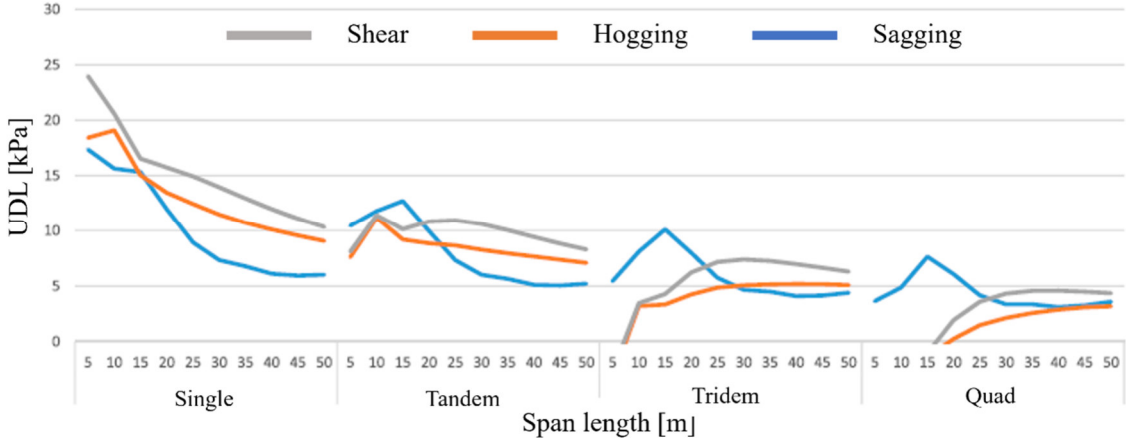


Figure 17: Required UDL for different axle group (van der Spuy & Lenner, 2019)

As can be expected the value of UDL decreases as the number of axles increase. A single axle configuration results in a maximum required distributed load of 24 kPa at 5 m span length and a minimum required of 6 kPa at 50 m span length. A distributed load of 24 kPa results in a very conservative design for longer span lengths. Adopting a single axle as currently mandated by TMH-7 loading, therefore, results in very conservative design of most bridges and is not advisable from an economical perspective. The results further show that current provisions in the TMH-7 NA model (as shown in Figure 15) for variable distributed loading are in fact correct with the larger span lengths requiring lower intensity of the UDL. As the number of axles increases the difference between the highest required and lowest required distributed load decreases, leading to a more economical design. From Figure 17, tridem and the quad axle configurations prove to be more suitable for longer span lengths in comparison to the single and double axle configurations. Although the required UDL decreases with an increase in span length the adoption of a constant value is not unreasonable as the ratio of dead load to live load for bridges increases at larger span lengths. Structures with long spans are dominated by dead loads, therefore, a slightly conservative variable load model for longer spans is not of a great concern as it provides a higher safety margin and low additional cost. It is therefore proposed to accept a constant UDL for the entire loaded length in order to simplify the load model. The decision to adopt a particular axle configuration can be now made, leading to either a tridem or a quad configuration.

Later work of (van der Spuy, 2020) with more refined GEV fitting proved that the extreme values were slightly different to those currently shown in Figure 17, and the calculated difference between the maximum and minimum UDL required to match the extreme values favoured the decision for a tridem axle configuration of 160 kN complemented by a UDL of 13 kPa, or basically a 40 kN/m. This is still conservative as discussed previously, as it only matches a single situation of hogging bending moment at 15m. Economic optimisation where the entire stock of bridges is considered would likely favour a decision of a lower UDL given that the span lengths are 15m at higher probability of failure, but overall

---

economic optimum is achieved. This point is important and must be investigated in future, when optimisation of NML is required.

A single lane traffic load model is typically calibrated for the slow, heavy lane as it was just shown. Loading in each of the additional notional lanes on a bridge deck is typically reduced by a factor less than one. This factor normally decreases even further as the number of the lanes on the bridge deck increases – hence the multiple lane factors need to be developed.

### **3.2 Multiple lane factors**

For multi-lane traffic, the critical loading event for a short to medium span bridge can involve extreme vehicles in one or more lanes. The main factor determining which case governs for the element under consideration is the transverse stiffness of the bridge. For example, a solid deck has a relatively deep slab and correspondingly high transverse stiffness. This results in a high degree of load sharing between lanes and a greater contribution to load effects from traffic in lanes remote from the location under investigation. It follows that maximum load effects for design tend to be due to adjacent heavy vehicles in multiple lanes rather than a single extreme vehicle. A beam-and-slab bridge, on the other hand, with only a thin slab of low stiffness connecting the beams exhibits limited lateral distribution. This results in much lower load sharing between lanes and the governing load case is more likely to involve a single extreme vehicle.

There have been many studies on lateral (or sometimes girder) distribution factors that quantify the contribution of loading in a lane to the load effect under consideration. The objective is to quantify load effects using a simple beam analysis (or influence line) for the most critical lane and scaling this result to consider the traffic in other lanes. A simple approach defines a component distribution factor as the LE caused by traffic in a given lane, expressed as a portion of the total (maximum) load effect value. The components for each lane should sum to unity. Component distribution factors can be found by passing a vehicle or axle loading along each lane and using a Finite Element model to calculate the resulting load effect. The resulting factors will depend on the vehicle chosen for the study but are not particularly sensitive to it. This approach is effectively assuming that influence line for any specified lane can be found by scaling the influence line for the most critical lane.

An interesting distribution factor approach is the *S/D* concept developed for the AASHTO code, evolving from (Newmark, 1948) through (Sanders & Elleby, 1970) to (Zokaie et al., 1991). Despite the range of approaches to lateral distribution factors, the essential idea is to eliminate the need to use an influence surface (or Grillage/Finite Element model) to determine LE.

(Zhou et al., 2016) describe some flaws with prevalent methods and present a formal general model for the problem, using a multivariate extreme value approach to quantify the MLFs appropriate for a given traffic stream, load effect, transverse distribution, and return period. This approach uses copulas to model the correlations at different probabilities between the different marginal distributions of each lane.

The approach is complex, but rational, and yields site-specific MLFs which are less conservative than those in codes, and so suitable for important bridges.

As discussed, notional load models used in standards typically use a combination of a uniformly distributed load and a set of point loads. Some standards use arbitrary set of point loads, other prefer that they represent a notional vehicle, bogie or tandem. The most critical or principal lane for the specified LE is subject to a lane load model. Portions of that principal lane loading are typically applied in other lanes to allow for the possibility of an extreme multi-lane loading event. These factors are distinct from the component distribution factors mentioned previously. But in essence, the load model derivation for loading on more than a single lane is achieved by the modification of the notional load model specified for the heavy slow lane.

### **3.2.1 Multiple lane factor independent of the structural solution**

To avoid the necessity to evaluate transverse stiffness and load sharing between structural components in specifying a load model, an approach based on multiple lane WIM data was developed by the author and a student under supervision to allow for considerations of extreme multi-vehicle events of desired non-exceedance (van der Spuy et al., 2019). Permutations of load effects due to recorded WIM data in different individual lanes allowing observation of side-by-side events in any number of lanes provide a basis for extrapolation and specification of multiple lane presence factors; an approach suited for the derivation of load models for design. Basically, a method is proposed to determine MLFs based on multiple lane WIM data by considering extreme value analysis of concurrent load effects in more than one lane without prior knowledge of the superstructure type. The method maximises the characteristic load in any one lane together with the characteristic concurrent total load and does not need to consider dependence and multivariate extremes as proposed in the method by (Zhou et al., 2018). Although the method is applied to free-flowing traffic in this paper, it can also be applied to congested traffic and considers the possibility of having more than one vehicle in any one lane. The method is thus suitable to any span length and can be extended to any number of lanes. By not relying on the superstructure type, the method is well suited to the development of a design code as it results in a single set of MLFs. In deriving the MLFs, all permutations of combinations of all lanes are investigated which makes the method suitable for the concept of applying load in the most adverse manner.

To apply the proposed method, it is necessary to have either multiple lane recorded WIM data or congested traffic loading data. In order to assess the ratio of load effects in adjacent lanes at extreme values it is necessary to predict extreme events at long return periods. The method proposed here is applicable to any number  $N$  of lanes, provided that  $N$  lanes of load effect data are available. It is necessary to ensure that WIM data is cleaned and well calibrated, as set out in Chapter 2.

The first step in the proposed methodology is to calculate a time history of load effects for each of  $N$  lanes by applying WIM data or congested traffic data to influence lines of various lengths, again as

discussed in Chapter 2. This is done for each load effect under consideration and for each span length to be considered for all  $N$  lanes. In this particular work, the load effects (LEs) considered are hogging moments for two span structures and sagging moments and shear for single span structures. Span lengths of interest depend on a specific code or assessment situation, but it is proposed to start at a span length of 10 m and to increase the span length in increments of 10 m or less. It is necessary to create convoys of vehicles from WIM data in order to capture the multiple vehicle occurrence in any single lane or adjacent lanes. The WIM file provides dates, time stamps, speed, axle weights and axle spacing of vehicles for each recorded lane. By using the time stamps and speed of each vehicle, it is possible to calculate the distance between vehicles. By calculating these distances, it is possible to assemble convoys of vehicles in each lane, which is essentially a spatial distribution of axle loads (point loads) spaced according to axle spacing and headways. As no acceleration or deceleration information is obtained from the WIM data, the relative position of vehicles in adjacent lanes becomes inaccurate if the convoys are too long. For this reason, shorter convoys can be built with only three following vehicles in any one lane; three vehicles are sufficient for short to medium span length bridges. The LEs in any lane for any span length can then be calculated as a function of time by moving the convoys over influence lines. To capture the relative position of vehicles it is suggested to have a short time increment (Enright, 2010b). By studying the load effect time history for each lane, it is possible to determine concurrent lane LEs at any time  $t$ .

WIM data is generally not available for periods equal to the required return period stipulated by a code. It is therefore necessary to extrapolate the calculated load effects to a chosen return period  $T$ . In this work a 5 % probability of exceedance is assumed in a 50-year reference period which is also used in the Eurocodes and the South African building design codes.

Extreme value theory is used in this study with monthly block maxima load effects; however, the procedure is formulated for any block size. Several studies have shown that bridge traffic load effects may be described by the Weibull extreme value distribution. However, to account for the possibility that the coincident lane load effects could approach the Gumbel extreme value distribution, it is proposed to instead use the Generalised Extreme Value (GEV) distribution. The GEV distribution does not require a predetermined choice of the distribution family from one of the Weibull, Gumbel or Fréchet extreme value distributions.

$$G(z) = \exp \left\{ - \left[ 1 + \xi \left( \frac{z - \mu}{\sigma} \right) \right]^{-1/\xi} \right\} \quad \text{Equation 18}$$

This equation describes the cumulative distribution function (CDF) of the GEV distribution for a random variable  $Z$  with  $\mu$  being the location parameter,  $\sigma$  the scale parameter and  $\xi$  the shape parameter. The shape parameter describes the tail of the underlying data set and is negative for a Weibull (bounded) extreme value distribution and positive for a Fréchet (unbounded) extreme value distribution. The Gumbel distribution is a special case of the GEV distribution with  $\xi = 0$  (Coles, 2001). Due to the

inherent bounded nature of traffic loading it is not unreasonable to allow only shape factors smaller than or equal to zero.

### Procedure

Considering  $N$  lanes on which independent load effect data is available over a period of time, the method treats all load effects and span lengths identically and can be used for any span length or skew decks, provided that the load effects can be calculated for each. In this work the procedure is applied as an example to span lengths between 10 m and 50 m in 10 m increments denoted by the set  $L \{10, 20, 30, 40, 50\}$ . It was found that that monthly blocks are sufficient to capture heavy vehicle concurrent multiple lane presence events without violating the independent and identically distributed (*iid*) condition of extreme value theory. Monthly blocks also maintain a good fit to the GEV distribution (Zhou et al., 2018). It is therefore necessary to have long run WIM data in order to have sufficient number of blocks so that a distribution can be fitted and that the extrapolation yields reasonable results.

The load effect data can be blocked into  $B$  consecutive monthly blocks and the maximum of each lane in every block can be calculated for each span length in the set. Denoting  $M_{n;b;L}$  as the maximum of the load effect data of lane  $n$  for block  $b$ , where  $n = 1, \dots, N$  and  $b = 1, \dots, B$  and  $L$  is the span length under consideration. This yields a sequence of monthly block maxima given by  $M_{n;b;L}$ . The Fisher-Tippet-Gnedenko theorem of extreme value theory and theorem 3.1.1 in (Coles, 2001) holds true for each lane sequence of block maxima, therefore the distribution of  $M_{n;b;L}$  can be approximated by a GEV distribution for every  $n = 1, \dots, N$  and each  $L$  in the set. The parameters of each GEV distribution are estimated by maximum likelihood using lane  $n$ 's monthly block maxima data.

Let  $\nu$  be the number of blocks within a one-year period, for monthly maxima thus  $\nu = 12$ . This leads to an exceedance probability,  $p$ , in the reference period given by Equation 19 with the probability of non-exceedance being  $1 - p$ .

$$p = \frac{1}{T\nu} \quad \text{Equation 19}$$

If each lane is evaluated individually at  $p$ , the return level for lane  $n$  is denoted by  $m_{n;p;L}$  i.e. the  $(1 - p)$ -th quantile of the GEV distribution fitted to the  $n$  lane block maxima for all  $L$ . Parameters for each lane  $n$  are estimated by maximum likelihood.

$$m_{n;p;L} = \mu_{n;L} + [\sigma_{n;L}((-\ln(1 - p))^{-\xi_{n;L}} - 1)]/\xi_{n;L} \quad \text{Equation 20}$$

From the  $N$  quantiles  $m_{n;p;L}$ , the lane with the largest quantile is designated as Lane 1. This is the reference value of a single lane loading scenario and is the extrapolated load effect which is used to calibrate a load model for the lane experiencing the maximum load effect. For Lane 1 the generic MLF is then given by

$$MLF_{1;p;L} = \frac{m_{1;p;L}}{m_{1;p;L}} = 1 \quad \text{Equation 21}$$

---

The single lane MLF is the maximum over all considered span lengths for all load effects.

Any two lanes can be considered by denoting them as  $r$  and  $s$  with  $1 \leq r < s \leq N$ .

Considering the maximum,  $M_{r+s;b;L}$ , of the sum for each block  $b$ , another sequence of block maxima data  $M_{r+s;b;L}^B$  is created consisting of the maximum concurrent LE sum of lanes  $r$  and  $s$  during each block  $b$ . Theorem 3.1.1 in (Coles, 2001) applied to this sequence leads to a GEV distribution,  $GEV_{r+s;L}$ , with parameters again estimated by maximum likelihood.

Denoting  $(1-p)$ -th quantile of  $GEV_{r+s;L}$  by  $m_{r+s;L}$  and carrying out the analysis for all  $\binom{N}{2}$  possible two lane combinations, leads to  $m_{2;L}^*$  for the combined maximum of these for each span length and load effect.

The load effect in the second lane,  $m_{2;L}$ , is obtained by subtracting the load effect of Lane 1 from the combined maximum  $m_{2;L}^*$ . The MLF for the lane with the second highest loading is then given by Equation 22:

$$MLF_{2;L} \equiv \frac{m_{2;L}}{m_{1;L}} \text{ per load effect} \quad \text{Equation 22}$$

This process is carried out over all span lengths for hogging, sagging and shear and the MLF for the second lane calculated for the second lane,  $MLF_{2;L}$ , as the maximum over these.

Iterating this process it follows that for any  $1 \leq n \leq N$  the  $n$  lane load effect is obtained as

$$m_{n;L} = m_{n;L}^* - m_{1;L} \sum_{i=1}^{n-1} MLF_{n-i}; \text{ for } 1 \leq n \leq N \text{ with } m_{1;L}^* = m_{1;L} \quad \text{Equation 23}$$

And in this case the MLF factor can be specifically determined according to the following relationship:

$$MLF_{n;L} \equiv \frac{m_{n;L}}{m_{1;L}} \quad \text{Equation 24}$$

The  $n$ -th lane MLF,  $MLF_n$ , can be determined by the maximum over all span lengths and load effects.

The described procedure then results in a set of multiple lane presence factors derived for all considered span lengths and load effects. As the maximum MLF factor is retained for each individual lane, the set is suitable for application in a design code. All permutations are considered, which effectively means the heaviest lane (MLF = 1) can be applied in any position transversely and subsequent lanes with lower MLF factors can be applied in sequence to achieve the most adverse effect.

### 3.2.2 Example Application with WIM data from South Africa

The proposed method is illustrated for a WIM site at Kilner Park on National Route 1 in the Gauteng Province of South Africa. The site has four lanes instrumented (two in each direction) as shown in *Fig. 1*. The time stamp resolution at this site is 0.01 s, however to reduce computational effort 0.02 s was used as an increment for the LE calculation. Three years of data were recorded from 2015 to 2017 and

cleaned, filtered and calibrated according to procedure in Chapter 2. The three years are deemed to be sufficient and yield enough blocks. Although this example illustrates free flowing traffic in opposing directions, the same procedure applies if all four lanes are recorded in the same direction or if congested traffic load effects are used, since the procedure requires only a spatial distribution of the recorded axle loads.

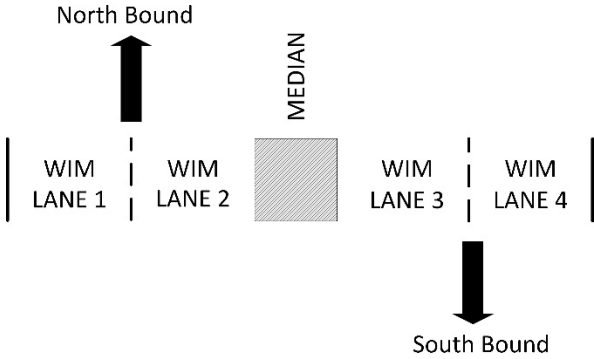


Figure 18: WIM station at Kilner Park, South Africa

In the here presented example, sets of monthly block maxima data were tested and shown to fit the GEV distribution well. To illustrate this, Figure 19 shows a quantile plot for the monthly maxima hogging moments in Lane 1. Adherence of the measured data to a straight line confirms that the GEV distribution is a suitable fit to the monthly maxima and that the data can be considered to be sufficiently *iid*.

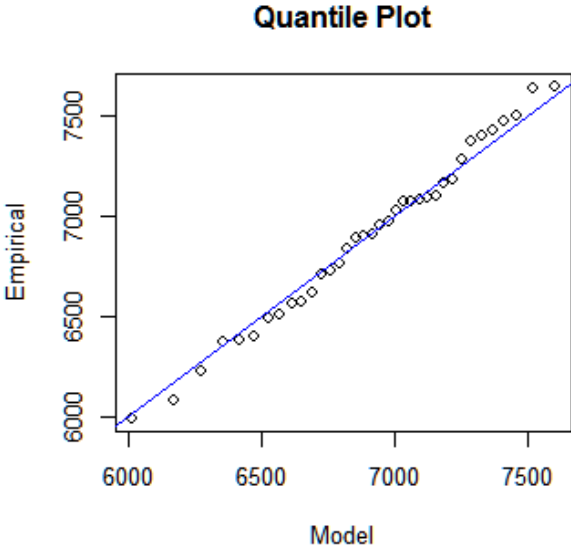


Figure 19: Quantile plot for Lane 1 monthly maximum hogging moments

The comprehensive results of extrapolated LE values for each lane equipped with WIM sensor can be found in (van der Spuy et al., 2019) , Table 7 provides the results of extrapolation for a single lane load effects considering just the 40m span length as an example in this work. The bold value shows the recorded maximum for each LE.



What is more interesting to report here is any permutations of combined lanes and extrapolated combined monthly maxima for each load effect – basically providing a characteristic load effect for any combination of lanes loaded simultaneously. To illustrate how to achieve a MLF in such situation results of two and three combined lanes are discussed in detail here

Table 7: Extrapolated load effects for a single lane traffic

Span length L (m)	Lane no	Hogging (kNm)	Sagging (kNm)	Shear (kN)
40	1	2655	6194	606
	2	3065	5956	596
	3	<b>3096</b>	<b>6835</b>	633
	4	2870	6502	<b>723</b>

. The combined effects from the two simultaneously loaded lanes are shown in Table 8 for the example 40 span length – to reinforce the idea, it is not the combination of maxima, but a combination of load effects from simultaneous records from the WIM station that is extrapolated to the characteristic value. It is conservative at this stage to combine all the lanes in a manner that any combination can govern the global bending moment and hence omit the fact that a hypothetical combination of Lane 1 and 4 will not affect in particular the actual structural member in consideration as the two lanes are not adjacent – the point of this work is to develop a robust method for the calculation of MLF values without considering the structural type. However, the overall results shown in (van der Spuy et al., 2019) do point to the fact that a typical maximum value of combined lanes is reached from two adjacent lanes are considered.

Table 8: Extrapolated load effects for any two lanes combined

Span length L (m)	Lane no	Hogging (kNm)	Sagging (kNm)	Shear (kN)
40	1, 2	4195	8914	845
	1, 3	4031	9418	823
	1, 4	4040	8513	798
	2, 3	4049	8694	<b>887</b>
	2, 4	4480	<b>9527</b>	868
	3, 4	<b>5423</b>	8762	885

With the information about combined LEs, a MLF can be calculated for each LE at each considered span length. Considering the example values for the 40m span length and a hogging moment in this instance, it follows that the particular MLF value of 0.75 is obtained from the maximum value for a single lane:

$$m_{1;40} = \max \{2655, 3065, 3096, 2870\} = 3096 \text{ kNm}$$

And from the maximum value of the combined lanes

$$m_{2;40}^* = \max\{4195, 4031, 4040, 4049, 4480, 5423\} = 5423 \text{ kNm}$$

by calculating the  $MLF_2$  factor according to the following, where a load effect in lane two  $m_{2;40}$  is given by

$$m_{2;40} = m_{2;40}^* - m_{1;40}(MLF_1) = 5423 - 3096(1) = 2327 \text{ kNm}$$

and finally the MLF value for the hogging moment is determined as:

$$MLF_{2;40} = \frac{m_{2;40}}{m_{1;40}} = 0.752$$

Following the procedures highlighted for the calculation of MLF at 40m, the comprehensive results for all load effects and all considered span lengths are summarized in Table 9 as per (van der Spuy et al., 2019).

Table 9: MLF values for two lanes

Span length L (m)	$MLF_{2;hog}$	$MLF_{2;sag}$	$MLF_{2;shear}$
10	0.571	0.204	0.258
20	0.628	0.259	0.279
30	0.514	0.228	0.342
40	<b>0.752</b>	0.394	0.227
50	0.632	0.339	0.439

To further illustrate the application of the obtained data and to determine the MLF factor for a third lane, the procedure is applied in a very similar manner, only the permutation of three lanes is considered to provide a maximum as per Table 10.

Table 10: Extrapolated effects for any three lanes combined

Span length L (m)	Lane no	Hogging (kNm)	Sagging (kNm)	Shear (kN)
40	1,2,3	<b>6141</b>	10923	1026
	1,2,4	5481	<b>12496</b>	<b>1206</b>
	1,3,4	5453	11972	1126
	2,3,4	5430	11498	1140

Following the shown procedures, the  $MLF_3$  for hogging moment is calculated from the combined maxima of

$$m_{3;40}^* = \max\{6141, 5481, 5453, 5430\} = 6141 \text{ kNm}$$

the value for load effect in lane three only is given as

$$m_{3;40} = m_{3;40}^* - m_{1;40}(MLF_2) - m_{1;40}(MLF_1) = 6141 - 3096(0.752) - 3096(1) = 717 \text{ kNm}$$

resulting in:

$$MLF_{3;40} = \frac{m_{3;40}}{m_{1;40}} = 0.232$$

To achieve all the results for the three combined lanes, the same procedures are repeated for all LE and all span lengths. The actual results are summarized in Table 11, where it can be seen that the highest MLF is obtained at 50m for the hogging moment. The reported negative values in Table 11 imply that the characteristic concurrent two lane load effects are larger than that for the three lanes loaded simultaneously and therefore the MLF for those cases is taken effectively as zero.

Table 11: MLF values for three lanes

Span length L (m)	$MLF_{3;hog}$	$MLF_{3;sag}$	$MLF_{3;shear}$
10	-0.051	-0.286	-0.18
20	0.215	-0.282	0.046
30	0.052	-0.142	0.065
40	0.232	0.077	-0.083
50	<b>0.281</b>	-0.069	0.039

To finish the example with WIM data at Kilner Park providing measurements at all four lanes, the last combination and permutations of all four lanes is considered. As the procedures are the same, they are omitted for clarity and only the resulting MLF values are reported here, as summarized in Table 12. Again, the hogging moment at 50m governs as it provides the highest value of MLF.

Table 12: MLF values for four lanes

Span length L (m)	$MLF_{4;hog}$	$MLF_{4;sag}$	$MLF_{4;shear}$
10	-0.154	-0.73	-0.673
20	-0.035	-0.474	-0.231
30	0.017	-0.496	-0.405
40	0.006	-0.106	-0.331
50	<b>0.091</b>	-0.234	-0.088

A combination of the results yield distinctive MLF factors for each lane of 1.00, 0.75, 0.28 and 0.09 for lanes one, two, three and four respectively.

In this case of this data from Kilner Park, MLF values are driven by hogging moments for span lengths between 40 m and 50 m, and decrease rapidly with increased number of lanes. This is natural, as the influence line for the hogging moment is in fact twice the length of the influence line for sagging moments and shears and hence has a larger number of vehicles involved in the permutations of the possible lanes. Again, the structural response is not considered, as only the combination of the load effects drives the derivation of the MLF factors and it could be in fact considered as true for the global behaviour, but perhaps conservative during the analysis of individual structural members as it could combine load effects from lanes not adjacent to each other. Yet, the developed procedure does follow the notion of critical load pattern.

In order to provide a certain form of validation and to compare the here reported MLF values with international codes, load effects were calculated for the Eurocode LM1, Australian code and the AASHTO HL-93 code for hogging, sagging and shear for span lengths between 10 m and 50 m. The maximum ratios between load effects in adjacent lanes were calculated. The values from the AASHTO code were normalised for comparison as the code has a different philosophy for the multiple lane factors. Of the three here considered codes, the LM1 shows the largest reduction in MLFs with an increased number of loaded lanes, refer to Table 13. The Australian and AASHTO codes show high marginal factors even in the fourth loaded lane and beyond, which points to a fact that even at extreme event there are significant side-by-side events in all four lanes. It is worth noting that, although different methodologies were followed in the various codes, the MLF values are at least comparable and to some extent validate the proposed method. Further data from other sites are necessary to allow for a better comparison.

Table 13: Comparison of MLF values

Code	Lane Number			
	1	2	3	4
EN 1991-2	1.00	0.59	0.32	0.21
AS5100.2	1.00	0.80	0.40	0.40
AASHTO	1.00	0.83	0.71	0.54
This study	1.00	0.75	0.28	0.09

Although a single set of MLFs is desirable for a design code and in principle the proposed method can deliver the factors, a careful consideration of the provided values point to the fact that for LE other the hogging and even shorter span lengths, the MLF values could be in fact reduced which would be particularly suitable in the assessment scenario.

---

## 4 Special consideration for design and assessment

Design situation is fundamentally different to the assessment situation when the unknowns and uncertainty are incorporated in the design loads and design resistances, that is a general load model that corresponds to a spectrum of situations and structural systems is taken as a basis for dimensioning the structure composed of estimated materials and its resistance. The development of a traffic load model is shown in Chapter 3. Again, it is emphasized that when a design standard for new bridges is developed, a notional load model is specified to give reliable estimates of characteristic maximum load effects for a range of bridge types and spans. The reliability calibration of the load model intends to secure a minimum required performance over the lifetime of the structure by specifying a target reliability value  $\beta_i$ . This results in partial factors for the considered limit state that are applied to the derived characteristic load (Steenbergen & Vrouwenvelder, 2010). The safety calibration of the design load model is intended to be optimized for the entire range of structures (Rackwitz, 2000), it is therefore inevitable that some bridges will be more heavily loaded than others. From the optimization perspective, it is wasteful to have a load model that results in widely different levels of conservatism for each load effect, yet from the practical perspective, it is needed for the design engineers. Care must be therefore taken in the specification of the span lengths and load effects against which the model will be developed.

For the assessment scenario the situation changes, as a specific bridge is considered in comparison to the entire stock. The characteristic maximum load effects can be factored and used directly in a bridge safety assessment (Pérez Sifre & Lenner, 2019). In developing a site-specific load model, the primary goal is not to be conservative but rather to minimize the range of conservatism while maintaining reliability for the load effects and spans considered by observing the site traffic. For instance, the American HL-93 notional load model is intended to generate the 75-year return period characteristic load effect for ‘normal vehicular use of the bridge’. WIM data was used to calibrate the US design load model (Nowak, 1996) and NCHRP Report 683 details a method to adjust the US HL-93 model using site-specific WIM data to obtain a site-specific load model for design or assessment. The ability to adjust a model is useful – some roads are subject to much heavier vehicles than others and their bridges need greater load carrying capacity, while other bridges will see the characteristic load with a very low probability.

It is therefore possible and, in fact, deemed necessary to consider site specific loading when assessing a bridge to obtain a loading more representative of the situation and remove any unnecessary conservatism tied to the design load model. It was already seen in Chapter 3, that a calibration of a load model for a certain load effect and a certain span length along with conservative assumption of multiple lanes factors suits well the design situation but can be adjusted for the assessment. From that perspective, the process can be fundamentally divided in two approaches that are aligned with the semi-probabilistic format that is familiar to the design engineers:

- Adjustment of partial factors for both load and resistance
- Adjustment of the characteristic values

Task Group 1.3 of the IABSE has recently investigated the use of the adjusted partial factors for the assessment of existing reinforced concrete bridges, the author of this habilitation is a contributing member of the task group. It resulted in a paper accepted for publication (Orcesi et al., 2023) that applies the method, an extract is provided in the following Section 4.1.

#### 4.1 Investigating partial factors for the assessment of existing reinforced concrete bridges

In accordance with the partial factor format provided in (EN 1990, 2002), the design (or assessment) values of the basic variables for resistance parameters  $R_d$  and for action parameters  $E_d$  depend on their characteristic values  $R_k$  and  $E_k$  respectively, i.e. values associated to a prescribed probability level. Nominal values may be defined when the probabilistic distribution of a basic variable is unknown.

Characteristic or nominal values should always be verified and updated (if needed) in order to reflect the actual conditions of an existing bridge. The design (or assessment) values are then derived from the characteristic values by dividing or multiplying by appropriate partial factors:

$$R_d = \frac{R_k}{\gamma_M}; E_d = \gamma_F E_k \quad \text{Equation 25}$$

where  $\gamma_M$  and  $\gamma_F$  denote the partial factors of resistance and action effect parameters, respectively. The values of partial factors specified in the codes depend on the target reliability values of considered consequence classes. Fixed values of partial factors can be set and/or procedures for adjusting partial factors can be provided.

In general, adjusting partial factors is recommended for situations with high upgrade costs, high failure consequences or in situations with non-standard conditions (improved production or execution quality, detailed information about resistance or load effect parameters, etc.). Such adjustment is intended to overcome a degree of approximation inherently associated with the fixed values.

Partial factors for materials may be adjusted if prior information (e.g. background information from the time of construction) or results of new tests and measurements performed in the existing structure are available. When adjusting partial factors for materials, the following aspects may be considered:

- Often the increase/decrease in the coefficient of variation of the material or geometrical property leads to a significant increase/decrease of the material partial factor. This means that if the material coefficient of variation is greater than that assumed in the design of new structures, for a fixed value of the reliability index, the assessment partial factor could be greater than that assumed in the design and, thus, its adjustment is recommended.
- Statistical uncertainty related to the number of test results could influence the value of the partial factor. For instance, a lognormal distribution can usually be assumed for concrete compressive strength in the design of new structures (see e.g. (prEN 1992-1-1, 2021) and its background

document by (Muttoni, 2021)). However, for a low number of tests (e.g. lower than 30), correction factors should be applied (see e.g. (EN 1990, 2002) and (prEN 1992-1-1, 2021)); this would yield an increase of the partial factor for concrete when compared to the value obtained without accounting for the additional statistical uncertainty related to the number of test results. If geometrical uncertainties are included in the partial factor for the material property (see e.g. (prEN 1992-1-1, 2021) and (Muttoni, 2021)), its adjustment could benefit from e.g. in-situ measurements on the existing structure.

- Resistance model uncertainties are sometimes included in the partial factor for the material property (see e.g. (prEN 1992-1-1, 2021) and (Muttoni, 2021)). Thus, if resistance models for the design are adjusted or expanded in their scope to allow the assessment of existing structures or new resistance models are used to assess existing structures, the degree of uncertainty of the models should be quantified and the material factor should be adjusted accordingly.

Note that according to the present practice, two alternative approaches can be adopted to specify partial factors (focusing on material factors as an example):

1. Either by determining a  $\gamma_M$ -value (single partial factor) on the basis of the probabilistic model of resistance covering uncertainties in the relevant basic variables such as in the material property, decisive geometrical variable, and in resistance model uncertainties,
2. or by considering separate partial factors e.g. for the material property,  $\gamma_m$ , resistance model uncertainty,  $\gamma_{Rd1}$ , and geometrical variation,  $\gamma_{Rd2}$  (unless a reasonably conservative nominal value is defined).

The first approach is traditionally adopted for shear and torsion resistance of reinforced concrete members. It has been proposed for instance for columns under pure compression by (Moccia et al., 2021), for shear resistance by (Bairán & Casas, 2018) and for bond of reinforcement by (Blomfors et al., 2019), now being incorporated into (prEN 1992-1-1, 2021) for bending and compression (Muttoni, 2021). The second approach is generally adopted in current codes, e.g. (EN 1992-1-1, 2004), and it is traditionally applied in a non-linear FE analysis (Cervenka et al., 2018).

Considering variable actions and the example of an unfavourable road traffic load effect,  $\gamma_Q$  can be obtained as follows:

$$\gamma_Q = \frac{Q_d}{Q_k} = \frac{F_{Q,t_{ref}}^{-1}[\Phi(-\alpha_E\beta), t_{ref}]}{Q_k} \quad \text{Equation 26}$$

where  $Q_d$  and  $Q_k$  denote design (assessment) and characteristic values of the traffic load effect  $Q$ , respectively;  $F_{Q,t_{ref}}^{-1}(\cdot)$  is the inverse cumulative distribution function (CDF) of maxima of  $Q$  during a reference period  $t_{ref}$  for which a target reliability index  $\beta$  is specified;  $\Phi$  is the cumulative distribution function of the standardised normal variable; and  $\alpha_E$  is the sensitivity factor of the action effect.

When specifically considering the traffic action on bridges as the variable action, particular care needs to be devoted to the definition of the characteristic value. To obtain the characteristic value, or the distribution of the maxima  $Q$  during the reference period, the traffic characteristics may be based on Weigh-in-Motion (WIM) measurements for the desired route as discussed in Chapter 3. When such traffic measurements are available, either direct numerical simulations (O'Brien & Enright, 2011) or statistical extrapolation of load effects (Caprani, 2005; van der Spuy & Lenner, 2019) can determine the characteristic and design (assessment) values directly. That could in fact alleviate the need for the definition of a partial factor, but numerical simulations have been rarely used in practice until now as WIM data is scarcely available. Furthermore, the load effect model uncertainty needs to be taken into account.

In the absence of WIM data, the characteristic value is commonly not updated while the partial factor is determined only by taking into account the chosen reference period and the target reliability  $\beta$  as specified in Section 2.4. Recently, an approach for the reduction of characteristic values in absence of WIM data was proposed (Perez Sifre & Lenner, 2021). The method is based on the readily available basic traffic counts. It may be helpful during the assessment situation when it is desirable to couple the reduced partial factor with the reduced characteristic values and avoid unnecessarily conservative choices regarding traffic load effects. It is particularly attractive for roads with very little heavy traffic.

While detailed discussion on selecting a reference period is beyond the scope of this section, it is interesting to note that the draft MC 2020 recommends the use of an annual reference period for assessment, mainly based on the following reasons:

Changing a reference period from e.g. 50 years to 1 year decreases the scatter of  $\beta$ -levels for different load ratios and fixed sensitivity factors (Meinen & Steenbergen, 2018).

- 1) Target levels do not need to be recalculated for existing structures assessed under different reference periods (often taken equal to the desired remaining service life).
- 2) An annual format is more consistent with regulations and acceptance criteria related to lifetime safety.
- 3) There is no need for averaging of human risks over longer periods. Human safety criteria are commonly defined based on an annual risk. Consideration of e.g. a 50-year reference period may result in the situation when human safety risks averaged over 50 years seem to be acceptable while actual annual risks may be initially low and increase above acceptable limits at the end of service life; for instance, due to excessive degradation.
- 4) An annual format is more suitable for rapid deterioration e.g. due to fatigue or corrosion – averaging over e.g. 50 years makes little sense when failure is likely in the last few years of the



---

considered lifetime, in which case the interpretation of a “generalized” failure probability over a reference period of 50 years becomes difficult to interpret.

The annual target reliability index should be fulfilled in each year of the service life of the structure. When the remaining service life of the existing structure is not specified, the annual target reliability index can then be used for a check until a subsequent re-assessment or the service life can be defined as a time instant after which the reliability criteria are no longer satisfied.

Further, changing the reference period from 50 years to 1 year requires adjusting the commonly applied sensitivity factors (EN 1990, 2002). These are predominantly proportionally dependent on coefficients of variation (COV) of basic variables. As the extreme value theory dictates that the COV of annual maxima of a variable action is larger than the COV of 50-year maxima, it follows that  $\alpha_{Q,1} > \alpha_{Q,50}$ . For standardisation purposes, it might be considered that  $\alpha_{E,1} > \alpha_{E,50}$  and  $\alpha_{R,1} < \alpha_{R,50}$ . (Meinen & Steenbergen, 2018) recommended to change  $\alpha_{R,50} = 0.8$  and  $\alpha_{E,50} = -0.7$  for a 50-year reference period to  $\alpha_{R,1} = 0.7$  and  $\alpha_{E,1} = -0.8$  for the 1-year reference period.

## **4.2 Adjustment of characteristic load value**

Several codes and research projects have implemented guidelines to account for the specific issue of the assessment of existing bridges. Modified design traffic load models, reduction of reference periods, lower safety levels and recalibrated partial factors are considered in the latest publications concerned with the load side of the issue (Allaix et al., 2016; BRIME, 2001; CAN/CSA-S6-06, 2006; Danish Road Directorate, 2004; ISO 2394, 2015; NEN8700, 2011). However, the use of site traffic conditions for the estimation of the load effects at a specific site is yet to be implemented in most of the codes or the application requires the use of extensive traffic data (Bailey, 1996), which may not be available. Other proposed methods are difficult to generalise and apply to other locations due to their simplistic and site-specific nature (ARCHES, 2009; Moses & Ghosn, 1985) or the methodology for the derivation of some factors presents shortcomings that could be potentially addressed (AASHTO LRFR, 2003). In contrast, the recently published methodology for site load factor approach (Pérez Sifre & Lenner, 2019) presents an opportunity to adjust static design traffic load models by making only use of simple traffic descriptors being observed on site. The advantage of this approach is precisely the easily obtainable traffic parameters that do not necessitate any instrumentations, such as Weigh-in-Motion at the site.

### **4.2.1 Example application with WIM data from South Africa**

In this section, a summary of the authors contribution to the development of site-specific load models based on simple traffic descriptors is summarized as per (Perez Sifre & Lenner, 2021) and compiled in a doctoral thesis under the supervision of the author (Pérez Sifre, 2020). It extends the proposed of site load-factor framework (Pérez Sifre & Lenner, 2019) initially developed for one lane traffic to include two lanes of truck traffic. The initial study was aimed at finding correlations between load effects and easily obtainable traffic descriptors such as average daily truck traffic and percentage of long vehicles

that are used to modify the design traffic load model. As a first step, a robust Monte Carlo simulation technique was proposed by using bivariate copula functions to account for the multivariate dependence between gross vehicle weight and axle loads. This method was validated by the comparison of generated and measured data.

Such routine enabled the generation of all the artificial traffic flows necessary to assess the influence of traffic characteristics on the extrapolated load effects. The second objective was to establish design load reduction factors – basically introducing straightforward reduction factors of the design load model based on simple, easily obtainable traffic descriptor. The results exhibited that an assessment traffic load model based on basic traffic descriptors is viable for the evaluation of existing bridges, hence a follow up study (Perez Sifre & Lenner, 2021) was accomplished to systematically account for all the uncertainty. These uncertainties are crucial for the overall calibration of the partial factors used in the semi-probabilistic context. A final reliability verification of the proposed approach and layering of the reduction factors is included in this work to ascertain that the safety levels defined in the code of reference are achieved (Perez Sifre & Lenner, 2021). The results are presented here.

The calculations in the mentioned studies were again based on the data collected in South Africa, same data from Roosboom station as used in Section 3.1.1. Yet any suitable traffic data collected anywhere can be used within the proposed framework. The developed procedure aims to deliver a general concept that is readily extrapolated to other regions. The focus was on sagging moments of single span bridges, shear forces over a support of single span bridges and hogging moments over the central support on double span bridges (where the total length of the continuous bridge is twice its span length). The complex dynamic amplification due to the interaction vehicle-bridge was not taken into account at this stage, as a different study by (Meyer et al., 2019) examined the behavior of the long multi-trailer trucks common in South Africa. Only the ultimate limit was considered in further calibrations, however slight modifications in the routine would make this methodology suitable for other verifications such as fatigue on bridges or performance of road pavements.

The proposed site load factor approach (SLFA) for the assessment of bridges is based on the calibration of individual load factors that are to be applied to the design traffic load model in order to better estimate the traffic loads being carried by a selected bridge. By observing differences in load effects between actual traffic site and the Roosboom reference station, there is an opportunity to modify the load model – a new load model for design is supposed to be derived from the Roosboom station, see Section 3.1.1 and a study by (van der Spuy & Lenner, 2019). The performance of the bridge can be assessed more accurately in terms of traffic load effects.

The main goal of the procedure was to evaluate the influence of a specific traffic characteristic that leads to a load reduction of the reference load as detailed by the following equation:

$$LF_i(x) = \frac{LE_i(x)}{LE_R} \quad \text{with } i = 1,2 \quad \text{Equation 27}$$

where  $LF_i$  and  $LE_i$  are the reduction factor and the characteristic load effect respectively for the  $i = 1,2$  site load factors. These correspond to the previously selected most influential factors - namely the ADTT and the percentage of long vehicles respectively (Pérez Sifre & Lenner, 2019). The  $x$  stands for a value of the descriptor for which the reduction factor is to be obtained.  $LE_R$  is the characteristic load effect obtained from the reference station.

Lower reference periods and correspondingly lower return periods tied to the remaining service life can be employed when assessing existing structures (Caspeele et al., 2013; ISO 13822, 2001). Load effects pertaining to the reference station (Roosboom in this case) or reference load model can be therefore extrapolated to desired lower return periods and compared to the characteristic load effects corresponding to the design traffic load model. The return period of the characteristic load effects for the design load model considered is currently considered as 975 years, or the same as for the development of LM1 in Eurocode as 5% exceedance in 50 years (van der Spuy & Lenner, 2018). Hence, an additional site load factor was introduced to capture the influence of possibly lower reference period for older bridges as shown in:

$$LF_3(x) = \frac{LE_R(x)}{LE_D} \quad \text{Equation 28}$$

where  $LF_3$  is the reference period factor,  $LE_R$  is the characteristic load effect from the reference simulation for  $x$  years of return period and  $LE_D$  the characteristic load effect obtained from the design traffic load model. Note again the difference between  $LE_R$  that corresponds to the value of crude extrapolated load effect, and  $LE_D$  that is corresponding to the value resulting from the application of developed load model.

Table 14: Return periods for various reference periods and probability of 5% of exceedance

Reference period (years)	Return period characteristic values (years)
50	975
40	780
30	585
20	390
10	195

Assuming different remaining service lives and a probability of exceedance of 5% in the reference period (EN 1991-2:2003), the reduced return periods are shown in Table 14. Any reference period could be in

principle selected, for instance annual reference period, however, if the reference period is related to the remaining service life of a bridge as suggested in the (ISO 13822, 2001), it does not seem practical to evaluate the performance of bridges with a remaining service life of one year. A minimum service life of 10 years was selected as a reasonable value.

Figure 20 schematically explains the concept of presented site load factors. The distance between the load effects mandated by the proposed design load model (van der Spuy & Lenner, 2019) and the reference simulation (Roosboom) represents the reference period site-load factor  $LF_3$ . It should be noted, that the proposed load model was conservatively established on the principle of worst load effect at critical span length.

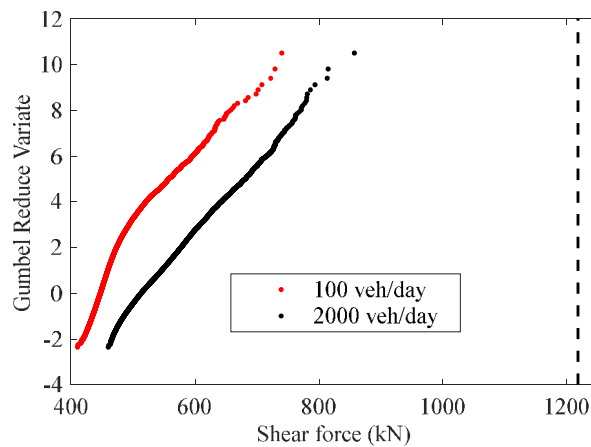


Figure 20: Site load factors concept - 50 m span length (Pérez Sifre, 2020).

The reduction shown here can be therefore largely contributed to a conservatism inherent to a load model and perceived reduction due to shorter remaining service life. Further reduction can be shown by the distance between the reference simulation (ADTT = 2000 veh/day) and any other simulation performed with different the ADTT represents the factor  $LF_1$ . Here, as an example, the ADTT is taken as 100 veh/day and the reduction in the shear force can be observed as decreasing approximately from 700 kN to 500 kN.  $LF_2$  is omitted for clarity with a simplifying assumption that the percentage of long vehicles does not change. Site load factors are proposed to be combined together using the following equation:

$$E_{ka} = E_{kd} \cdot \prod_{i=1}^3 LF_i \quad \text{Equation 29}$$

where  $E_{ka}$  is the assessment characteristic load effect,  $E_{kd}$  the design characteristic load effect, and  $LF_i$  the site load factors.

Simulations are performed for a variety of ADTT and percentage of long vehicles for two lane traffic. The load effects are extrapolated to the different return levels as indicated previously by fitting probability distributions such as Gumbel and Weibull to the tail of the histograms of load effects (B. Enright, 2010; O'Connor & O'Brien, 2005). To simplify the fitting process of extreme value functions to the data that is seldom independent and identically distributed, graphical techniques such as probability plots are used to validate the adherence of the tail data to the selected probability distribution.

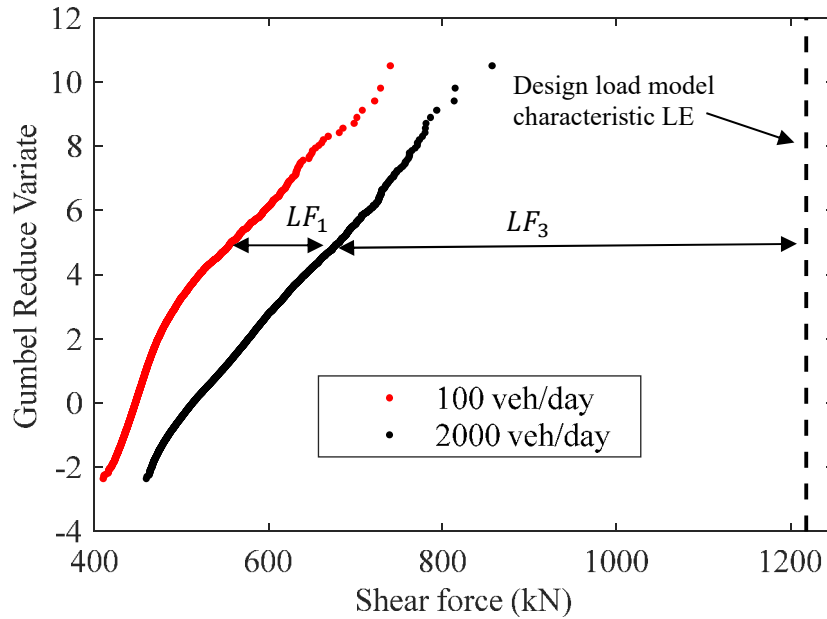


Figure 21: Site load factors concept - 50 m span length (Pérez Sifre, 2020).

For full details about the calculation of the characteristic load effects refer to (Pérez Sifre, 2020). presents, as an example site load factors  $LF_1$  for the sagging moment (single span bridges) in variation of ADTT as a function of different span lengths. Note, 2000 veh/day served as the reference traffic for the calibration of design load model (P. van der Spuy & Lenner, 2019), therefore intuitively ADTT > 2000 exhibits factors above 1.0 while ADTT < 2000 shows lower values.

Table 15: ADTT site load factors  $LF_1$  – sagging moment.

Span length (m)	ADTT (veh/day)				
	100	500	1000	2000	4000
10	0.89	0.92	0.97	1.00	1.03
20	0.89	0.93	0.98	1.00	1.05
30	0.88	0.93	0.97	1.00	1.04
40	0.87	0.93	0.97	1.00	1.04
50	0.87	0.93	0.96	1.00	1.05

#### 4.2.2 Uncertainty and partial factors

The definition of a simple semi-probabilistic approach that is suitable for its application in the industry requires the evaluation of different sources of uncertainties that affect simplified calculations and resulting safety levels. Most of design and assessment approaches found in modern codes utilise the concept of partial factors to account for all uncertainties and mandate a minimum required safety level. When assessing the accuracy of the results pertaining to concepts discussed in this work the following general sources of uncertainty are to be investigated:

1. Epistemic uncertainty - lack of recorded traffic data. Lack of measured data can be compensated for by the generation of hundreds of years of traffic (Enright et al., 2011). Consequently, the generated samples are larger than those typically resulting from WIM data only and thereby reducing the effect of uncertainty due to lack of data.
2. Accuracy of the WIM data. The accuracy of the recorded traffic data is an important aspect that can have implications on the determination of the extreme load effects as proven by (O'Connor & O'Brien, 2005). It might require a calibration of the data or a correction of the load effects through a partial factor. A minimum class C(15) per definition of (COST 323, 1998) is recommended for span less than 50m while less accurate data may be used for spans over 50 m. The WIM data used in this section have been recalibrated and the accuracy evaluated following the criteria available in (de Wet, 2010). The accuracy is determined as suitable or at least class C(15), which according to the review literature avoids the need for further corrections (O'Connor & O'Brien, 2005).

Particular aspects of uncertainty discussed at this point include:

1. Aleatoric uncertainty: randomness of basic variables. Values cannot be fixed deterministically. Partial factors assure low probabilities of exceedance of high load effects.
2. Model uncertainty: Mathematical models used in the structural verifications are an idealization of the real phenomena. This uncertainty accounts for the deviations in the results due to simplifications and is estimated using the recommendations found in specialised literature (Allaix et al., 2016; Steenbergen & Vrouwenvelder, 2010; Sýkora et al., 2013).
3. Statistical uncertainty in the determination of the characteristic load effects: Monte Carlo simulations present a variability especially visible towards the upper tail of the load effects. The selection of different tails used in the extrapolation, therefore, may deliver different characteristic load effects. The simulation of long periods of traffic to some extent alleviates this problem, however, this uncertainty is evaluated and considered in the determination of the characteristic traffic load effects.
4. Statistical uncertainty in the estimation of the traffic descriptors: The method developed by requires basic estimation of the ADTT and the percentage of long vehicles for the calculation of the site-specific load effects. Measuring these descriptors for a short period might incur errors in the estimation, as traffic flow is not constant throughout all periods. Errors can lead to incorrect selection of the site load factors and therefore potentially incorrect values of the site-specific load effects.

Semi probabilistic codes address the issue of uncertainty and prescribed safety levels by the implementation of partial factors for both design and assessment of existing structures (Caspeele et al., 2016).

The formulation of partial factors adopted was a variation of definitions used in (Caspeele et al., 2013; Lenner, Keuser, & Sýkora, 2014) to result in the following definition:

$$\gamma_Q = \gamma_{Ed,q} \cdot \gamma_q \cdot \gamma_e \cdot \gamma_l \quad \text{Equation 30}$$

where  $\gamma_Q$  is the partial factor of the variable action and  $\gamma_{Ed,q}$  stands for the partial factor accounting for the model uncertainty in the estimation of the load effects. The reliability-based partial factor  $\gamma_q$  accounts for the aleatoric uncertainty of the action effect. The additional partial factors  $\gamma_e$  and  $\gamma_l$  introduced in the referenced contribution account for the uncertainty in the calculation of the characteristic load effects and the variability in the estimation of the traffic descriptors necessary for the application of the model.

The calibration of the partial factors was performed based on concepts applied in the calibration of the design partial factors, also known as the design value method (Caspeele et al., 2013). Reduced reference periods  $t_{ref}$  were further considered here with adjusted target reliability levels as recommended for the assessment of existing structures. (Retief, Viljoen, & Holický, 2019) propose the target reliability values  $\beta_T$  (50 years) for South Africa as shown in Table 16. Values for the assessment of existing structures are determined using cost optimization methods and societal risk criterion and are compared to the design values of the national South African code (SANS-10160-1, 2009). Note that these values are valid in the South African context and application of the presented method in other regions should consider the local target reliability indices. For general derivation of target values refer to (Rackwitz, 2000).

Table 16: Proposed target reliability indices  $\beta_T$  in South Africa.

SANS 10160-1	RC2	RC3
Design	3.0	3.5
Assessment	2.0	2.6

RC2 and RC3 refer to the failure consequences class (medium and high consequences of failure respectively) as proposed by the Eurocode (EN-1990, 2002). RC3 class is omitted from the calibration in the presented work with the focus on short to medium span length bridges that generally fall under RC2 class. The shorter remaining service life of existing structures is captured by using Equation 31 and the reduced reference period results are shown in Table 17. **Chyba! Nenalezen zdroj odkazů.** All the target reliability indices below correspond to the same annual probability of failure.

$$\Phi(\beta_{T,n}) = [\Phi(\beta_{T,1})]^n \quad \text{Equation 31}$$

The application of the previous equation is valid if the actions have independent statistical maxima in each year. In reality, this is not always true and the maxima of actions in subsequent years are correlated.

A more general expression is investigated by (Holický et al., 2018) concluding that the assumption of annual independence accepted in many codes may lead to larger failure probabilities:

$$\Phi(\beta_{nk}) = [\Phi(\beta_1)]^{n/k} \quad \text{Equation 32}$$

here  $\beta_{nk}$  is the reliability index for a  $n$  reference period and independence interval  $k \leq n$  (mean time period for which the failures in subsequent periods of  $k$  years are considered to be mutually independent). The difficulty in the application of this equation is the definition of the independence interval  $k$ .

Table 17: Target reliability indices – various reference periods.

Reference period (years)	Target reliability index	
	Design	Assessment
1	4.04	3.31
10	3.46	2.61
20	3.27	2.36
30	3.15	2.21
40	3.07	2.09
50	3.00	2.00

Sensitivity factors  $\alpha_E$  for the loads required for the calibration of partial factors were initially taken as a simplification from (EN 1990, 2002) for the 50-year reference and hence equal to:

$$\alpha_E = \alpha_{E,50} = -0.7 \text{ (dominant action)}$$

$$\alpha_E = \alpha_{E,50} = -0.28 \text{ (accompanying action)}$$

Despite the new developments and transition to annual values (Meinen & Steenbergen, 2018) the use of these values is commonly accepted in practice for the calibration of partial factors for a wide range of engineering structures (König & Hosser, 1982). The validity of the value  $\alpha_E = -0.7$  for the traffic used in this study is also verified in (Pérez Sifre, 2020).

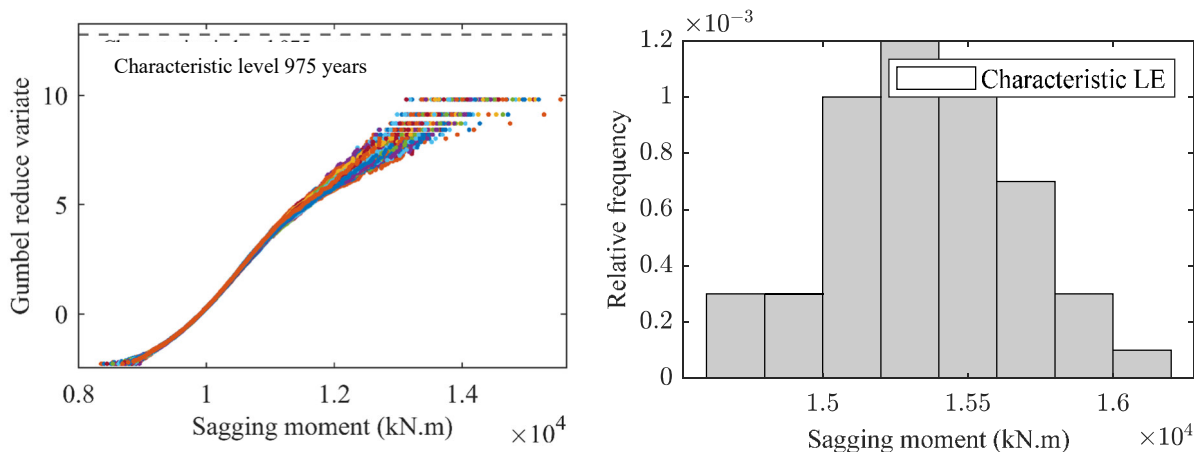


Figure 22: Sagging moments as a result of simulations (Perez Sifre & Lenner, 2021)



### 4.2.3 Uncertainty in the determination of the characteristic load effects

Generation of artificial traffic data using Monte Carlo simulations is accompanied by an inherent variability, which essentially means that the end results obtained in simulations may be different due to randomness of the sampling process. The selection of different runs of simulations used for the extrapolation results in different characteristic values of the load effects. Long run simulations are a way to reduce the variability of values located away from the extreme tail (Enright & O'Brien, 2013). Values at the desired return level can be directly read off from the distribution or plot without the need for extrapolation methods. By generating hundreds or thousands of years of traffic, it is possible to improve the accuracy of the results. Long run simulations are therefore important for the sought-after results; however, they are extremely time-consuming and are not always viable. A combination of relatively long simulations and the use of extrapolation methods, avoids the need for extremely long simulations and still delivers suitable characteristic values of the load effects (Enright, 2010; Pérez Sifre, 2020). This section evaluates the error introduced in the estimation of the characteristic load effects and proposes partial factors to account for it.

Figure 22 shows exemplarily a 50 m span length sagging moment calculated based on a 2000 veh/day of artificial traffic. Five thousand years of traffic are simulated and therefore corresponding hundred individual samples of 50 years traffic are shown in different colours. The histogram in Figure 22 corresponds to the relative frequency of sagging moments extrapolated to 975 years based on each of the 50-year samples. The variability of the extrapolated values depending on the sample selected is noticeable.

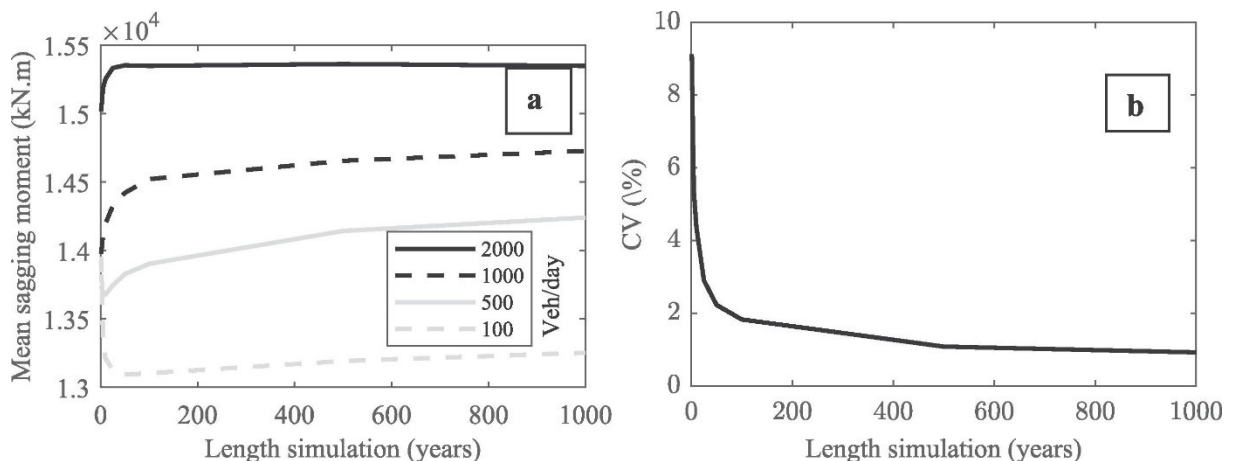


Figure 23: Uncertainty in the estimation of the characteristic load effects (Pérez Sifre & Lenner, 2021)

This extrapolation was sequentially repeated for different sample sizes and for various values of the ADTT. The sample mean and COV of every extrapolated scenario are calculated at the return period of 975 years. For instance, if 1000 years are simulated and split in 10 different samples of 100 years then 10 different characteristic values at a return period of 975 years are obtained. As an example, Figure 23 shows the mean value of the sagging moment for a 50 m span bridge plotted with different ADTT. The

change of the mean COV (%) for all span lengths and ADTTs with the simulation length is shown in Figure 23. Note the rest of the spans and simulations present similar results, for full details refer to (Pérez Sifre, 2020).

The values for both the mean and the COV converge for all ADTTs with increased simulation length. Short simulations are not as reliable and deliver less consistent results. This can be observed in Figure 23 where 100 veh/day sagging moment happened to be higher than 500 veh/day sagging moment. The mean COV varies from approximately 9% for one-year samples and decreases gradually to reach values lower than 1% for samples of 1000 years. Plotted values show that the simulation of long periods of traffic reduces the uncertainty of extrapolated LE as previously stated.

Table 18: Fitted distributions and partial factor  $\gamma_e$

Load effect	Span length (m)	Distribution	Mean	Standard deviation	$\gamma_e$
Sagging (kN·m)	10	Normal	1412	25.6	1.04
	20	Normal	3780	68	1.04
	30	Normal	7589	140	1.04
	40	Normal	11470	183	1.03
	50	Normal	15349	322	1.04
Shear (kN)	10	Normal	577	12	1.04
	20	Normal	931	23.1	1.05
	30	Normal	1118	22.7	1.04
	40	Normal	1188	25	1.04
	50	Normal	1304	21.5	1.03
Hogging (kN·m)	10	Normal	990	16	1.03
	20	Normal	2493	48.3	1.04
	30	Normal	4476	106.5	1.05
	40	Normal	7758	142.5	1.04
	50	Normal	10267	103.6	1.02

The partial factor  $\gamma_e$  accounting for this uncertainty is calibrated using the 2000 veh/day simulation as it was the largest of the simulations performed (5000 years of traffic). Individual samples of 100 years are selected from a total of 5000 years. They are subsequently used for the extrapolation to the characteristics values of the load effects, delivering inherently 50 values per load effect and span length. Selecting shorter individual samples would provide a total higher number of characteristic values, however, could overestimate the partial factor  $\gamma_e$  (higher COV as seen in Figure 23). If longer individual samples were to be selected from the 5000 years simulated, the number of characteristic values would

be insufficient to fit a probability distribution and model the uncertainty. The calculation of the partial factor  $\gamma_e$  is performed by fitting Normal distributions to the histograms of load effects and selecting a high fractile as in:

$$\gamma_e = 1 - \text{COV} \cdot \alpha_{E,50} \cdot \beta_T \quad \text{Equation 33}$$

where COV is the coefficient of variation of the Normal distribution,  $\alpha_{E,50} = -0.7$  is the sensitivity factor and  $\beta_T = 3.0$  is the reliability index selected in this work to avoid excessive numbers of factors; naturally a different value can be chosen in more accurate calibration. The values of  $\gamma_e$  shown in Table 18 are generalised for the evaluation of this type of uncertainty regardless of the traffic conditions, reference period or reliability level adopted. Note that partial factors shown in this section are a pre-calibration based on the assumed sensitivity factor  $\alpha_{E,50}$ . The actual value of  $\alpha_{E,50}$  may differ significantly (Lenner & Sýkora, 2016), therefore leading to a recalibration of the factors proposed here.

#### 4.2.4 Estimation of the traffic descriptors uncertainty

The proposed assessment approach relies on the idea that the assessing engineer can obtain the basic information about traffic flowing over the bridge assessed. The ADTT and the percentage of long vehicles are necessary for the application of the method in the here presented case. Both parameters are easily obtainable either visually or by the installation of simple equipment on the roads.

Traffic flow is non-stationary process and it presents daily, weekly and seasonal fluctuations. Measuring traffic on different days may lead to different estimates of traffic descriptor values, subsequently also to different reduction factors. Both the ADTT and the average percentage of long vehicles tend to stabilise with the increasing number of days measured. Ideally, long measurements should be taken to ensure accurate values. In practice, this is not always possible and just a few days of data might be available.

This section analyses the influence of the uncertainty in the estimation of the traffic descriptors in relation to the length of the measurements. To account for the uncertainty, correction factors  $\gamma_t$  (traffic factors) are proposed.

Figure 24 shows the COV of the ADTT and the percentage of long vehicles for different lengths of measurements (days of traffic measured) based on the data recorded at the Roosboom WIM station. Values show a larger variability attributed to the ADTT. The decrease of COV with the length of the measurements presented in both figures indicates an improvement in the estimation of the traffic descriptors.

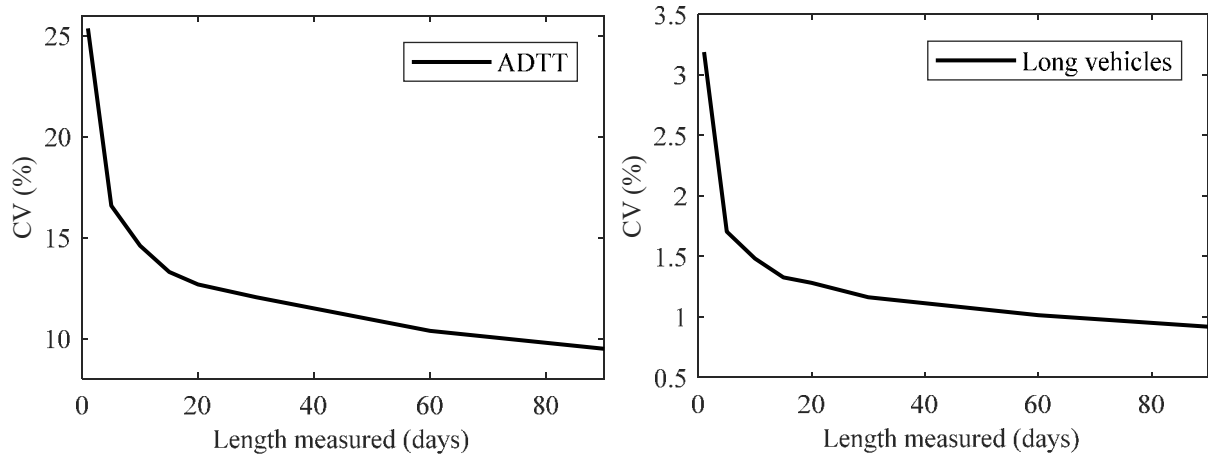


Figure 24: Variation of COV for ADTT and percentage of long vehicles with the length of the measurements (Pérez Sifre, 2020).

The uncertainty in the estimation of the traffic descriptors eventually affects the estimated LE for the site being assessed. Values of the ADTT and percentage of long vehicles are transformed into site load factors. Important deviations in the estimation of the mentioned traffic descriptors could lead to incorrect site load factors and therefore to the calculation of LE that are not representative of the site. Multiplication of both  $LF_1$  and  $LF_2$  factors leads to the combined site load factor. Figure 25 exemplarily shows the combined site load factors for the same load effect, the span length and five days measured.

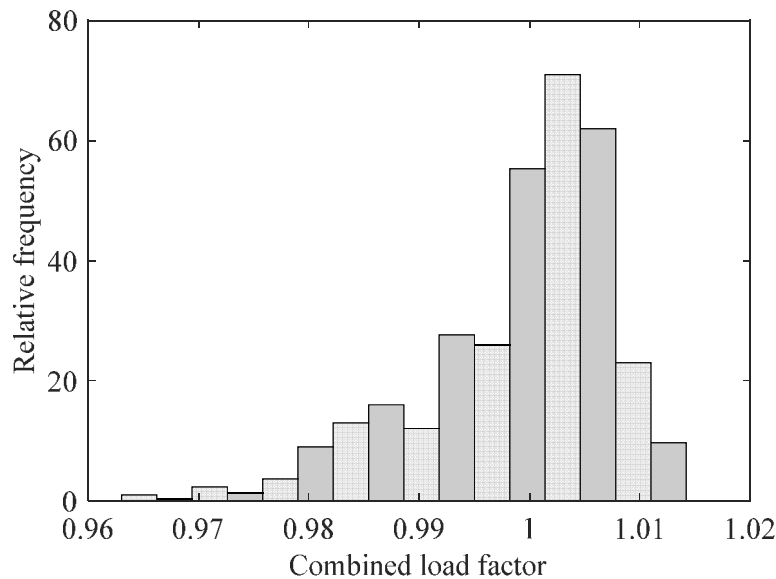


Figure 25: Relative histogram of combined load factor (Pérez Sifre, 2020).

Distributions of modified load effects are calculated using Equation 32, the site load factors are used here instead of deterministic values:

$$E_{ka} = E_{kR} \cdot \prod_{i=1}^2 LF_i \quad \text{Equation 34}$$

where  $E_{ka}$  stands for the distribution of the assessment characteristic load effects,  $E_{kR}$  the reference station characteristic load effects, and  $LF_i$  the distributions of site load factors. Figure 26 shows an example of the histogram obtained and the fitted probability distribution (GEV) using maximum likelihood estimation. The peak of the histogram is the most probable characteristic load effect, equal

to  $E_{kR}$ . Long measurements of the traffic descriptors with low variation deliver  $\prod_{i=1}^2 LF_i = 1$  and therefore  $E_{ka} = E_{kR}$ .

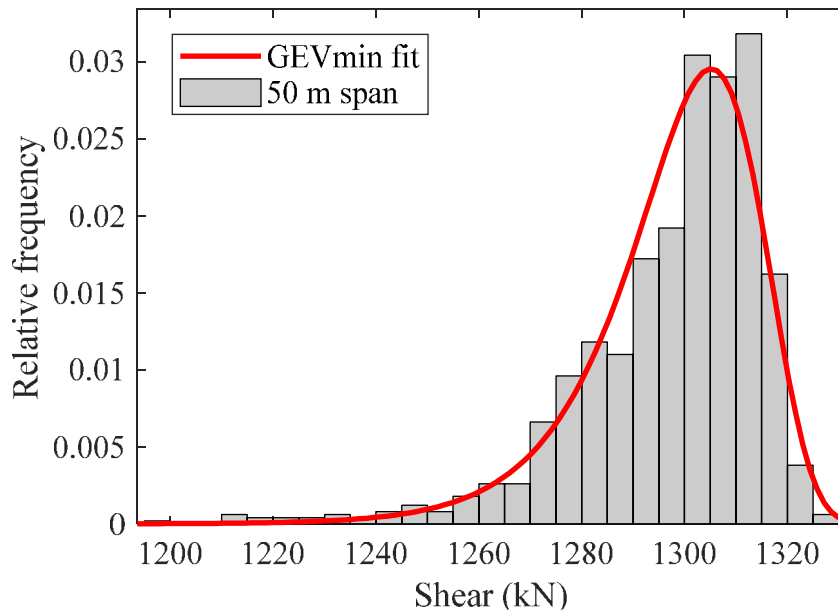


Figure 26: Relative histogram of modified shear force and fitted distribution (Pérez Sifre, 2020)

The shape of the histogram is explained not only by the dispersion of the traffic descriptors but also by the shape of load factors functions. These site load factor curves present higher gradients for lower values of the traffic descriptors and vice versa. This means that the internal forces are highly sensitive to lower values of the of the traffic descriptors and less sensitive to higher values, where the load scenarios that create the most extreme load effects are similar. Two values of traffic descriptors located the same distance from the mean but each one on each side of the histogram would lead to the same modification of the load effects in absolute terms if the correlation was linear. However, due to the variations in the gradient, lower values induce higher modifications, thus the histograms tend to present larger lower tails. Two values of ADTT shown in Figure 27 are 1000 veh/day apart from the original ADTT (2000 veh/day). The lower value (1000 ADTT), however, leads to a modification of negative 4% and while higher value (3000 ADTT) to positive 1%. Lower ADTTs produce numerically higher modifications, hence the shape of presented the histograms.

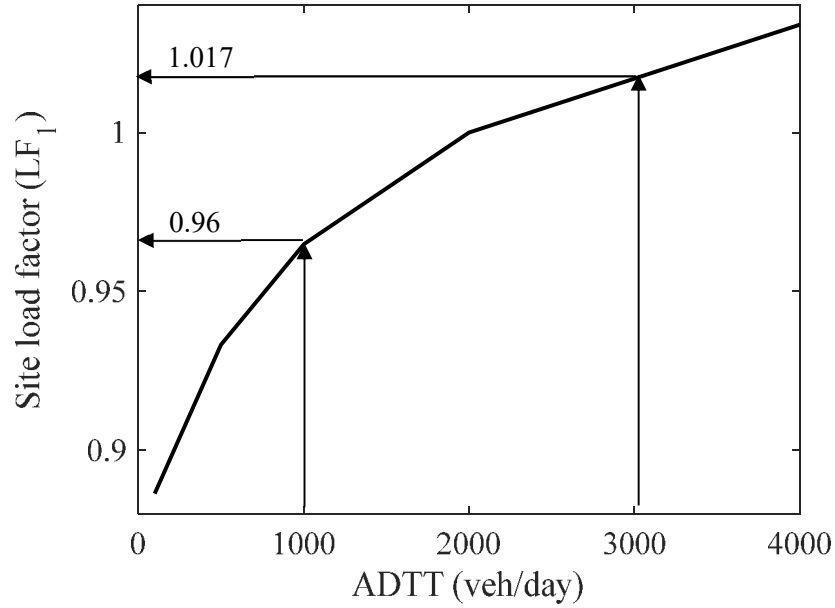


Figure 27: Site load factor  $LF_1$ - shear force 50 m span length (Pérez Sifre, 2020)

The partial factor  $\gamma_t$  accounting for the uncertainty in the estimation of the traffic parameters is further introduced here. The intention of this partial factor is to alleviate deviations in the estimations of traffic descriptors that could potentially lead to extreme reductions of the original characteristic load effects and therefore unsafe scenarios. For instance, measuring the traffic flow for a short period might lead to incorrect values of the traffic descriptors and consequently incorrect characteristic LE. The partial factor  $\gamma_t$ , calibrated using traffic data, is meant to account for these deviations of the estimated characteristic LE that are mitigated once the factor is applied to the estimated LE delivering a more accurate value. This can be mathematically expressed as indicated in:

$$P(E_k < E_{kR}) = \Phi(-\alpha_E \cdot \beta_T) \quad \text{Equation 35}$$

where  $E_k$  is the assessment characteristic low effect estimated using short measurements of the traffic descriptors and  $E_{kR}$  is the actual assessment characteristic load effect based on long measurements of the traffic descriptors (peak of the histogram in Figure 26). Equation 35 is equivalent to saying that the probability of observation of a characteristic load effect  $E_k$  below the real value  $E_{kR}$  is tied to the required reliability level  $\beta_T$ .

It is the lower tail of the histogram of the modified load effects that captures the required probability, therefore the partial factor is calculated as a low fractile as indicated in the following equation:

$$\gamma_t = \frac{E_{kR}}{F_{GEV}^{-1}(\Phi(-\alpha_E \cdot \beta_T))} \quad \text{Equation 36}$$

where  $E_{kR}$  the reference station characteristic load effects that normalises the partial factor,  $F_{GEV}^{-1}$  is the inverse cumulative distribution function (CDF) of the generalised extreme value (GEV) minima distribution,  $\Phi$  is the CDF of the Standard Normal distribution,  $\alpha_E$  the sensitivity factor and  $\beta_T$  the target reliability index. The selected  $\beta_T$  is 3.0 that corresponds to a 50-year reference period according to Table 16. As previously discussed, selecting different  $\beta_T$  for each reference period leads to a high number of factors. This is equivalent to the selection of a fixed fractile for the calibration.

Figure 28 shows the mean value of the traffic partial factors  $\gamma_t$  of all the span lengths for the three load effects. Partial factors decrease with the period measured reflecting the reduction in the uncertainty in the estimation of the traffic descriptors mentioned previously. Sagging moment and shear force partial factors are lower than hogging moments. The hogging moment is greatly affected by the span length of the bridge and the ADTT. For short structures and lower ADTTs only single truck scenarios are creating the most extreme events. For larger spans and higher ADTT scenarios involving more trucks gain importance. This consequently affects the site load factors creating substantial variations in their gradient, thus leading to larger reductions of the hogging moment (higher uncertainty) than observed in the other two load effects by increasing the traffic partial factors. This uncertainty is greatly mitigated if the traffic descriptors are measured for longer periods.

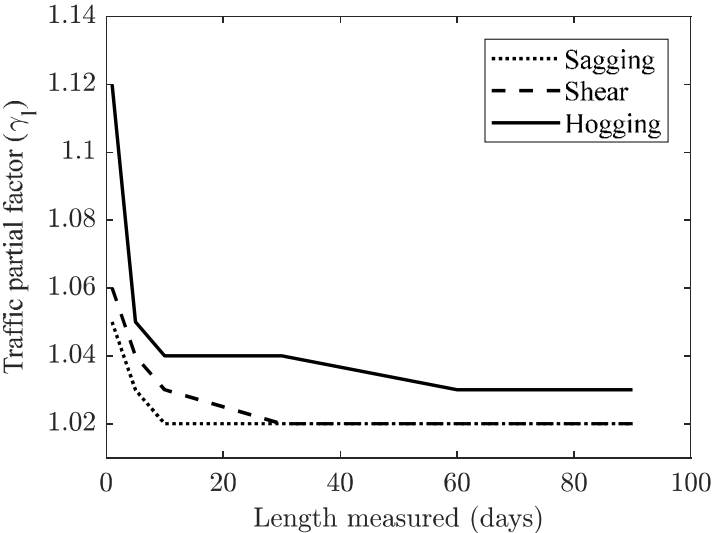


Figure 28: Mean traffic partial factors – all span lengths and load effects (Pérez Sifre, 2020)

Ideally, the traffic descriptors should be estimated using extensive data sets. In such case, the uncertainty in estimation of traffic characteristics can be neglected and the partial factor  $\gamma_t$  can be considered as equal to 1. Measurements for periods larger than ten days do not lead to substantial variations in the traffic partial factors. On average, and with reasonable accuracy, five days could be used. This period should be considered as a minimum for the estimation of the traffic characteristics descriptors. The use of shorter periods for the estimation of traffic parameters partially undermines the benefits of the reductions achieved with the application of the site-load factors and is therefore not recommended. To avoid biased estimations, measurements should be always taken on working days in months where the economic activity is normal.

Note that the partial factors shown in this section are a pre-calibration based on the assumed sensitivity factor  $\alpha_E = -0.7$ . The actual influence of this uncertainty might differ from the accepted value  $\alpha_E$  significantly, therefore affecting the factors proposed here. Section 4.2.7 presents more details.

#### 4.2.5 Reliability based partial factor

The reliability-based partial factors  $\gamma_q$  can be obtained by comparing the assessment  $E_d$  and characteristic  $E_{ka}$  values of the load effects according to the following equation:

$$\gamma_q = \frac{E_d}{E_{ka}} \quad \text{Equation 37}$$

Characteristic load effects are obtained as values with a probability of exceedance of 5% in the selected reference period, in this contribution equal to 50 years. Design load effects, however, are a function of the target reliability  $\beta_T$  and the sensitivity factors  $\alpha_E$  leading to a probability of exceedance  $P_{exd}$ :

$$P_{exd} = \Phi(-\alpha_E \cdot \beta_T) \quad \text{Equation 38}$$

where  $\Phi$  is the CDF of the Standard Normal distribution. If the concept of return period is applied to the calculation of the design values, the probabilities of exceedance for the design and assessment and the reference periods considered lead to the return periods  $RP$  in Table 19.

Table 19: Design values return periods for design and assessment and characteristic return period (years) – various reference periods (years)

Reference period	Design $RP$	Assessment $RP$	Characteristic values $RP$
10	1291	289	195
20	1798	396	390
30	2180	475	585
40	2497	539	780
50	2774	594	975

Note that the concept design values of the load effects, calculated as high fractiles of the distribution of load effects, should not be confused with the design (versus assessment) evaluation scenario referring to the reliability level. Design load effects are obtained by extending the performed extrapolations to design return periods. The reliability based partial factors  $\gamma_q$  can be therefore calculated according to Eq. 37.

Table 20 shows a simplified list of the chosen partial factors for various reference periods. A partial factor is calibrated for each load effect and span length. However, the highest, thus conservative among these values is shown here for simplicity incurring only in a 3% error. The observation of values equal and below 1.0 for the assessment can be easily understood by examining the return periods listed in Table 19. For reference periods of 20 years and longer, the characteristic return period is higher than the assessment (design value) return period, thus the partial factors obtained below 1.0.



Table 20: Reliability-based partial factors  $\gamma_q$

Reference period (years)	Design	Assessment
10	1.09	1.02
20	1.07	1.00
30	1.06	1.00
40	1.05	0.99
50	1.05	0.99

#### 4.2.6 Model uncertainty partial factor

According to the fib Bulletin 80 (Caspéele et al., 2016) the model uncertainty partial factor  $\gamma_{Ed,q}$  can be assumed as 1.12 for unfavourable variable actions disregarding the reference period. This value is also assumed here for ease in the calibration of the partial factors. It is noted, that consideration of different values for different reference period may lead to more accurate estimation of the model uncertainty based on the target  $\beta_T$  (Sýkora et al., 2013).

#### 4.2.7 Final partial factors

The previous model uncertainty and reliability based partial factors,  $\gamma_{Ed,q}$  and  $\gamma_q$  respectively, are to be multiplied to obtain a single final partial factor as follows:

$$\gamma_Q = \gamma_Q^* \cdot \gamma_t \cdot \gamma_e \quad \text{with} \quad \gamma_Q^* = \gamma_{Ed,q} \cdot \gamma_q \quad \text{Equation 39}$$

where the factor  $\gamma_Q^*$  is equivalent to the typically defined partial safety factor  $\gamma_Q$  (Caspéele et al., 2016b). In the context of this contribution, is modified by additional factors  $\gamma_t$  and  $\gamma_e$ . The intermediate partial factor  $\gamma_Q^*$  presented in Table 21 avoids the need of multiplying two factors and in practice appears as a single value.

Table 21: Intermediate partial factors  $\gamma_Q^*$

Reference period (years)	Design	Assessment
10	1.22	1.14
20	1.20	1.12
30	1.19	1.12
40	1.18	1.11
50	1.17	1.11

#### 4.2.8 Reliability verifications

The proposed layering of partial factors and traffic load factors was verified by employing reliability principles and the overview is provided in this section. A reliability analysis assured that the proposed

methodology achieves the desired level of safety for the traffic loads. Prior to the calculation of the reliability indices, the influence of the proposed uncertainties was evaluated to verify the pre-calibrated partial factors. The reliability verifications were performed using FORM analysis implemented in the package UQLab for Matlab (Marelli & Sudret, 2014).

The performed reliability analysis only considered the traffic load effects while ignoring any resistance components. This was achieved by isolating only the design load and the load corresponding to the assessment scenario – or the actual loads. The relative importance of the load effects was initially expressed with the assumed sensitivity factor  $\alpha_E = -0.7$ , therefore the reliability level of the traffic load effect was formulated as  $\beta_E = -\alpha_E \cdot \beta_T$ . The failure mode was defined as the instance of the actual traffic load effects exceeding the design traffic level (Basson & Lenner, 2019). This is mathematically expressed as the limit state specified as:

$$Z = E_{kd} \cdot \gamma_Q^* \cdot \frac{\theta_t}{E_{kR}} \cdot \theta_e \cdot \prod_{i=1}^3 LF_i - \theta_{E,Q} \cdot E_Q \quad \text{Equation 40}$$

where  $E_{kd}$  is the characteristic load effect of the design traffic load model (van der Spuy & Lenner, 2019),  $\gamma_Q^*$  the partial factor as detailed in Equation 37,  $\theta_t/E_{kR}$  the traffic descriptors uncertainty,  $\theta_e$  stands for the uncertainty in the calculation of the characteristic load effects,  $LF_i$  the traffic load factors,  $\theta_{E,Q}$  the model uncertainty and  $E_Q$  corresponds to the distribution of the load effects obtained from the long simulations and tied to a reference period.

The uncertainty in the determination of the characteristics values  $\theta_e$  as well as the uncertainty of the traffic descriptors  $\theta_t$  in the limit state are initially evaluated for importance by the FORM analysis. The assumed  $\alpha_E = -0.7$  used in the pre-calibration can differ from the actual importance of these variables. Therefore the first set of reliability analysis is intended to evaluate the importance of the uncertainties in the investigated limit state and recalibrate the factors if necessary. With newly recalibrated factors reflecting the verified importance, the substantiation of layering of the partial factors and site load factors can proceed.

The variables in the limit state Equation 38 are obtained from the artificial traffic generated previously and tables of factors fully available in (Pérez Sifre, 2020). Table 22 presents the sensitivity factors  $\alpha_e$  and  $\alpha_t$  for the uncertainty in the calculation of the characteristic load effects and the traffic descriptors uncertainty, respectively, at different span lengths and load effects.

By observing the differences in obtained results, the previously assumed value of  $\alpha_E = -0.7$  for each variable is not appropriate. It is necessary to recalibrate the partial factors to cater for the variables obtained at the reference station. Naturally, different traffic conditions and underlying distributions might result in different values than those observed in Table 22. It is however expected that dominating variables remain the same, and same sensitivity factors will be observed for various traffic conditions.

Table 22: Sensitivity factors FORM

Load effect	Span Length (m)	$\alpha_e$	$\alpha_t$
Sagging	10	0.17	0.07
	20	0.17	0.08
	30	0.17	0.06
	40	0.17	0.07
	50	0.18	0.08
Shear	10	0.17	0.07
	20	0.17	0.06
	30	0.17	0.06
	40	0.17	0.06
	50	0.17	0.06
Hogging	10	0.18	0.05
	20	0.17	0.06
	30	0.17	0.12
	40	0.18	0.07
	50	0.19	0.06

According to here obtained results partial factor  $\gamma_e$  (uncertainty in the determination of the characteristic load effects) is recalibrated to a value of 1.01. Owing to the very low values of the sensitivity factor  $\alpha_t$ , the importance of this uncertainty in the global reliability is negligible and the partial factors  $\gamma_t$  are, therefore, excluded from the assessment method proposed here. It should be noted that the low influence of the uncertainty in the estimation of the traffic descriptors  $\theta_t$  has been determined with an assumed length of measurements of five days. For the exclusion of this uncertainty from the model to be valid, a minimum of five days is therefore necessary for the estimation of the traffic descriptors from traffic counts. Shorter periods of observation could lead to large sensitivity factor and therefore yield the  $\gamma_t$  partial factor again relevant. The exclusion of the partial factors  $\gamma_t$  is based on the results obtained in this publication using the local traffic and cannot be generalised. Other countries applying the proposed approach are advised to verify the influence of the traffic descriptors uncertainty before discarding it.

The main goal of this section is the verification of the partial factors and traffic load factors layering. Given the elimination of irrelevant factors, a limit state Equation 38 can be simplified. The failure mode is defined here as the instance of the actual traffic load effects exceeding the design traffic loads used in the structural verification (characteristic values and recalibrated partial factors):

$$Z = E_{kd} \cdot \gamma_Q^* \cdot \gamma_e \cdot \prod_{i=1}^3 LF_i - \theta_{E,Q} \cdot E_Q \quad \text{Equation 41}$$

The results of interest delivered by the FORM analysis are the probability of failure  $p_f$  (the probability that the actual loads exceed the design loads) or the equivalent reliability index  $\beta$ . The verification is successful if the reliability index  $\beta$  obtained in the FORM analysis is higher than the target reliability index for the traffic load effects  $\beta_E$ , therefore the maximum probability of failure intended is not exceeded.

Three traffic scenarios are considered in this verification. These scenarios cover for different traffic conditions (light and heavy traffic) and evaluation conditions (design and assessment with different reference periods):

1. Newly generated traffic with an ADTT of 500 veh/day, 25% of long vehicles and an assessment evaluation with a reference period of 10 years corresponding to target reliability index  $\beta_{E,10}=1.83$  ( $\beta_{E,1}=2.31$ ) (10 and 1 referring to the reference period). This traffic would be representative of a minor road in a rural area with a very light traffic.
2. ADTT=100 veh/day and % of long vehicles= 87%, long traffic data available (traffic uncertainty excluded) and design evaluation with a reference period of 10 years Corresponding to target reliability index  $\beta_{E,10}=2.42$  ( $\beta_{E,1}=2.83$ ).
3. Reference station traffic conditions (Roosboom) and design evaluation with a reference period of 50 years. Therefore, the target reliability index  $\beta_{E,50}=2.1$  ( $\beta_{E,1}=2.83$ ).

The distributions of load effects are obtained for every scenario fitting probability distribution to the already generated traffic. The rest of the variables are described in previous sections. Table 23 shows the reliability indices obtained for the load effects, the span lengths studied and the three scenarios described.

The intended reliability index for traffic loads  $\beta_E$  is achieved in all cases and, therefore, the layering proposal of partial factors and traffic load factors is validated. The differences found between the reliability index achieved and the intended reliability level  $\beta_E$  can be attributed to simplifications of the partial factors as well as mainly the difference between the design values obtained using the methodology presented previously and the design values obtained as the fractile  $\Phi(-\alpha_E \cdot \beta_T)$  from the distribution of load effects  $E_Q$ . The two instances (Scenario 1 – shear and hogging – 10 m span length) where the calculated value is below the target value can be attributed to the previously detailed reasons, furthermore, the differences are insignificant and not a concern regarding the validity of the results.

Table 23: Reliability indices

Load effect	Span Length (m)	Scenario 1	Scenario 2	Scenario 3
		$\beta_{E,10}=1.83$	$\beta_{E,10}=2.42$	$\beta_{E,50}=2.10$
Sagging	10	1.83	2.69	2.35
	20	2.12	2.62	2.40
	30	2.24	2.56	2.40
	40	2.21	2.53	2.39
	50	2.34	2.69	2.50
Shear	10	1.81	2.54	2.32
	20	2.03	2.69	2.39
	30	2.11	2.58	2.41
	40	2.18	2.54	2.35
	50	2.29	2.61	2.37
Hogging	10	1.80	2.68	2.30
	20	1.95	2.5	2.29
	30	1.86	2.44	2.36
	40	2.14	2.71	2.35
	50	2.42	2.89	2.24

### 4.3 Application of the site load factor approach with

The general procedure for the application of the site load factor approach is illustrated based on South Africa data along with the here derived partial factors summarised in Table 24 as follows:

1. Collection of the necessary information is the first step for the application of the approach. Traffic measurements have to be taken to estimate the relevant traffic descriptors, in the case of this document corresponding to the ADTT and the % of long vehicles. A minimum of five days of traffic data collection is recommended. A possibly shorter remaining service life of the structure together with an appropriate reliability level should be established
2. The estimated traffic descriptors are used to obtain the site load factors  $LF_1$ ,  $LF_2$  and  $LF_3$  for each of the three load effects considered. The new characteristic load effect is obtained using Equation 32 repeated here for convenience, where  $E_{kd}$  is the characteristic load effect obtained using the relevant design load model (van der Spuy et al., 2019):

$$E_{ka} = E_{kd} \cdot \prod_{i=1}^3 LF_i$$

3. The design value of the load effects is finally obtained by multiplying  $E_{ka}$  by the final partial factors  $\gamma_Q$  summarised in Table 24. The reference period and reliability level are the required inputs in this table.

 Table 24: Partial factors  $\gamma_Q$ 

Reference period	Design	Assessment
10	1.24	1.15
20	1.21	1.13
30	1.20	1.13
40	1.19	1.12
50	1.18	1.12

One example of the application of the site load factor approach is presented further to clarify the presented procedure.

### Example application – Simply supported bridge

The example is exploring a simply supported bridge with one lane per each direction located on a road with relatively lower truck traffic. The structure does not present structural deficiencies, however, owing to its age the evaluation is performed for the lowest reference period and assessment target reliability level. Table 25 summarises the assumed characteristics of the structure and traffic used for this example.

Table 25: Summary of data for the bridge evaluation.

Bridge arrangement	Simply supported
Span length	20 m
ADTT (one lane)	750 veh/day
Percentage of long vehicles (one lane)	70%
Remaining service life (reference period)	10 years
Reliability level	Assessment

Site load factors  $LF_1$ ,  $LF_2$  and  $LF_3$  are obtained from (Pérez Sifre, 2020) only for the relevant internal forces that is the sagging moment and the shear force. In this instance, interpolation is needed to obtained both factors ( $500 < 750 < 1000$  veh/day;  $50 < 70 < 87.5\%$  long vehicles). Table 26 details the load factors  $LF_1$ ,  $LF_2$  and  $LF_3$ , the final global factors as well as the resulting modified UDL (compared to design values of 30 kN/m first lane L1 and 22.5 kN/m second lane L2,) along with the intensities for tridem

loads (compared to design values of 160 kN each axle first lane L1 and 120 kN each axle second lane L2).

Table 26: Site load factors and modified load model (two lanes)

Load effect	$LF_1$	$LF_2$	$LF_3$	Global	UDL per lane L1/L2 (kN/m)	Tridem loads per lane L1/L2 (kN)
Sagging	0.96	0.98	0.55	0.51	15.3/ 11.5	81.6/61.2 (per axle)
Shear	0.96	0.98	0.66	0.62	18.6/ 14.0	99.2/74.4 (per axle)

The reference period factor  $LF_3$  could be selected per lane for a lateral distribution of loading. The comparison of the characteristic load effects obtained from the design load model and the modified model are presented in Table 27.

Table 27: Comparison of characteristic load effects

Load effect	Design LM	Modified
Sagging (kNm)	6490	3310
Shear (kN)	1310	820

The partial safety factor according to the previous data is  $\gamma_Q = 1.15$ . Design load effects are finally obtained multiplying the modified load effects by the partial factor  $\gamma_Q$ . The most apparent difference can be contributed for  $LF_3$  accounting for the conservatism in the uncalibrated design load model at this particular span length.

#### 4.4 Conclusions

The previously presented results based on the site load factor approach for one lane of traffic (Pérez Sifre & Lenner, 2019) were enhanced here for two lanes of traffic (Perez Sifre & Lenner, 2021). All sources of uncertainty related to the parameters involved in the determination of load effects are evaluated and used as a basis for the calibration of several partial factors. Moreover, it is proposed to utilise layering of partial factors and site load reduction factors. This layering, as routinely used in the semi-probabilistic context, is verified using reliability techniques as to adhere to minimum safety levels. The reliability indices obtained in this process are always at minimum equal to the target reliability values proposed in the national guidelines.

Traffic load models for a bridge assessment present a challenge. The site load factor approach offered here is a straightforward method, based on easy obtainable traffic parameters without any need for extensive instrumentation. The method aims to provide a more accurate estimation of static load effects. Depending on the traffic encountered at a site and the values specified by the design load model, the application of the developed procedures can lead to a substantial reduction of the static load effects for

the assessment. It also allows for a reduction of target reliability values and reference periods to suit the needs of a particular assessment problem.

The presented method is suggested for the assessment of existing bridges; however, it can also serve similar purposes when renovating or constructing a road on a route where WIM is available. The estimation of the traffic flow in the new scenario for a precise calculation of the traffic loads is the key factor here but can be in principle aided by numerical simulations. Depending on the traffic flow it may actually lead to either a reduction, which is likely due to inherent conservatism in load models; or to an increase should the simulated intensity exceed the traffic used for the calibration of the load model. Furthermore, although based on the specific case of South Africa, is general and can be adapted to any country or region. Lastly, the method as proposed can be readily extended to include dynamic amplification with the caution of more uncertainty induced by complex the vehicle-structure interaction.



---

## 5 Example reliability assessment

Discussions in Chapter 3 and Chapter 4 reveal that design codes are typically developed to cater for a variety of load cases and variety of structures while securing acceptable performance and acceptable level of safety over the desired reference period, or the or in other words adhere to the reliability index  $\beta$ . There is inherently built-in conservatism that may result in increased safety margins for ordinary structures under common loads.

On contrary, in the assessment situation the described conservatism should be avoided. The adjustment of partial factors based on different target reliabilities can be particular attractive when the performance of the bridge according to the code cannot be achieved and the economical optimisation of the required reliability level yields a lower acceptable value, refer to (Sykora et al., 2014). Another option beyond the adjustment of partial factor is the probabilistic assessment, or reliability assessment of the structure with probabilistic models for all variables and essentially an evaluation of the given limit state:

$$p_f = p(E > R) \quad \text{Equation 42}$$

where the probability of failure  $p_f$  is the probability that the loading  $E$  exceeds the resistance  $R$  in a specified reference period, while the corresponding reliability index is taken as a measure of the probability failure of the structure in that reference period:

$$\beta = -\Phi(p_f) \quad \text{Equation 43}$$

where  $\Phi$  denotes the standardized normal distribution and  $\beta$  is therefore a transformation of the probability of failure,  $p_f$ , and a higher  $\beta$  implies a lower  $p_f$ .

A study by (Lenner et al., 2021) is presented in this work is to illustrate the investigation into the reliability performance of highway bridges designed according to a certain code. In this case the South African code TMH-7 is used as a suitable example (Basson & Lenner, 2019).

### 5.1 Reliability performance of bridges with WIM data from South Africa

Past studies have identified deficiencies in traffic load model of the South African code for design of bridges, TMH-7 (Anderson, 2006; Oosthuizen et al., 1991). In response, the performed study by (Lenner et al., 2021) is focused on the reliability performance of TMH7 for the normal traffic conditions. The performance at the ultimate limit state (ULS) is investigated, with the traffic load effect taken as static bending moment at midspan of a simply supported bridge (excluding dynamic effects arising from to the complex vehicle-structure interaction). The study presented here is limited to only the free flow traffic, which is typically assumed to govern extreme traffic load effects for short to medium span bridges ranging from 5 to 50 metres (Bruls, Croce, Sanpaolesi, et al., 1996). Dynamic investigations of traffic loads on road bridges of are summarized in a different work by (Meyer et al., 2021) under the supervision of the author of this text.

In achieving the study's purpose to investigate the performance of the code, reliability analyses were performed for two case studies based on actual traffic load effects derived from WIM data available in South Africa. For each analysis, reliability indices were obtained as the indicative measure of the safety level. The results were compared to the target reliability values from existing standards to draw inferences regarding the performance of TMH-7 for normal traffic loading. The particular investigations were split in:

- A case study based on WIM data obtained from Roosboom station, where the data served in reference studies shown in Section 3.1.1 and Section 4.2.1. In this case, traffic load extremes of a single lane were investigated and compared to the design values from the traffic load model.
- A case study focused on WIM data from Kilner Park, where the data were used in MLF investigation in Section 3.2.2. In this case, a full probabilistic analysis of a critical element including its resistance evaluation is presented.

The scope of each case study is dictated by the number of traffic lanes measured at the WIM site. For Roosboom only the slow (outer) lane data per direction are available, which is a limitation for a full probabilistic reliability analysis. This is why the focus is only the modelling of traffic load extremes. Using the semi-probabilistic approach, the traffic load effects are assigned with a fixed sensitivity factor  $\alpha$  and the design value is derived from the data as an appropriate fractile of a fitted probability distribution. The second case study based on the data from Kilner Park then provided a fully probabilistic reliability analysis. Two lanes per direction were measured at this site and it was therefore possible to develop a meaningful loading due to collected WIM data on a typical bridge deck. A 20 m two-lane, single span bridge was selected as a representative example. A critical element reliability analysis was carried out including the resistance, permanent and traffic load effect variables. A sensitivity analysis followed to determine the relative significance of the basic variables on the obtained reliability indices.

### **5.1.1 Roosboom case study (RCS)**

The first case study presented here based on (Lenner et al., 2021) consists of a reliability analysis considering isolated traffic load effect based on seven years of WIM data for a single lane, basically comparing the code values with those obtained from measured data. It was first necessary to obtain the distribution function describing the WIM based load effect and then formulate the limit state function. This enabled the calculation of the reliability index by means of the First Order Reliability Method (FORM). Sagging bending moment of a simple span beam were considered in increments of 5m for 5m to 50m span length in order to limit the scope.

Consideration of single loading events leads to a distribution of the load effects that need to be described by a probability distribution. As discussed at length in Chapter 2, there are different approaches that vary from utilising basic fitting of a normal distribution to the population or to the tail (Nowak, 1993;

---

Nowak & Rakoczy, 2013; Soriano et al., 2017) to the more common extreme value theory and tail fitting (Coles, 2001; Enright, 2010; Leahy et al., 2015)

A block maxima approach was adopted in this study as it is a proven and effective technique in studying extreme traffic events, refer to Section 2.6.1. It essentially isolates a maximum event in each block. To utilise the technique, the underlying assumption is that the data must be independent and identically distributed *iid* (Coles, 2001), with a minimum size of a block equal one day (Caprani, 2012). However larger blocks tend to remove variations in observations and yield data that better adheres to the *iid* requirement. Considering seven years of available recordings, monthly maxima of the bending moment were used in the presented study. On contrary to the approach specified in 2.6 and 3.2, a simplified methodology as developed by (Holický, 2013) was adopted to explore a wide range of extreme value distributions and to illustrate the process. The method of (Holický, 2013) is particularly useful in finding applicable models by plotting the skewness and the coefficient of variation of the data set against plotted distributions. Considering the obtained monthly blocks for each span length and evaluating the statistical properties of the monthly maxima, the sample skewness and coefficient of variation, denoted by  $\alpha$  and  $V$  respectively, are used to plot data points on the developed diagram for each span length.

Figure 29 clearly indicates the fit of the data to various distributions including the GEV family, i.e. the Gumbel, Fréchet and Weibull distribution. The  $V$  ranges between 0.08 and 0.10, which indicates a relatively narrow distribution shape in comparison to the characteristics of daily and weekly maxima where  $V$  ranges 0.12 to 1.16 and 0.10 to 0.14 respectively, see (Basson, 2020) for full details. All span lengths have a positive skewness (right tail) equal to or less than 0.8, except for a 15 m span that has a small negative skewness (left tail). Furthermore, the skewness for the 10 m and 15 m spans can be observed as close to zero, which indicates a distribution that approaches a normal distribution, refer to (Basson, 2020).

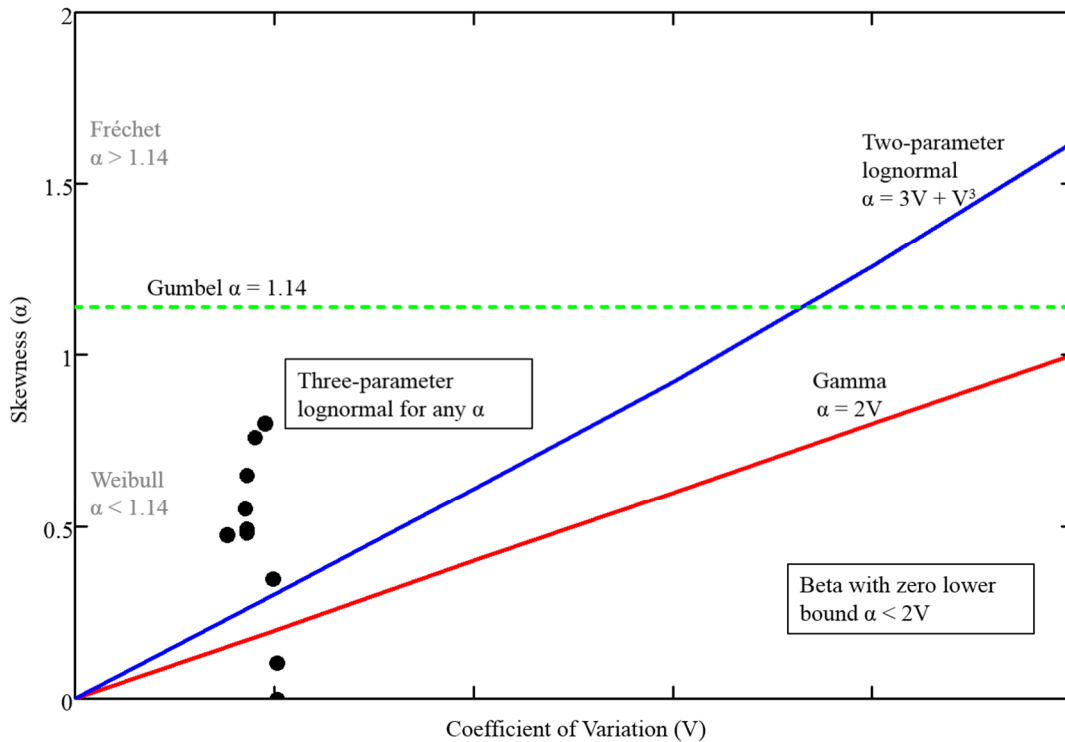


Figure 29: Relation between skewness and coefficient of variation for monthly maxima for each span length RCS; the points indicate  $V$  and  $\alpha$  for various span lengths (Basson, 2020)

Most of the points in Figure 29 are located above the two-parameter lognormal line, which suggests that the three-parameter lognormal (LN3) distribution or Weibull distribution (for maxima) is appropriate for modelling the monthly maxima. The GEV distribution can be used conveniently, as it approaches the Weibull distribution when the skewness is less than 1.14. Both the LN3 and GEV distribution are asymmetrical and have three model parameters. Both models are flexible in allowing for both positive and negative skewness and can thus cater for different sample characteristics obtained from the different span lengths. As a result, the LN3 and GEV distribution are further investigated with an aim to decide on an appropriate model.

Goodness-of-fit tests performed assess the suitability of both the LN3 and GEV distribution in representing the monthly maxima. The tests consist of diagnostic plots and the modified Anderson-Darling (AD) test hypothesis testing. For each considered distribution, the model parameters are inferred by the maximum likelihood estimation (MLE). Visual inspection of the diagnostic plots for all span lengths shows that both models fit the data well. The points on the probability plots adhere to a straight line and a good fit is seen for the density plots. For illustrative purposes, the Q-Q plots obtained for a 5 m span are shown in Figure 30 for LN3 and in Figure 31 for GEV. The AD test is used as a numerical measure to substantiate the results obtained from the diagnostic plots. When the  $p$ -value obtained from the AD test exceeds the significance level, the data can be represented by the selected model. A significance level of 0.05 is typically accepted (Fisher, 2006). The LN3 distribution is converted to a normal distribution (Holický, 2013). As documented by (Lenner et al., 2021) the  $p$ -values exceed 0.05, which indicates that the monthly maxima can be represented by a LN3 distribution. Similar  $p$ -values

were obtained for the GEV distribution, although higher values are seen for 10 to 20 m spans. The results agree with the diagnostic plots that both the LN3 distribution and the GEV distribution can be used to adequately represent the monthly maxima.

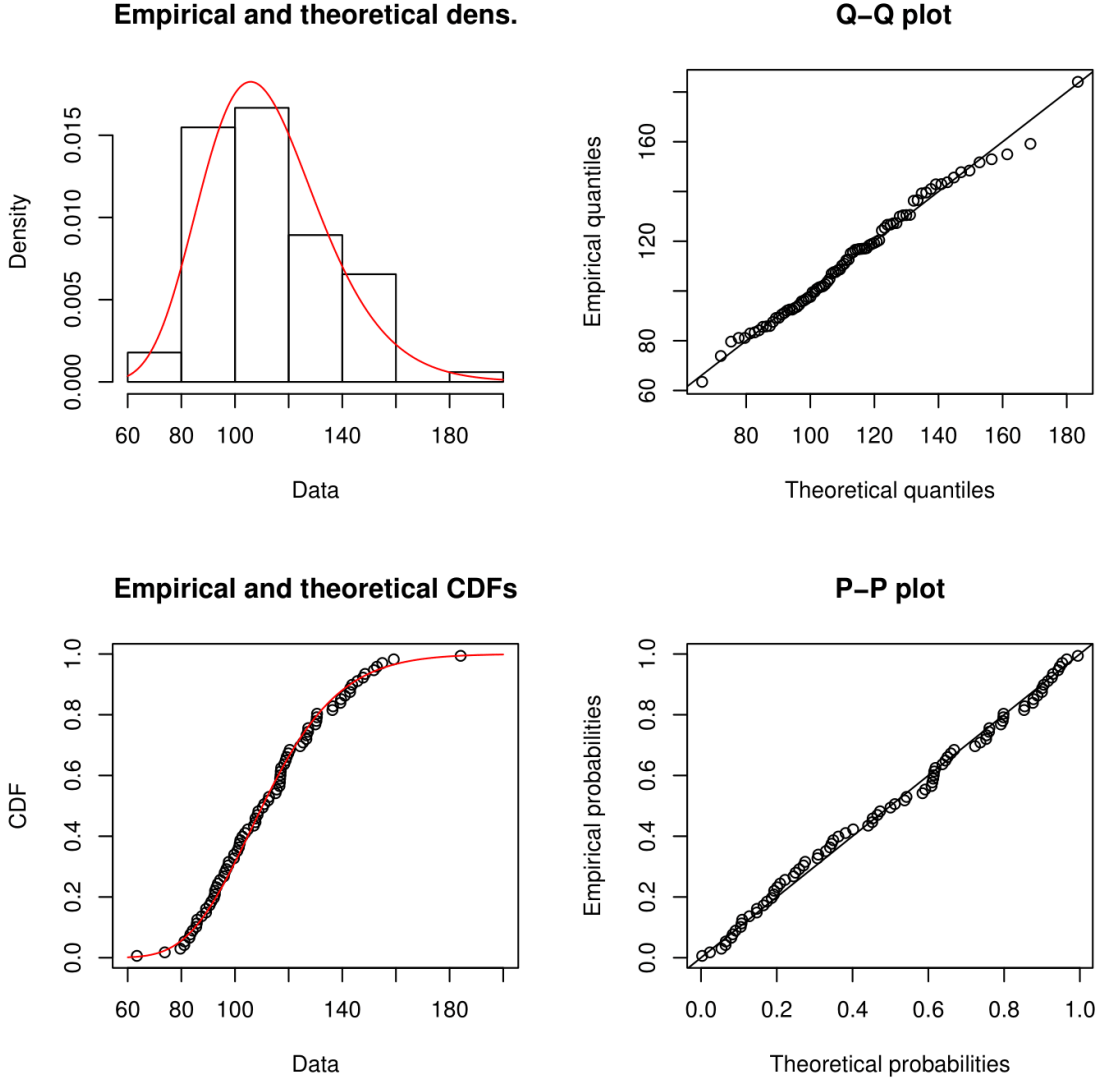


Figure 30: Diagnostic plots for the monthly maxima of a 5 m span RCS represented by the LN3 distribution (Basson, 2020)

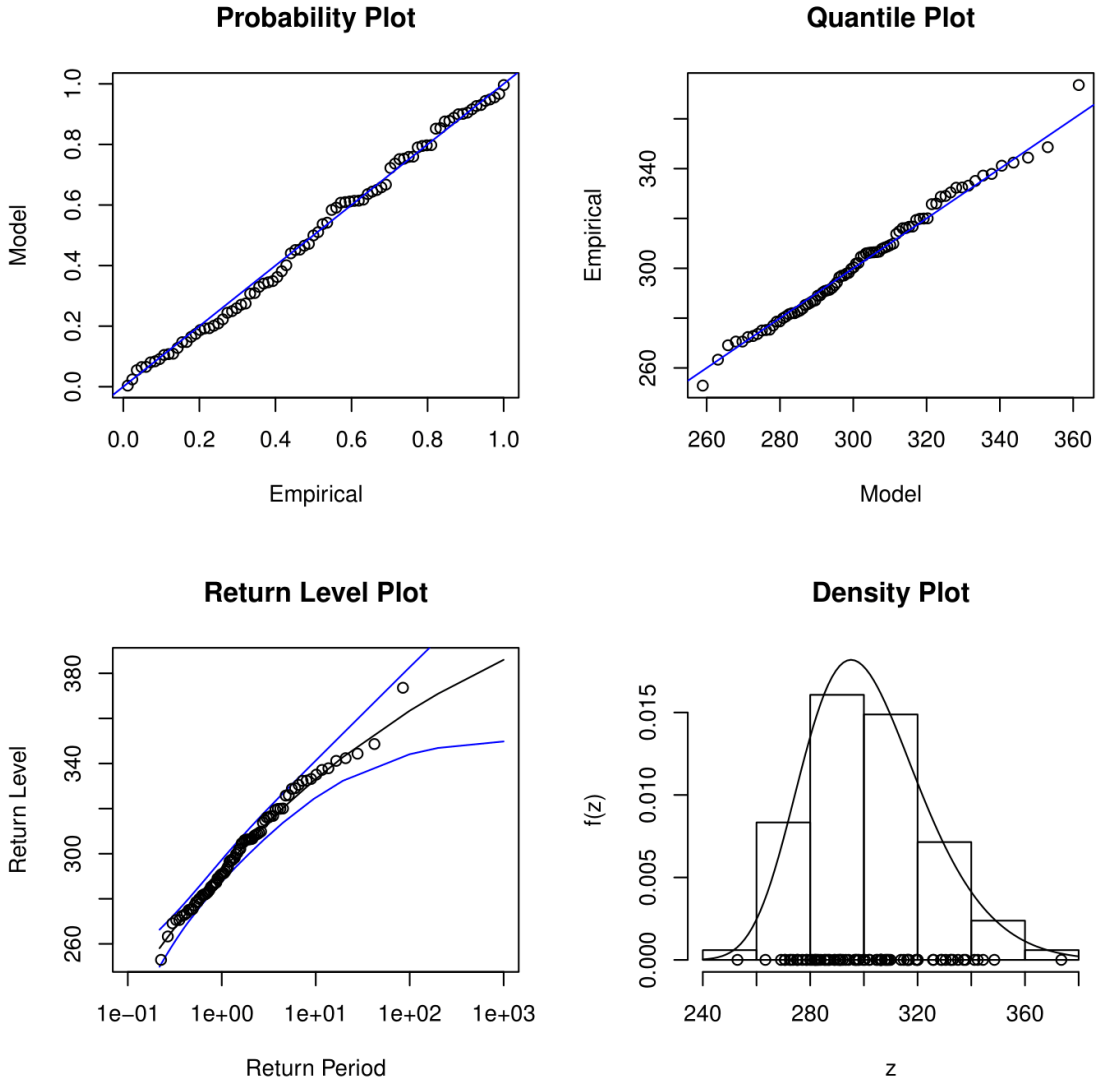


Figure 31: Diagnostic plots for the monthly maxima of a 5 m span RCS represented by the GEV (Basson, 2020)

**Design Load Effect**

The overall reliability level, described by the reliability index  $\beta$ , can be split into the resistance part  $R$  and load effect part  $E$ , refer to (ISO 2394, 2015a). For this case study, the load effect part is of interest, where the reliability level is expressed with the load effect index  $\beta_E$  equal to  $\alpha_E\beta$ . The variable  $\alpha_E$  is a sensitivity factor of traffic load effects obtained from FORM. This describes the relative importance of the load effects in obtaining  $\beta$  and is accepted in this work as -0.7 for dominant action as recommended by (EN 1990, 2002; ISO 2394, 2015a). This  $\alpha_E$  value is deemed appropriate for shorter spans, while it may be reduced for longer spans with dominant permanent load, see (Lenner & Sýkora, 2016).

When only traffic load effects are analysed, a reliability criterion can be defined as the instance when the actual traffic load effects exceed the design load effect. A reference period of 50 years is chosen in order to provide for comparison with the target reliability commonly listed in codes. Therefore, the actual load effects derived from the WIM data should correspond to a 50-year maximum. The design load effect can then be described as a fractile of the 50-year maximum load effect distribution  $F_{50}(x)$ .

---

The probability of failure  $p_f$  is then approximated by the probability that the design load effect  $e_d$  is exceeded by the traffic load effects  $E$  as shown in Equation 44. Then Equation 45 is used to estimate the overall  $\beta$ , where the probability distribution function of a standardised normal distribution  $F_U(x)$  relates  $\beta$  to  $p_f$ ,

$$p_f = P(E > e_d) = 1 - F_{50}(e_d) \quad \text{Equation 44}$$

$$p_f = F_U(+\alpha_E\beta) = F_U(-0.7\beta) \quad \text{Equation 45}$$

where  $F_U(\cdot)$  denotes the cumulative distribution function of the standardised normal variable and  $F_{50}(\cdot)$  is the 50-year maximum load effect distribution.

To obtain the maximum load effect distribution for a 50-year period, the monthly maxima distribution is statistically projected by raising the probability distribution function  $F(x)$  to an appropriate power  $n$ . For each span length, the 50-year maximum load effect distribution was obtained from both the LN3 distribution and the GEV distribution of monthly maxima. Depending on the selected model, the characteristics of the projected maximum load effect distribution differ. According to (Castillo et al., 1996), a lognormal distribution fitted to maximum values converges to a Gumbel distribution as the power  $n$  tends to infinity.

The Weibull distribution for maxima, represented by the GEV distribution, has a finite upper bound and its maximum domain of attraction remains a Weibull distribution (Castillo, 1988b). The concern with using the maximum Weibull distribution, is that the upper bound remains unchanged irrespective of the reference period projected to. This means that the 50-year maximum load effect distribution has the same upper bound as the monthly maxima distribution. This could potentially be problematic as the design load effects may exceed the bound determined by the distribution function parameters.

The physical argument that might justify the upper bound could be formulated on the basis of legal limits for axle and vehicle loads. However, the concern about frequent overloading of trucks makes this argument doubtful. Further, the LN3 distribution shows a similar fit to the monthly maxima as the GEV distribution and its unbounded right tail (for positive skewness) allows for the thorough investigation of the design load effects. As a result, a LN3 distribution is adopted in this particular case (Lenner et al., 2021) for the monthly maxima of traffic load effects.

### **Reliability analysis for traffic load effects**

The limit state function  $Z$  defines the desired failure mode for the investigation as per Equation 45. Model uncertainty  $\theta_E$  was introduced in the presented contribution as a lognormal distribution with a mean of 1.0 and a COV of 0.1 according to the commonly used in literature (fib COM3 TG3.1, 2016; JCSS, 2001b). The design load effect  $e_d$  is a deterministic value calculated according to TMH7 NA loading, while  $E_{50}$  was described by the 50-year maximum load effect distribution with a LN3 distribution. FORM was implemented to estimate failure probability for each span length.

$$Z = e_d - E = e_d - \theta_E E_{50} \tag{Equation 46}$$

The traffic load effects are derived from the WIM data for a single traffic lane as obtained from a previous study (van der Spuy & Lenner, 2019). To make a meaningful comparison with TMH-7 it was necessary to investigate different scenarios. The concept of notional lane as defined in TMH7 is different to the actual traffic lane, meaning that a notional lane is often narrower than a traffic lane. As a result, a number of different notional lanes can be fitted to a bridge deck which in reality only carries a single traffic lane (bridges are built to accommodate not only a traffic lane, but also shoulders). Four design scenarios were defined, with a first assumption of one traffic lane corresponding to one notional lane followed by the opposite view of a single traffic lane occupying a deck which is designed for three notional lanes. The same is carried out for two possible traffic lanes and three and two notional lanes respectively. A summary of the scenarios under consideration is provided in Figure 32.

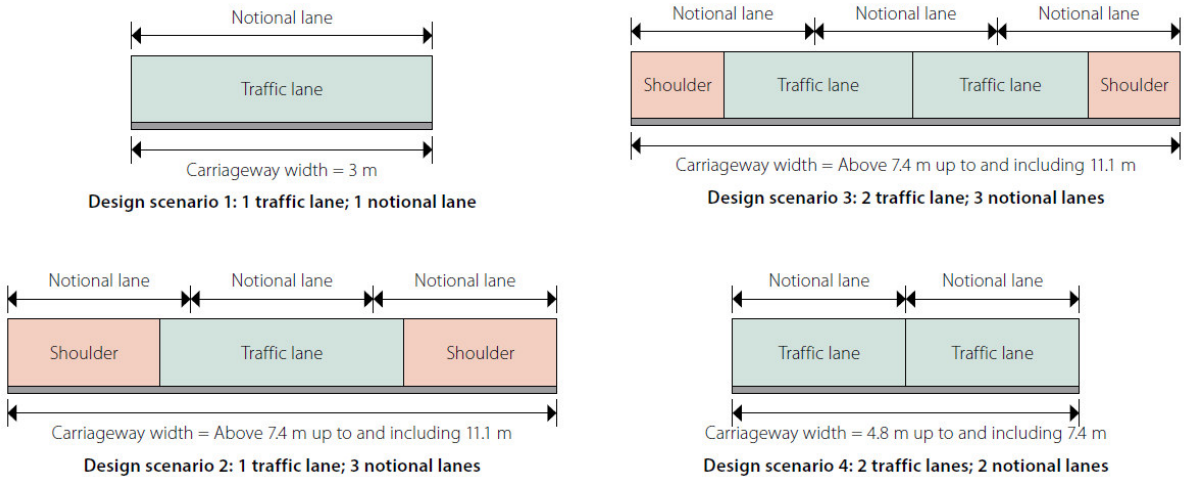


Figure 32: Design Scenarios (Lenner et al., 2021)

The WIM data in this case study is limited to a single measured lane, i.e. the slow lane. To investigate a two-lane bridge, the slow lane data needs to be utilised in such a way as to find representative load effects for the adjacent lane. A conservative assumption was made that the second lane of loading could be obtained by multiplying the slow lane load effects with a MLF = 0.75 as derived in Section 3.2.2. The calculated reliability indices  $\beta$  for each span length are given in Table 28.

Table 28: Overall reliability indices  $\beta$  provided for each design scenario and corresponding to a 50-year period of RCS.

Span length (m)	Design scenario 1	Design scenario 2	Design scenario 3	Design scenario 4
5	-1.2	9.7	3.8	-0.7
10	-1.6	10.8	4.2	-0.7
15	1.2	15.0	7.5	2.3
20	1.7	10.6	6.1	3.2
25	2.8	10.3	6.2	3.6
30	3.8	10.6	6.6	3.9



Span length (m)	Design scenario 1	Design scenario 2	Design scenario 3	Design scenario 4
35	4.3	10.4	6.4	3.9
40	5.1	10.1	6.3	3.8
45	5.2	10.2	6.5	4.0
50	5.6	10.7	6.9	4.4

In order to make a meaningful comparison of the obtained results for a 50-year reference period (EN 1990, 2002) recommends  $\beta_t = 3.8$  while the South African Standard (SANS-10160-1, 2009) uses a  $\beta_t$  of 3.0 for the same reference period. It is readily observed that the way each scenario is defined, is fundamental to the obtained reliability index. The extreme case of one notional lane to one traffic lanes shows very low  $\beta$  (therefore high probability of failure) for short spans while for spans  $\geq 25$  m the performance is deemed satisfactory. The poor performance in this scenario can be contributed to the way notional lane is defined, and that it is physically impossible to have one notional lane equal to one traffic lane. It is neglecting the mandatory shoulders on the roads – meaning the deck width is always wider than a traffic lane and therefore necessitates more notional lanes during the design.

On the other hand, the case of wide shoulders results in a scenario where three notional lanes are compared to a single traffic lane. In this case the obtained values show high reliability, mostly in excess of  $\beta = 10$ , leading to very low probability of failure. Care must be exercised in this case, as this is pointing only to the global action effects and it might not necessarily be true to a critical element of a bridge, for instance a single girder in a multi-girder deck. Yet, it does provide an insight into the performance of NA loading and the inherent conservatism in the definition of notional lane width. Design Scenarios 3 and 4 exhibit similar results, where two traffic lanes are considered and again, when the number of notional lanes is matched with the number of reflected traffic lanes, a poor reliability performance is observed. At the same time, for all considered scenarios, the longer span lengths prove to show satisfactory performance when a target  $\beta$  of 3.0 or even 3.8 is considered.

### 5.1.2 Kilner Park case study (KPCS)

The second case study utilises the same data as Section 3.2.2 - three consecutive years of WIM data for the two outer traffic lanes in both directions measured at Kilner Park (van der Spuy et al., 2019).

An example structure is selected for the investigation focused both on the resistance and loading side of the limit state equation. The chosen structure corresponds to a typical bridge in South Africa - A 20 m reinforced concrete bridge as twin spine deck. The effect of individual lane loading and load distribution between the two main girders is investigated in this case study.

### Bridge deck analysis and design

The cross-sectional properties of the designed bridge deck, together with the traffic lane arrangement, are illustrated in Figure 33. Two actual traffic lanes of 3.7 m width each are considered with necessary surfaced shoulders on both sides. The deterministic analysis reveals that a single spine beam is the critical member in the design. The permanent loads for the design include the dead load of the bridge deck, typical F-shape Type A parapets and asphalt road surfacing with a thickness of 40 mm. NA loading per TMH-7 (excluding dynamic effects as in the previous case study) was applied to the grillage model using three design notional lanes that correspond to the considered deck width as per requirements of TMH-7. The ULS mid-span moment for the considered beam according to the analysis equals to 11,600 kNm hence resulting in 29 Y40 steel bars required for flexural resistance (450 MPa yield strength, typical rebar strength in South Africa).

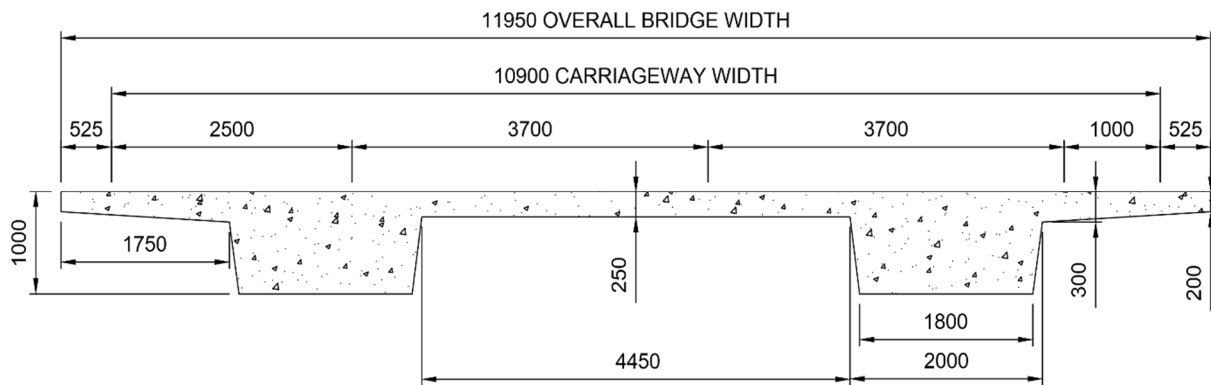


Figure 33: Cross-section of bridge deck with traffic lane arrangement (units in mm) of KPCS (Basson, 2020)

The transverse stiffness of the considered superstructure was a key factor for the load effects due to traffic as captured by the WIM. By using the transverse influence line for the critical element (Figure 34 and Figure 35) it was possible to capture the load sharing effect and determine how much of the total load was resisted by the single spine. The lateral load distribution factor (LLDF) numerically describes the contribution of each WIM lane to the bending moment in the investigated girder. Uncertainty in the lateral load distribution was accounted in the probabilistic analysis by load effect model uncertainty  $\theta_E$  as in the previous case study. A scenario of the normal traffic lanes along with a scenario of a bridge utilised by narrower three traffic lanes was investigated. The second loading scenario was provided in order to capture the possibility that a bridge initially designed for two traffic lanes with three notional lanes may actually be utilised as a three-lane bridge with reduced shoulders. Eight different load cases were considered in total as summarised in Table 29, where Nb1, Nb2 are north bound lanes 1 and 2, while Sb1, Sb2 are south bound lanes 1 and 2. Lane 1 in each direction is considered as the slow, heavy lane.

Table 29: Load cases considered KPCS.

Load Case	Permutations
1	Nb1; Nb2
2	Sb1; Sb2
3	Nb2; Nb1
4	Sb2; Sb1
5	Nb1; Sb1
6	Sb1; Nb1
7	Nb1; Nb2; Sb2
8	Sb1; Sb2; Nb2

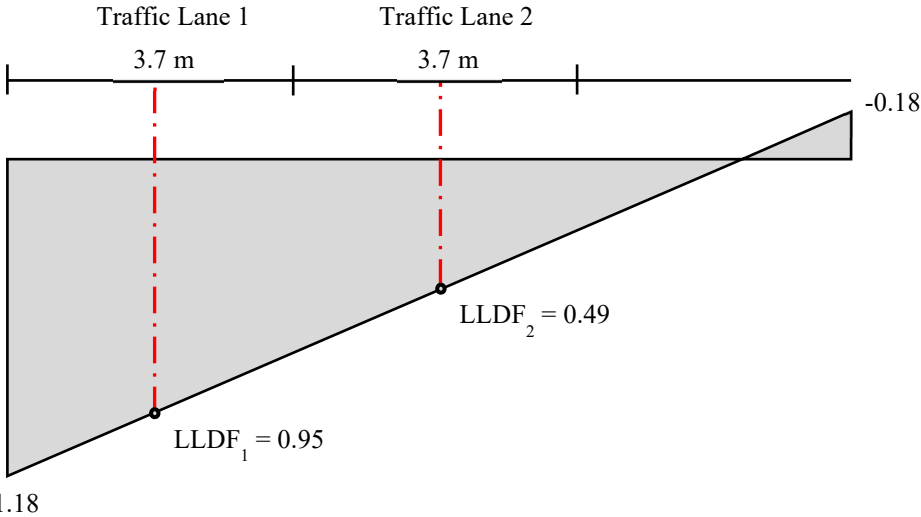


Figure 34: Lateral load distribution factors corresponding to the position of traffic load effects in two lanes (Basson 2020)

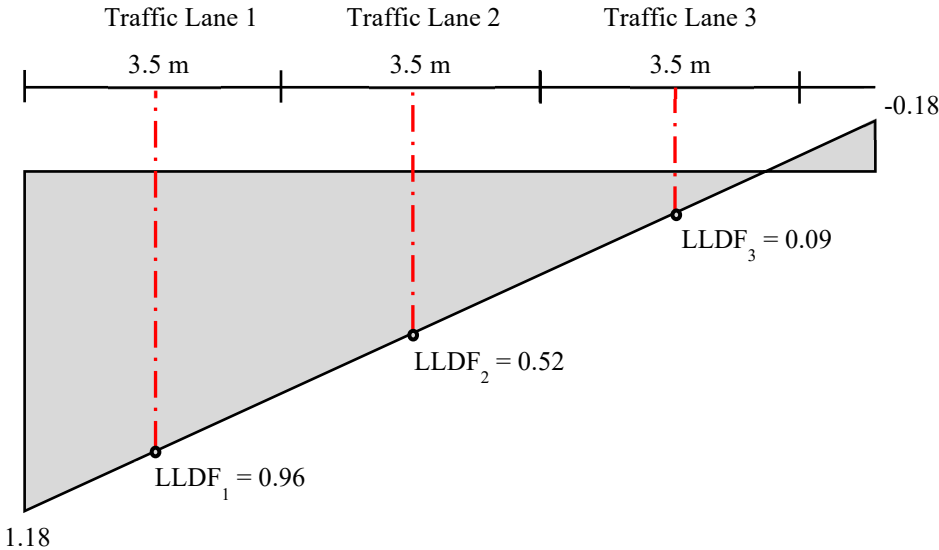
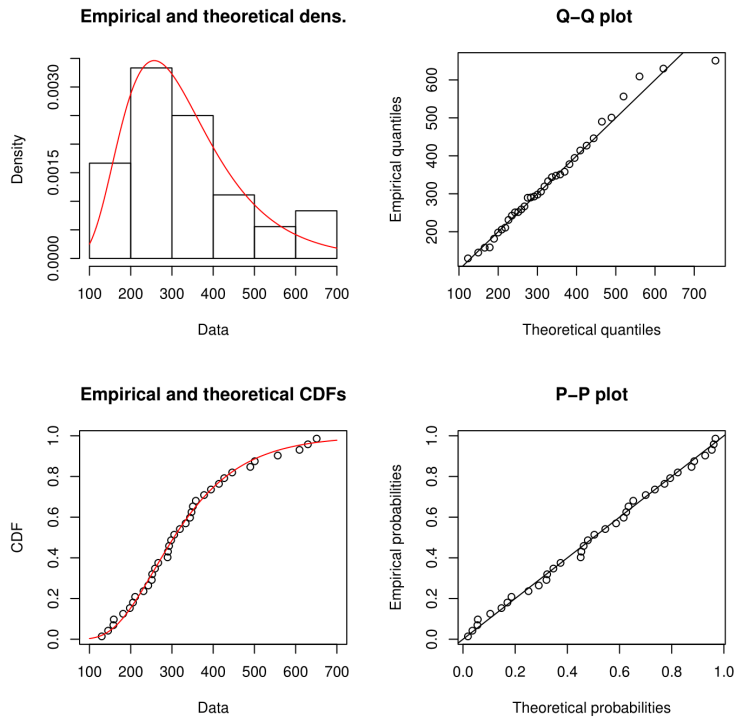


Figure 35: Lateral load distribution factors corresponding to the position of traffic load effects in three lanes (Basson, 2020)

**Probabilistic modelling of traffic load effects**

The monthly maxima combined for two opposite travel directions, representing the extreme traffic load effects for the critical spine beam were modelled and assessed similarly to the Roosboom Case Study. Figure 36 illustrates the characteristics of each load case and relates the sample skewness to the coefficient of variation. It is observed that the sample skewness varies considerably, which can be conveniently captured by the LN3 distribution. Consistently with the RCS, the use of the Weibull distribution was avoided as the fixed upper bound was deemed to be unjustified. As only extracted load effects from (van der Spuy & Lenner, 2019) were available for this project, it was impossible to determine the cause of the high skewness for the single load effect situated in the Fréchet domain.

The moment parameters for the LN3 distribution were estimated using MLE. Visual inspection of the diagnostic plots shows that the LN3 distribution fits the combined monthly maxima well. For illustrative



purposes,

Figure 37 shows the Q-Q plot for the load case when the two traffic lanes in the southbound direction are considered. As in the first case study, the adopted probabilistic model provides only an approximation of the upper tail behaviour and detailed analysis might improve traffic load extremes predictions. The 50-year maximum load effect distribution can again be obtained by Equation 9, where  $F(x)$  is the probability distribution function of the LN3 distribution describing the combined monthly maxima.

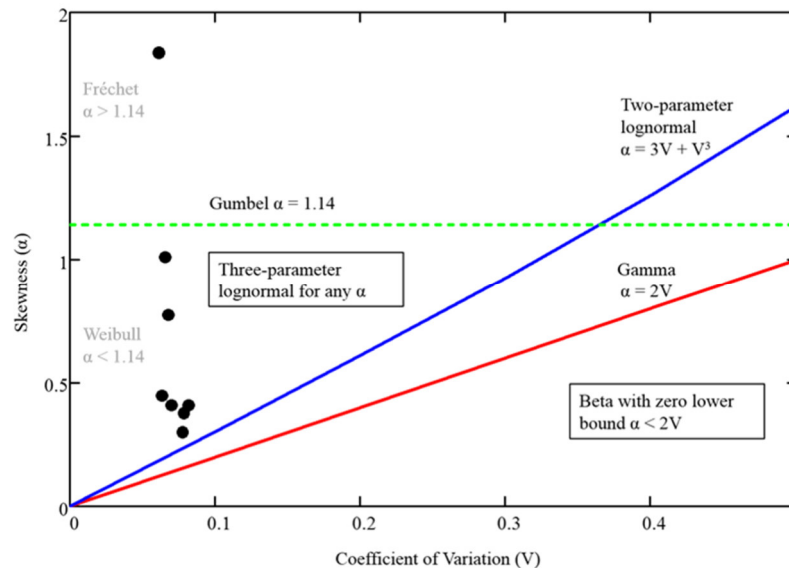


Figure 36: Relation between skewness and coefficient of variation for monthly maxima for each span length KPCS; the points indicate  $V$  and  $\alpha$  for various span lengths (Basson, 2020)

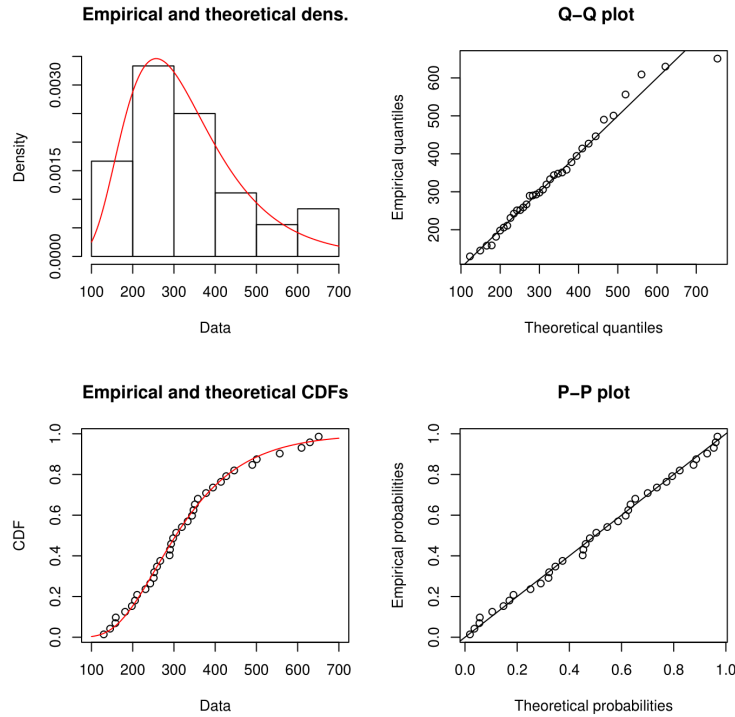


Figure 37: Diagnostic plots for two south bound lanes combined of KPCS fitted with the LN3 distribution (Basson, 2020)

**Formulation of limit state function for the critical element reliability analysis**

The limit state function in Equation 47 is used to determine the reliability performance of the bending moment capacity of the critical spine beam at ULS. The function consists of independent basic variables that describe the resistance, permanent load, traffic load effects and model uncertainties relevant to the critical spine beam to produce this equality:

$$Z = \theta_R f_y A_s \left[ 1 - \frac{f_y A_s}{1.34 f_{cu} b d} \right] d - \theta_G (G + G_w) - \theta_Q Q \tag{Equation 47}$$

Table 30 defines the basic variables presented Equation 46 with respective probabilistic models. Due to ambiguities in model uncertainty models presented by various researchers, two different models of uncertainty for the resistance are further investigated in order to assess the sensitivity of their parameters.

Table 30: Conventional probabilistic models describing the basic variables in the limit state function.

Name of basic variable	Symbol of basic variable (X)	Unit	Distr. type	Mean ( $\mu_X$ )	Standard deviation ( $\sigma_X$ )	Reference
Dead load	$G$	kNm	N	$G_k$	$0.05\mu_X$	(Holický, 2009)
Superimposed dead load	$G_w$	kNm	N	$G_{wk}$	$0.1\mu_X$	
Traffic load (50 years)	$Q$	kNm	LN3	Based on moment parameters of 50-yr maximum load effect distribution		

Name of basic variable	Symbol of basic variable ( $X$ )	Unit	Distr. type	Mean ( $\mu_X$ )	Standard deviation ( $\sigma_X$ )	Reference	
Concrete strength	$f_{cu}$	kPa	LN	$f_{cu,k} + 1.645\sigma_X$	$0.18\mu_X$	(Holický, 2009)	
Yield strength	$f_y$	MPa	LN	$f_{y,k} + 1.645\sigma_X$	30		
Effective flange width	$b$	m	Det	$b_k$	0	Measured in-situ	
Effective depth to reinforcement	$d$	m	N	$d_k$	$0.02\mu_X$	(Lenner & Sýkora, 2016)	
Area of reinforcement	$A_s$	m <sup>2</sup>	N	$1.02*A_s$	$0.02\mu_X$	(Steenbergen & Vrouwenvelder, 2010)	
Permanent load model uncertainty	$\theta_G$	-	N	1	$0.07\mu_X$	(Lenner & Sýkora, 2016)	
Traffic load model uncertainty	$\theta_Q$	-	LN	1	$0.1\mu_X$	(Allaix et al., 2016b; Sýkora & Holický, 2012)	
Resistance model uncertainty	Model 1	$\theta_R$	-	LN	1	$0.06\mu_X$	(Allaix et al., 2016b)
	Model 2	$\theta_R$	-	LN	1.1	$0.1\mu_X$	(Sýkora et al., 2015)

Note: abbreviations for distributions N – normal, LN – lognormal, Det - deterministic

### Reliability analysis results

Reliability analysis of the critical element was again performed using FORM. Overall reliability indices  $\beta$  obtained for each load case depend on the selected model of the resistance model uncertainty  $\theta_R$ . For Model 1, the obtained  $\beta$  values range between 6.2 and 7.8, whereas for Model 2, the values range between 6.2 and 7.0. The lowest  $\beta$  was obtained for Load case 8, when three traffic lanes were positioned on the bridge and the slow lane in the southbound direction had the largest loading contribution on the critical spine beam. It is seen that an addition of another traffic lane is not as influential as in the RCS due to the reduced influence of additional lane according to the transverse stiffness.

The range of  $\beta$  values is contributed to the varying statistical moments for  $Q$  amongst the load cases under consideration. The higher the mean, coefficient of variation and skewness of the traffic load effects, the lower the obtained  $\beta$  values are. Depending on whether the traffic moves in the northbound or southbound direction and whether a slow lane or a fast lane is located above the critical spine beam, the moment parameters describing the traffic load effects vary. The results show the importance of investigating different load cases to find the governing load case for the critical member under consideration. For future studies, it is recommended to identify and separate different loading event types. By fitting distributions to the individual loading event types, the accuracy of the probabilistic models should improve. This will also lend further support to the assumption of independent identically distributed extremes of traffic load effects. The results also show that the coefficient of variation of  $\theta_R$  influences  $\beta$ , which agrees with literature (Allaix, 2007; Holický & Retief, 2005)

When comparing the results to target reliability indices  $\beta_t$  of 3.8 and 3.0, the obtained  $\beta$  values were significantly higher. This observation shows that TMH7 NA load model exhibits satisfactory reliability performance for the bending capacity of a critical elements of a 20 m twin spine deck, but might be deemed uneconomic. According to (Matos et al., 2019) uneconomically high  $\beta$  values (larger than 5-6) could be expected for structures in a good condition. The high  $\beta$ -levels are also in agreement with the results of the previous study (Teichgräber et al., 2018) who found many sources of “hidden safety” in the traffic-load model LM1 in EN 1991-2, leading to ~25% overdesign. Future research should investigate other bridge deck types for a 20 m span to determine whether the reliability results concur with the results of the twin spine deck. In addition, it is also recommended to investigate shear as a failure model.

### Sensitivity analysis results

The FORM analysis also provides the sensitivity factors  $\alpha$  for all basic variables. The factor indicates the influence of a variable on the obtained  $\beta$ . As  $|\alpha|$  numerically increases, so does the significance of the basic variable. Note that  $\sum \alpha^2 = 1$ , when all the basic variables in the limit state function are considered in the summation. Thus,  $\alpha^2$  describes the relative importance of each basic variable. The primary focus of the sensitivity analysis was Load Case 2, 3 and 8, where the lowest  $\beta$ -values were obtained. Variables  $Q$ ,  $\theta_R$ ,  $f_y$  and  $\theta_Q$  show the largest significance, with  $Q$  and  $\theta_R$  having the highest  $\alpha$ -values. Considering the two models for  $\theta_R$ , Figure 38 provides the relative importance  $\alpha^2$  of the most significant variables for Load Case 2, 3 and 8. From Model 1 to Model 2, the coefficient of variation of  $\theta_R$  increases and, in response, the relative importance of  $\theta_R$  also increases, whereas  $Q$  becomes less significant. This would justify considering a reduced value of the sensitivity factor for traffic load effect, well below |0.7|. However, as a next step of future research it is recommended to verify and improve the theoretical probabilistic models used for the basic variables, especially  $\theta_R$ . Actual data would improve the uncertainty quantification of a variable, which in turn would improve the accuracy of  $\alpha^2$  and the obtained  $\beta$ .



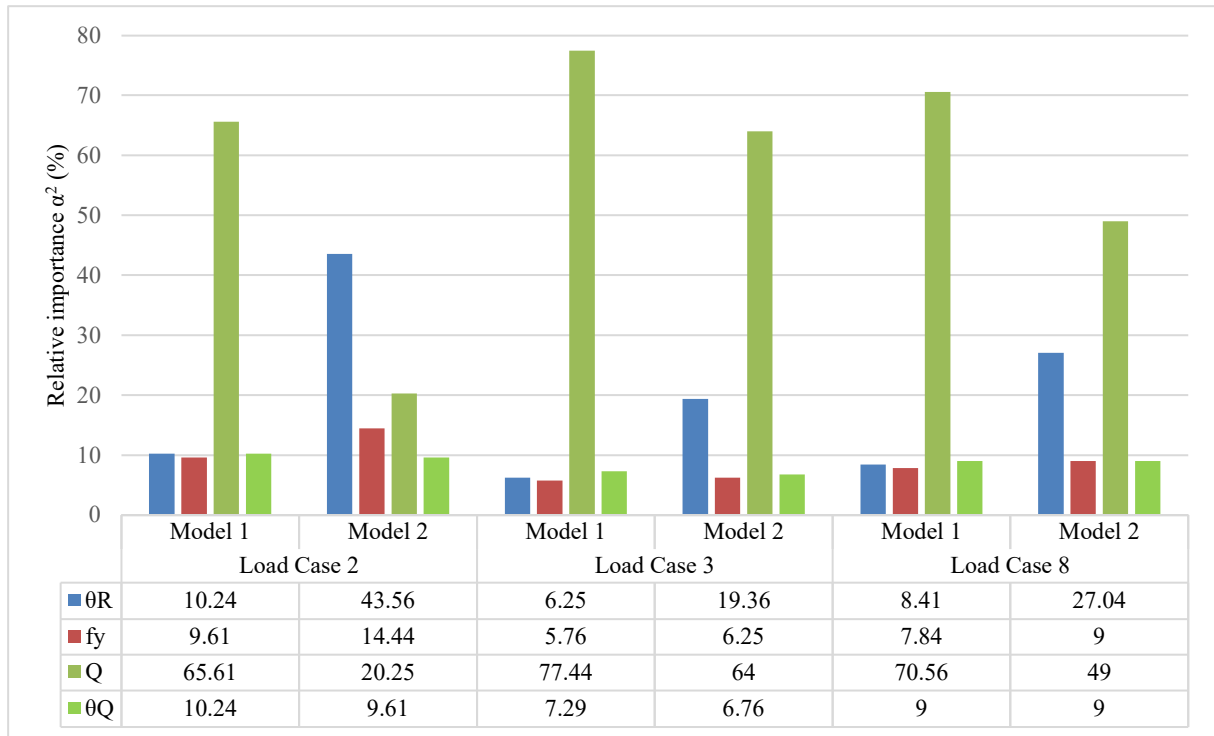


Figure 38: Relative importance  $\alpha^2$  of the resistance model uncertainty  $\theta_R$ , yield strength  $f_y$ , traffic load (50 years)  $Q$  and traffic load model uncertainty  $\theta_Q$

## 5.2 Discussion

In the presented analysis, uncertainty in WIM was neglected. The previous studies (Jacob & Feypell-de La Beaumelle, 2010; Morales-Napoles & Steenbergen, 2014) classified WIM systems into low-speed (5-15 km/h) and high-speed (normal speeds of the traffic flow). The latter of interest here - are expected to have accuracy of 10-25% for 95% of vehicles, while the accuracy of the former is much higher (estimated to 3–5%). The accuracy depends on the calibration of a WIM system; the key issue is to remove possible biases particularly for high vehicle weights. When the bias is correctly removed (as assumed in this study), uncertainty in WIM measurements is deemed to have a small influence on predicted traffic load effect extremes. A work by (de Wet, 2010) shows that WIM errors in South Africa are generally less than 10%. The accuracies mentioned here fall within the B(10) accuracy class of COST 323 which are suitable for the development of bridge live load studies (COST 323, 1998). (O'Connor & O'Brien, 2005) show that an accuracy as low as C(15) does not have an appreciable effect on predicted extreme values. Yet, this is to be investigated in detail within further research.

The here presented example study of reliability assessment was limited to the investigation of static effects only. If DAF were included,  $\beta$ -levels would mostly increase as typically conservative nominal value of DAF is considered in design while measurements typically suggest very low dynamic amplification due to heavy traffic (besides effects on local or short-span members). DAF commonly exhibits an inverse proportionality between the dynamic amplification and vehicle weight and a number of lanes, and a reduction in its scatter with increasing weight and number of lanes (Lenner & Sýkora,

2016; O'Connor & Enevoldsen, 2007). As the results of this study are presented only for sagging moments, it is suggested to interpret the achieved reliability performance of the code with caution.

### 5.3 Conclusions and recommendations

The Roosboom Case Study, considering separately traffic load effects with an assumed sensitivity factor  $\alpha_E = -0.7$ , indicated that NA loading generally performs well for spans ranging from 15 to 50 metres in length. However, a poor reliability performance was seen for short narrow span bridges, especially for 5 m and 10 m spans. That is, when the number of traffic lanes is equal to the number of notional lanes for NA loading. The findings agree with (Anderson, 2006) and (van der Spuy & Lenner, 2019) who also found deficiencies in the NA loading for short span and narrow bridges. The generally acceptable performance of the rest of the bridges could be contributed to the relatively high partial factor, but mostly to the nature of the notional lane definition of the NA load model. Owing to the geometry of a typical highway bridge, more notional lanes of the NA model are used for design than the bridge can physically carry. The Roosboom case study is valuable, as it identified deficiencies in TMH7 for normal traffic conditions, and it also identified span lengths that achieve a high reliability performance. This implied that the design load model could be optimised to be more cost efficient for a range of bridges. To study a reliability performance of a critical element, the Kilner Park case study entailed investigation of a single spine of a 20m twin spine deck. The results agreed with the Roosboom case study and satisfactory performance was observed. In fact, the obtained  $\beta$ -values range between 6.2 and 7.8 and far exceed the target levels  $\beta_r$  of 3.8 and 3.0 as required by the Eurocode and the SANS codes respectively.

---

## 6 Special loads on bridges

As discussed in the previous Chapter 4 and Chapter 5, the design provisions in most codes provide insufficient guidance for the assessment of existing structures and as a result, the assessment of an existing bridges using techniques provided for structural design may yield unsatisfactory performance of the structure even if the bridge is able to carry the loads with sufficient reliability. Hence the discussed techniques for the adjustment of partial factors or the adjustment of characteristic value of the normal traffic in Chapter 4. However, for both the design of new and the assessment existing road bridges, a further consideration should be given to special or permit vehicles, special loads and military traffic as discussed in a paper published by (Lenner & Sýkora, 2016) that forms the backbone of this Section. These vehicles are referred to as well-defined or special.

For well-defined vehicles, the axle loads and their spacing are known as this information is utilised in order to obtain more accurate estimates of load effects. The actions due to a single well-defined vehicle can be described with less uncertainty when compared to the load effect of a generalised traffic flow that aims to cover the real traffic at its extreme value of specified reference period. The generalised traffic may also cover possible trends, dynamic interaction of bridges with different types of vehicles and the influence of future political decisions with regard to new traffic concepts (Hanswille & Sedlacek, 2007; O'Brien et al., 2014). As the loading due to special vehicles often needs to be treated on a case-specific basis, the related considerations can hardly be entirely covered by the design codes. In fact, the provisions in the bridge codes regarding special vehicles seem to be limited (Markova, 2013) and thus the loads due to special vehicles are commonly treated in engineering practice similarly as the normal traffic.

The aim of this Section is to provide guidance and to report on traffic loads imposed by special, well-defined vehicles for the reliability assessment of existing road bridges, focusing on the Ultimate Limit State (according to (EN-1990, 2002) for the basis of structural design). The goal of the initial investigation was to propose appropriate values of partial factors for such loading.

To achieve the goal and in accordance with (EN 1991-2, 2003a) for traffic loads on bridges, the characteristic load associated with a single crossing of a special vehicle was taken as a nominal value. The distinction between single crossing and repeated crossings of the same vehicle was made. In the latter case it was considered that a permit or an authorisation is issued for a period of one year.

It was further assumed that weights and axle loads of special vehicles are guaranteed by measurements, or can be precisely determined on the basis of calculations and experience with similar transports. That is why the proposed approach took no account for possible overloading as particularly intentional overloading needs to be classified as a malevolent action or human error that is commonly deemed beyond the scope of design standards. In most cases human errors are eliminated by quality control rather than reliability elements such as partial factors that normally disregard actual failure frequencies

significantly affected by human errors. The quality control in this assumed case was represented by weight measurements.

### 6.1 Loads due to special vehicles

Traffic load models for special vehicles are included in in order to introduce a possibility to design and size the bridge for potential exceptionally heavy loading. This may be necessary for industrial areas or selected routes where extremely heavy vehicles may travel frequently. The basic design models of special vehicles are listed in an increasing manner according to axle loads and number of axles. Specific design models should cover abnormal loading considering country-specific conditions. However, the models describe a specified loading intensity rather than real vehicles. The load values may be given individually for each newly designed bridge according to the local conditions. This warrants a sufficient structural resistance when the permission to cross a bridge for a special vehicle is needed. Loads due to heavy civil vehicles can be described by the LM 3 models in Annex A to (EN 1991-2, 2003a) whilst military vehicles are defined according to the NATO standardisation agreement (STANAG 2021, 2006).

It is important to note that the design process may ensure a required structural resistance for normal traffic, but it does not guarantee any authorised crossing by a specific special vehicle. The load effect of such a vehicle must be assessed individually and compared to the resistance levels. The authorised special loading may then take form of a vehicle transporting heavy freight, or a military vehicle in an emergency or crisis situation when response to a threat is necessary.

Generally, three Traffic Situations were distinguished in the referenced study:

1. Special traffic load along with normal traffic.
2. Special traffic load only with no other traffic allowed on the bridge.
3. Special traffic load under strictly defined conditions in terms of the vehicle's position and speed with no other traffic allowed.

It was decided that should a specific vehicle be authorised to cross a bridge, properties of the vehicle must to be known in advance for estimation of the load effects. That is why it was hereafter accepted that the axle loads and axle spacing of the vehicle under consideration are known and the load effect can be calculated with enhanced accuracy.

Traditional semi-probabilistic safety concept is based on the use of partial factors for both resistance and loading. (EN-1990, 2002) lists the partial factors for actions commonly considered in verifications of limit states. The provisions for military vehicles including the Military Load Classification system were recently investigated and the partial factors calibrated in (Lenner et al., 2014). It may be understood from (EN 1991-2, 2003a) that special vehicles under the LM 3 provisions are treated with partial factor  $\gamma_Q$  for traffic loading that is generally applied to normal traffic conditions described by the design model LM 1.

---

A comparison of the LM 1 and LM 3 models reveals the following:

- LM 1 attempts to represent the characteristic load of real traffic with its predicted trends, while the special loading relates to a single, well-defined vehicle.
- The characteristic value of the LM 1 model corresponds to a 1000-year return period. For special vehicles the mean value is commonly accepted as a characteristic value. Consequently, a considerable reliability margin is thus included in the characteristic value for normal traffic compared to special vehicles.
- Dynamic effects are included in models for normal traffic in current bridge codes; they need to be assessed separately in the case of special vehicles.

For these reasons using the same partial factors for the LM 1 model and for well-defined special vehicles is inconsistent and calibration is needed in order to specify more appropriate partial factors for the load effects due to special vehicles.

### 6.1.1 Load Combinations

Partial factors  $\gamma_Q$  derived in the presented study are intended to be applied in conjunction with the load combination rules given in (ISO 22111, 2007) that are consistent with ASCE, AS/NZS (Australian/ New Zealand Standard) standards and Eurocodes. As an example the load combination rule (6.10a,b) of (EN-1990, 2002) is shown here; with no prestressing applied, the reliability verification format can be written as (a less favourable expression is decisive):

$$R_d \geq E_d = \sum_j \gamma_{G,j} G_{k,j} \text{ "+" } \sum_i \gamma_{Q,i} \psi_{0,i} Q_{k,i}; \quad j \geq 1, i \geq 1 \quad \text{Equation 48}$$

$$R_d \geq E_d = \sum_j \xi_j \gamma_{G,j} G_{k,j} \text{ "+" } \gamma_{Q,1} Q_{k,1} \text{ "+" } \sum_i \gamma_{Q,i} \psi_{0,i} Q_{k,i}; \quad j \geq 1, i > 1 \quad \text{Equation 49}$$

where  $R$  denotes resistance;  $E$  load effect;  $\gamma$  partial factor;  $G$  permanent action effect;  $Q$  variable action effect;  $\xi$  reduction factor for unfavourable permanent actions; and  $\psi_0$  factor for combination value of a variable action. The subscripts "d" and "k" denote design and characteristic values, respectively. The symbol "+" implies "to be combined with" and  $\Sigma$  "the combined effect of". Note that favourable variable actions are not considered in structural verifications based on the partial factor method.

In principle the partial factors  $\gamma_X$  and the characteristic values  $X_k$  shall be based on real material properties and actions. Values of the factors  $\xi$  and  $\psi_0$  are to be accepted from a relevant standard such as (EN-1990, 2002).

The load effect due to a special vehicle  $Q_{\text{spec}}$  was assumed to be a leading variable action and thus other variable actions (normal traffic, wind, thermal actions etc.) were always considered by their combination values  $\psi_{0,i} Q_{k,i}$ . The effect of a special vehicle should consistently dominate over the effect of normal traffic for the bridges of short to medium spans. For long span bridges the special vehicle will likely affect reliability of local structural members rather than reliability of main girders.

The partial factor  $\gamma_G$  should be assessed considering available information regarding permanent actions (taking into account possible geometrical measurements and material tests); in particular the distinction between structural design and assessment of an existing bridge should be made. For simplification the partial factor  $\gamma_G$  was considered in the referred study as follows:

- A reduced value 1.15 ( $\xi \gamma_G$ ) may be accepted for the assessment of an existing bridge when measurements of geometry and volume densities are available and uncertainties in the effect of permanent actions are significantly reduced.
- In other cases, including the design phase or assessment with insufficient data on permanent actions, a value of  $\gamma_G$  recommended in a relevant standard should be accepted.

Equation 50 can then be simplified to:

$$R_d \geq E_d = \sum_j (\xi_j) \gamma_{G,j} G_{k,j} \text{ “+” } \gamma_{Q_{spec}} Q_{k,spec} \text{ “+” } \sum_i \gamma_{Q,i} \psi_{0,i} Q_{k,i} \quad \text{Equation 50}$$

where ( $\xi$ ) indicates that the reduction factor may be applied. With respect to the three Traffic Situations indicated in Section 6.1, the following remarks are made:

1. Special vehicle along with normal traffic – when using Eurocodes, the load model LM 1 associated with the partial factor  $\gamma_Q$  is typically combined with the special vehicle and its partial factor  $\gamma_{Q_{spec}}$ ; other actions covered by the term  $\sum_i \gamma_{Q,i} \psi_{0,i} Q_{k,i}$  may include wind or thermal actions etc.
2. Special traffic load only with no other traffic allowed – the partial factor  $\gamma_{Q_{spec}}$  is consistent with Traffic Situation 1 since the uncertainties related to the load effect due to a special vehicle are essentially unchanged.
3. Special traffic load under strictly defined conditions in terms of position and speed of the vehicle; no other traffic allowed – in this situation the partial factor  $\gamma_{Q_{spec}}$  may be different from those accepted in Traffic Situations 1 and 2 due to the controlled crossing where uncertainties in the load effect may be significantly reduced.

Transient design situations with respect to temporary conditions of the bridge due to crossing(s) of a special vehicle are considered in this contribution. Accidental design situations like crisis or emergency situations (due to e.g. natural catastrophes or the state of war) are not treated here.

### 6.1.2 Load effect of the special vehicle

It was proposed by (Lenner & Sýkora, 2016) to address the design load effect of a special well-defined vehicle according to its characteristics that differ from traditional traffic loading. Hence it was assumed that the load effect due to the passage of a special vehicle  $Q_{spec}$  can be obtained as follows:

$$Q_{spec} = \theta \delta Q_{stat} \quad \text{Equation 51}$$

where  $\theta$  denotes the model uncertainty in estimation of the load effect from the load model,  $\delta$  is the dynamic amplification factor and  $Q_{\text{stat}}$  is the static load effect including uncertainties in measurements of weights and spacing. In principle all the variables in Eq. 51 are to be treated as random variables.

Therefore, the characteristic value  $Q_{k,\text{spec}}$  is the product of characteristic values of the three basic variables that can be realistically taken equal to their mean values,  $Q_{k,\text{spec}} = \mu_{Q_{\text{spec}}} = \mu_{\theta} \mu_{\delta} \mu_{Q_{\text{stat}}}$ . The design load effect is then expressed using an appropriate partial factor:

$$Q_{d,\text{spec}} = \gamma_{Q_{\text{spec}}} Q_{k,\text{spec}} \quad \text{Equation 52}$$

Assuming lognormally distributed  $\theta$  and  $\delta$ , and a normal distribution of  $Q_{\text{stat}}$  (Lenner, 2014), a lognormal distribution can be considered for the load effect  $Q_{\text{spec}}$  since greater variability is associated with both  $\theta$  and  $\delta$  rather than with a well-described  $Q_{\text{stat}}$ . Based on these assumptions the partial factor  $\gamma_{Q_{\text{spec}}}$  is obtained as:

$$\gamma_{Q_{\text{spec}}} = Q_{d,\text{spec}} / Q_{k,\text{spec}} = [\mu_{Q_{\text{spec}}} \exp(-\alpha_E \beta \text{COV}_{Q_{\text{spec}}})] / \mu_{Q_{\text{spec}}} = \exp(-\alpha_E \beta \text{COV}_{Q_{\text{spec}}}) \quad \text{Equation 53}$$

where  $\alpha_E$  denotes the FORM sensitivity factor,  $\beta$  the target reliability index discussed in Section 7 and  $V_{Q_{\text{spec}}}$  the coefficient of variation of  $Q_{\text{spec}}$ , estimated as follows:

$$\text{COV}_{Q_{\text{spec}}} \approx \sqrt{(\text{COV}_{\theta}^2 + \text{COV}_{\delta}^2 + \text{COV}_{Q_{\text{stat}}}^2)} \quad \text{Equation 54}$$

where  $\text{COV}_{\theta}$ ,  $\text{COV}_{\delta}$  and  $\text{COV}_{Q_{\text{stat}}}$  are the coefficients of variation of model uncertainty, dynamic amplification and of static load effect, respectively.

Note that normal distribution of the loading is deemed appropriate since the properties, such as axle load and axle spacing, are normally distributed variables. This is supported by the evaluation of traffic loading and measurements of axle loads where all the applied vehicular loading followed a normal distribution (Bogath & Bergmeister, 1999).

## 6.2 Stochastic models for the load effects

Stochastic models for load effects due to special vehicles were then developed considering two possible crossing conditions:

- Special traffic load unrestricted – special loading with no restriction in terms of velocity or position on the bridge – Traffic Situations 1 and 2.
- Special traffic controlled – special loading with reduced velocity (< 5 km/h) and restricted transverse position on the bridge – Traffic Situation 3.

The stochastic model for well-defined special loading can be assessed in terms of uncertainty related to axle loads and spacing of axles. Assuming no bias in estimating  $Q_{\text{stat}}$ , the coefficient of variation of the static load effect is of particular interest. Conclusions regarding variability of the static load were drawn

from (Lenner, 2014) where numerical simulations were employed in order to quantify the expected static load effect due to passage of military vehicles over bridges. It established the effect of an uncertainty tied to the axle loads and geometrical properties of a military vehicle. Only a single vehicle on a span was simulated. The static system was represented by the relevant influence lines for simply supported, fixed and continuous beams, thus encompassing most of common structural systems. The definition of military vehicles was similar to that of special vehicles accepted here.

Using Monte Carlo simulations, random properties of vehicles were generated according to specified mean values and coefficients of variation for both axle loads and axle spacings (Lenner, 2014). The mean values were selected according to (STANAG 2021, 2006). Coefficients of variation were selected more broadly, so as to cover a wide range of situations relevant also for the variability of heavy trucks. The simulations also reflected possible uneven, random distribution of vehicle weight to axle loads and the differences between axle loads of a vehicle in motion and their static values. However, it is emphasised that significant unexpected distribution of axle loads should be mitigated during transport by measures such as restraining movements of the load on a trailer, or appropriate increase of characteristic values of axle loads in reliability verification.

It was concluded that if a vehicle defined by its axle loads and axle geometry is considered, then the variation of its static load effect  $COV_{Q_{stat}}$  is largely dependent on the coefficient of variation of axle load while the coefficient of variation of axle spacing is of minor importance. The span length  $L$  is an additional decisive factor in estimating the coefficient of variation of static load  $COV_{Q_{stat}}$ . The extensive analysis revealed the range of  $COV_{Q_{stat}}$  from 0.03 to 0.07. It was additionally shown that a value of  $COV_{Q_{stat}}$  in the given range has only a marginal influence on the reliability as indicated by the probabilistic reliability and sensitivity analysis. Therefore, it is sufficient to accept  $COV_{Q_{stat}} = 0.05$  for static load effect due to the passage of special vehicles.

In general, the dynamic effect of traffic load is influenced by a number of factors, such as maximal bridge span length, bridge natural frequency, vehicle weight, axle loads, axle configuration, vehicle suspension properties, position of a vehicle on the bridge, quality of pavement, stiffness of structural members, etc. Considerable differences exist between various approaches and no consensus has been reached among the scientific community. However, a large contribution may be attributed to vibrations of the vehicle induced by the road profile roughness, depending on the velocity and surface unevenness between the approach and the bridge deck (Cantieni, 1992).

An increase of static loading leads to a decrease of mean value of the dynamic amplification  $\mu_\delta$  (in some cases approaching unity) and also results in a reduction of its coefficient of variation (Gonzalez, 2012; Hwang & Nowak, 1991). Therefore, the dynamic component attains a minimum at the maximum loading level. A similar pattern can be observed for articulated vehicles and increasing number of axles interfering with the bridge response. Recent testing and calibration of variable loading was accomplished within the project Assessment and Rehabilitation of Central European Highway Structures ARCHES



(ARCHES, 2009). For heavy loads and smooth roadways the amplification factors typically remained below 1.1.

The dynamic response is influenced by the unevenness at the bridge approach or a damaged roadway surface. A rough road profile or a small bump can in some cases produce a significant increase of dynamic effects. Figure 39 and Figure 40 show the results adapted from (González & Znidaric, 2009) where statistical properties of dynamic amplification were numerically investigated. In this example, the *Truck* represents the normal traffic conditions while the *Crane* is selected for exceptionally heavy loading. It is observed that the mean values of the dynamic amplification factor due to the heavy loading exhibit insignificant variability for different situations A to C (A – smooth surface, B – 2cm bump and C – 4cm bump). Coefficient of variation is less than 0.10 at shorter span lengths and below 0.05 at span lengths over 7 m. For shear response, dynamic amplification exhibits similar patterns.

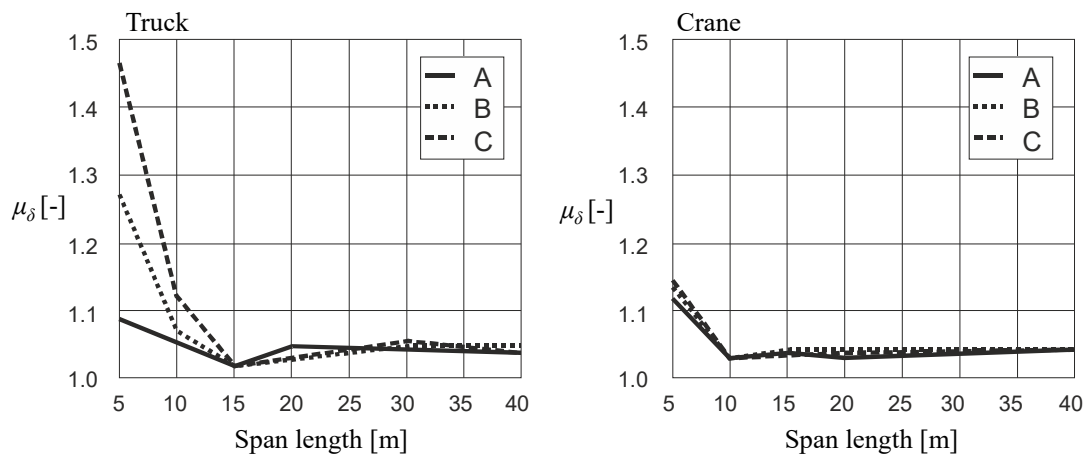


Figure 39: Mean value of dynamic amplification for bending in midspan: A – smooth surface, B – 2cm bump and C – 4cm bump (Lenner & Sýkora, 2016)

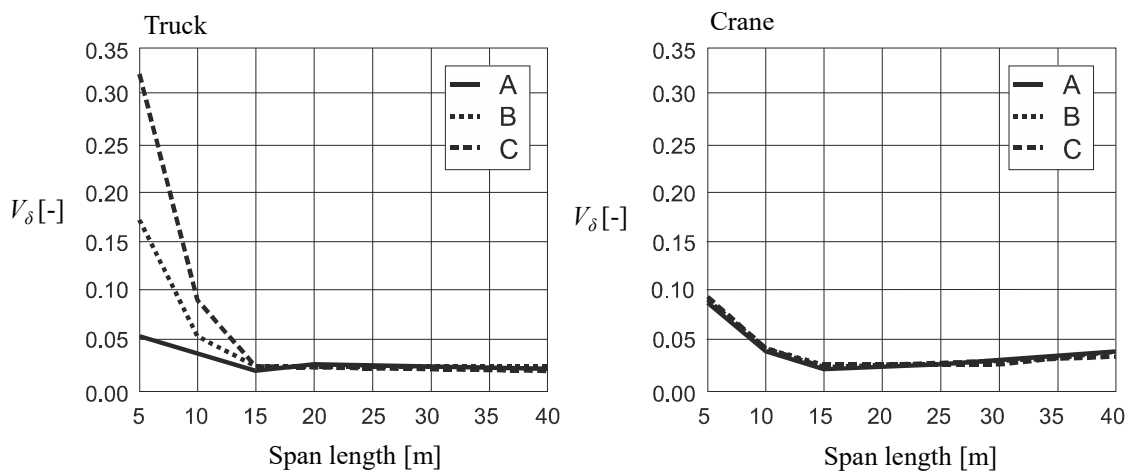


Figure 40: Coefficient of variation of dynamic amplification for bending in midspan: A – smooth surface, B – 2cm bump and C – 4cm bump (Lenner & Sýkora, 2016)

Besides road profile roughness, the dynamic amplification stochastic properties are to a certain extent dependent on the considered span length. The characteristic (mean) value of dynamic amplification  $\delta$  is clearly tied to the bridge length or natural frequency. The largest amplification of the static load and its variation  $V_\delta$  is generally observed at short span lengths. However, it should be noted that the mean value of dynamic amplification can be actually reduced for long vehicles crossing short spans. In this case, only few axles contribute to the loading and the resulting effect is positively influenced by rigidity of the vehicle or trailer, this is further elaborated by a study considering multi-trailer long vehicles (Meyer et al., 2021). Considering a typical pavement settlement in front of a short bridge, some axles of long rigid vehicles may actually jump over the bridge and thus reduce the transfer of forces between axles and the deck; or the interference between the axles of articulated vehicles results in considerable damping effects. The mean value in such a case must be assessed with caution. At the same time, the study by the author and his PhD student (Meyer et al., 2021) clearly shows that each vehicle in the general traffic stream has its loading frequency based on the length and axle configuration and is it this own frequency along with the natural frequency of the bridge that play a key role in the dynamic amplification.

It is important to realise that the coefficient of variation  $COV_\delta$  affects the value of the partial factor, while the expected mean value influences the total load effect (Eqs. 53 and 54). It was suggested in the study of load effects due to the well-defined vehicles to accept the values proposed by ARCHES for the *Crane* as relevant for special heavy vehicles. From Figure 39 and Figure 40 the following values of the mean ( $\mu_\delta$ ) and coefficient of variation ( $COV_\delta$ ) of the dynamic amplification factor were recommended for crossings by heavy special vehicles:

$$\begin{aligned} \text{For } 5 \text{ m} \leq L \leq 10 \text{ m: } \mu_\delta &= 1.15 - 0.02 \times (L - 5 \text{ m}); \quad COV_\delta = 0.1 - 0.01 \times (L - 5 \text{ m}) \\ \text{For } L > 10 \text{ m: } \mu_\delta &= 1.05; \quad COV_\delta = 0.05 \end{aligned} \quad \text{Equation 55}$$

These values consider the variation due to profile roughness or a bump between the approach and the deck. However, site-specific conditions should be carefully evaluated. Any seriously adverse conditions for dynamic amplification, such as rough profile or exceptionally short span lengths, can be then mitigated by demanding a controlled crossing. For exceptionally smooth profiles  $\mu_\delta = 1.05$  and  $COV_\delta = 0.05$  can be regarded for any span length.

According to Equation 55 the mean value of the dynamic amplification ranges from 1.05 to 1.15. It was assumed that an appropriate unbiased value is considered when determining the characteristic load effect and the mean value is thus not reflected in estimating the partial factor when the calibration of the partial factors is done for special vehicles.

Note that for the controlled crossing conditions, vehicular speeds of 5 km/h are sufficiently low to consider a quasi-static loading (González, Dowling, et al., 2010). In accordance with Annex A to (EN 1991-2, 2003a) the dynamic amplification factor need not be applied for the controlled crossing.

According to the Probabilistic Model Code (JCSS, 2001a) the model uncertainty is generally a random time-invariant variable accounting for effects neglected in the models and simplifications in the mathematical relations. Model uncertainty in the load effect  $\theta$  should cover numerous aspects including idealization of supports, composite actions of structural members, computational options (e.g. in FE analysis), description of input data and other effects not covered by a load effect model such as deviations from expected load distributions. The Model Code (JCSS, 2001) provides limited guidance regarding the selection of mean values and coefficients of variation.

A unit mean and  $COV_\theta = 0.07$  for permanent action and  $COV_\theta = 0.10$  for traffic load were therefore recommended for the development of partial factors (Steenbergen & Vrouwenvelder, 2010). (O'Connor & Enevoldsen, 2009) list the classes of uncertainties for variable loading regarding the level of confidence in modelling. The classes depend on a structural system, geometric properties and crossing mode where conditional (controlled) passage is usually associated with a higher level of confidence and thus low uncertainty in the loading model.

It can be concluded that the model uncertainty is largely influenced by the static system and the level of confidence in applied loading. The mean in the study by (Lenner & Sýkora, 2016) was generally considered as 1.0. The controlled crossing conditions was selected as associated with a reduced coefficient of variation  $COV_\theta = 0.07$ , while general crossing with uncontrolled position of the vehicle on the bridge deck was chosen as  $COV_\theta = 0.10$ .

### 6.3 Sensitivity factors and load ratio

Sensitivity factor  $\alpha$  indicates the influence of a particular variable in the limit state on the resulting reliability. These factors depend on the stochastic properties of both resistance and loading variables and can be in principle estimated for general use. (EN-1990, 2002) (Annex C) and (ISO 2394, 2015) allow for the following approximations for actions again as:

$$\alpha_E = \alpha_{E,50} = -0.7 \text{ (dominant action)}$$

$$\alpha_E = \alpha_{E,50} = -0.28 \text{ (accompanying action)}$$

However, as noted by (Lenner & Sýkora, 2016) appropriate values of the sensitivity factors should be estimated on a case-specific basis since they have a considerable influence on the partial factor  $\gamma_{Q_{spec}}$  and subsequently on the decision about crossing. They can be calculated using the FORM analysis.

It was shown during the investigation of military vehicles representing well-defined loads (Lenner et al., 2014) that the ratio  $\kappa$ , describing the relationship between permanent and variable loading (Gulvanessian & Holicky, 2005), is a key parameter affecting sensitivity factors:

$$\kappa = M_G / (M_G + M_Q) \quad \text{Equation 56}$$

where  $M_G$  denotes the characteristic permanent load effect and  $M_Q$  the characteristic traffic load effect.

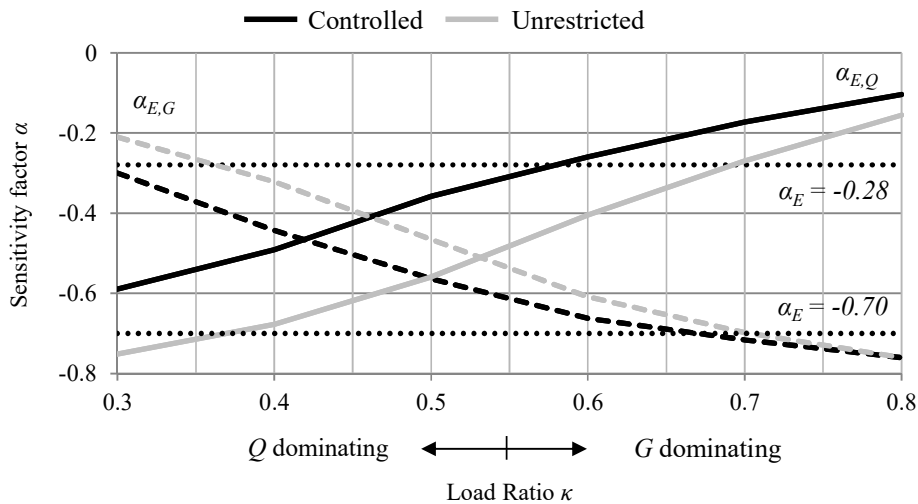
The bending limit state of reinforced concrete beam was therefore investigated in detail in a subsequent study and analysed using FORM (Lenner & Sýkora, 2016). Flexural resistance was described according to (EN 1992-1-1, 2004; EN 1992-2, 2005). Probabilistic models for all relevant variables given in Table 31 were adopted from (Braml, 2010; Sýkora et al., 2013). For controlled and general traffic conditions the respective statistical parameters are listed in Table 32.  $COV_{Q_{spec}}$  is calculated according to Eq. 54. The higher coefficient of variation for dynamic effects was omitted in the study, considering smooth profiles and/or span lengths over 10 m. Figure 41 shows the selected resulting sensitivity factors  $\alpha_{E,G}$  and  $\alpha_{E,Q}$  for permanent and variable actions, respectively, in relation to the load ratio  $\kappa$ .

Table 31: Stochastic models of basic variables for bending limit state (Braml, 2010; Sýkora et al., 2013)

Variable	$X$	Distr.	$\mu_X/X_k$	$COV_x$
Yield strength reinforcement	$f_y$	LN	490/560	0.054
Reinforcement area	$A_s$	N	1	0.02
Concrete comp. strength	$f_c$	LN	30/40	0.15
Uncertainty in resist. model	$\theta_R$	LN	1.1	0.1
Geometry	$b, d$	N	1	0.02

Table 32: Coefficients of variation for different traffic situations considered in the sensitivity analysis

Traffic situation	$COV_{Q_{stat}}$	$COV_\delta$	$COV_\theta$	$COV_{Q_{spec}}$
Special traffic load – controlled (Traffic Situations 2 and 3)	0.05	--	0.07	0.09
Special traffic load - unrestricted (Traffic Situation 1)	0.05	0.05	0.10	0.12


 Figure 41: Variation of the sensitivity factors  $\alpha_{E,Q}$  and  $\alpha_{E,G}$  with the load ratio  $\kappa$  (Lenner & Sýkora, 2016)

It appears that the influence of each random variable considerably depends on the load ratio. Clearly, an absolute value of the sensitivity factor for variable action  $\alpha_{E,Q}$  attains its maximum at a low load ratio indicating a dominant variable action whilst absolute  $\alpha_{E,G}$  is minimal.

Generally, the results in Figure 41 indicate that decreasing the variability of traffic loading decreases its associated sensitivity factor and increases the sensitivity factor for permanent loading. The numerical

investigation confirms that the leading action is likely to have a larger influence on the reliability although better described variables are likely to yield lower values of  $\alpha$ . Furthermore, flexural resistance is associated with relatively small uncertainties and thus the importance of load effects as expressed by the  $\alpha$ -factors increases. The exact value of  $\alpha$  is principally important as overly conservative approximations result in unnecessarily high partial factors. However, the  $\alpha$ -factor needs to be selected with caution to warrant adequate performance under various loading scenarios.

Depending on the level of involvement and required level of reliability verification, the following approaches to estimation of  $\alpha_E$ -factors can be accepted:

1. The approximate values given in standards (i.e.  $\alpha_E = -0.70$  for the leading action and  $\alpha_E = -0.28$  for accompanying actions) can be adopted, providing conservative values for most practical cases.
2. The values can be obtained from Figure 41 for a given ratio  $\kappa$ , provided that the assumptions made in this section apply for an investigated bridge.
3. The FORM analysis can be used to estimate  $\alpha_E$ -values.

#### 6.4 Multiple crossings

The previous analysis provides the methodology for establishing parameters of the load effect due a single crossing. In this section multiple crossings of the same vehicle or vehicles of the same type during the period covered by permit are investigated. For the authorisation a typical period of one year, during which  $n$  crossings take place, is considered.

Model uncertainties  $\theta$  and all resistance variables are a priori assumed as time-invariant components of the limit state function, and therefore are deemed independent of the number of crossings. On the other hand, the dynamic load effect obtained as the product of dynamic amplification and static load effect,  $Q_{\text{dyn}} = \delta Q_{\text{stat}}$ , is deemed to vary for each crossing due to inherent randomness of influencing factors such as velocity of the vehicle, its position on the bridge, bridge vibrations, and the effect of surface unevenness. In the absence of statistical data it is further assumed that  $Q_{\text{dyn}}$  can be described by identically distributed, independent random variables  $Q_{\text{dyn},i}$  ( $i = 1, 2, \dots, n$ ). This is a conservative assumption as static load effect and dynamic amplification are additionally affected by factors likely independent of the number of crossings, including bridge natural frequency, axle loads and configuration. Consequently, the values  $Q_{\text{dyn},i}$  are positively correlated.

The cumulative distribution function of the maximum dynamic load effect due to  $n$  crossings,  $Q_{\text{dyn},n}$ , is obtained as follows:

$$F_{Q_{\text{dyn},n}}(x) = F_{Q_{\text{dyn}}}(x)^n \quad \text{Equation 57}$$

A fully probabilistic model is developed for the maximum load effect  $Q_{\text{spec},n} = \theta Q_{\text{dyn},n}$ . Figure 42 illustrates the variation of its mean  $\mu_{Q_{\text{spec},n}}$  and coefficient of variation  $COV_{Q_{\text{spec},n}}$  with  $n$  for  $COV_{\theta} =$

0.1 and  $COV_\delta = COV_{Q_{stat}} = 0.05$ . The mean value increases with an increasing number of crossings, while the coefficient of variation is nearly independent of  $n$ . The former represents the nominal (characteristic) value while the latter affects the partial factor as follows from Eq. 51.

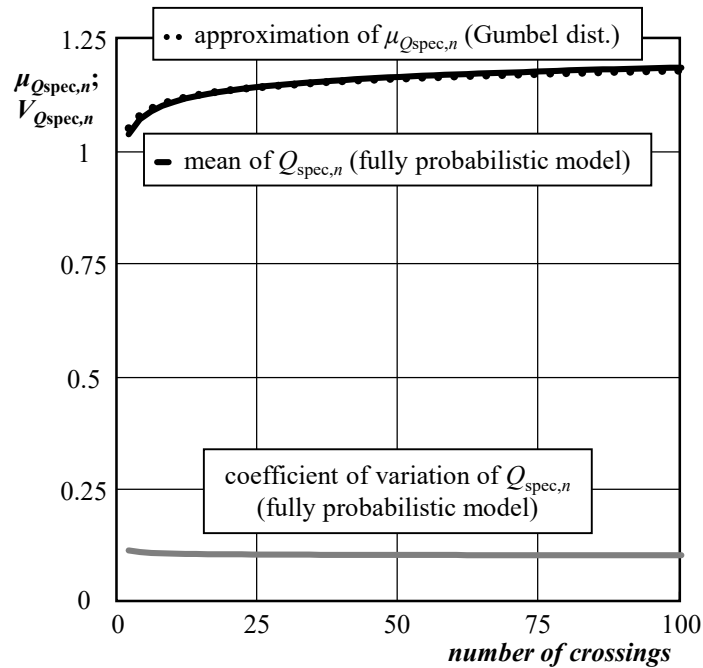


Figure 42: Variation of  $\mu_{Q_{spec,n}}$  and  $COV_{Q_{spec,n}}$  with  $n$  (for  $COV_\theta = 0.1$  and  $COV_\delta = COV_{Q_{stat}} = 0.05$ ) (Lenner & Sýkora, 2016)

That is why it is proposed to keep the partial factor  $\gamma_{Q_{spec}}$  independent of the number of crossings while the characteristic value should be adjusted with respect to  $n \geq 2$  using the following ratio:

$$\frac{Q_{k,spec,n}}{Q_{k,spec}} = 1 + V_{Q_{dyn}} \left[ \frac{4 \ln n - \ln(\ln n) - 1.377}{2\sqrt{2 \ln n}} \right] \quad \text{Equation 58}$$

Equation 58 provides the mean value of the maximum of  $n$  identically distributed, independent normal variables with unity mean and coefficient of variation  $V_{Q_{dyn}} \approx \sqrt{(COV_\delta^2 + COV_{Q_{stat}}^2)}$  (Ang & Tang, 1975). The approximation gives estimates close to those based on the fully probabilistic model as shown in Figure 42. Additional comparisons with the fully probabilistic approach reveal that, for any  $n$ , the proposed approach is sufficiently accurate for the controlled crossing associated with  $COV_\theta = 0.07$  as well as for higher uncertainty in dynamic amplification associated with  $COV_\delta = 0.1$ . The differences in design value,  $\gamma_{Q_{spec}} \times Q_{spec,k}$ , are less than 5%. Consequently the proposed approach is recommended for practical applications.

---

## 6.5 Target reliability for crossing by special vehicles

A risk-informed decision making (economic optimisation) should be conducted in order to justify the authorisation of individual or multiple crossings. In addition, human safety levels should also be adhered to whenever normal traffic is allowed to cross a bridge along with the special vehicle.

When the special vehicle is crossing a bridge along with normal traffic, risks of persons not involved in the transport should not be increased as compared to normal traffic situations. For existing bridges (Steenbergen et al., 2015) proposed the following annual target levels  $\beta_{\text{hs}}$  based on societal risk criteria:

- $\beta_{\text{hs}} = 2.7$  for span length  $L \leq 20$  m,
- $\beta_{\text{hs}} = 3.3$  for  $20 \text{ m} < L \leq 50$  m,
- $\beta_{\text{hs}} = 3.7$  for  $50 \text{ m} < L \leq 100$  m,
- $\beta_{\text{hs}} = 4.4$  for  $L > 100$  m.

These values can be accepted as minimum requirements for multiple crossings and annual permits. For instance, for medium-span bridges ( $20 \text{ m} < L \leq 50 \text{ m}$ ), economic optimisation dominates target reliabilities for  $B / C_f < 0.001$  while for higher ratios human safety criteria become decisive (Lenner & Sýkora, 2016). In the former case the benefit is too low to accept risks related to possible failure; in the latter case lower target reliability could be justified by the benefit, but minimum human safety levels need to be adhered to. For the latter case normal traffic can be restricted during crossing when lower target reliability level needs to be considered.

These target levels should be recalculated for different reference periods  $t_{\text{ref}}$  for which permits could be issued. The guidance provided in (EN-1990, 2002) assumes independent failure events in subsequent reference periods. However, this assumption cannot be accepted in the analysed case as the failure events are nearly fully correlated and the target reliabilities tend to be independent of a reference period (Vrouwenvelder, 2002). That is why it is proposed here to accept the aforementioned  $\beta_{\text{hs}}$ -values for the assessment of crossing irrespectively of a reference period  $t_{\text{ref}}$ . However, this approach can be accepted only for short reference periods, say one year or the period between main inspections, for which it can be reasonably assumed that conditions of the bridge with respect to e.g. deterioration of construction materials or pavement do not change significantly.

## 6.6 Partial factors

The here presented investigation and definition of all necessary stochastic parameters allowed for the calculation of partial factors. According to Eqs. 52 and 53 the necessary input parameters include the target reliability, sensitivity factors and coefficients of variation that can be adjusted as shown in previous sections. It is important to note that a careful review of their applicability to each considered situation is necessary. Moreover, the suggested modification of partial factors is aimed at the global

verification only. Additional local checks with modifications of the target reliability and sensitivity factors might be necessary.

As an example, partial factors are calculated and plotted in Figure 43 for the target reliability  $\beta$  from 2.7 to 4.4 and for a range of the load ratio  $\kappa$ . Partial factor  $\gamma_{Q_{\text{spec}}}$  is calculated in accordance with Eq. 53  $V_{Q_{\text{spec}}}$  is chosen as 0.12 for unrestricted traffic conditions and as 0.09 for the controlled crossing.

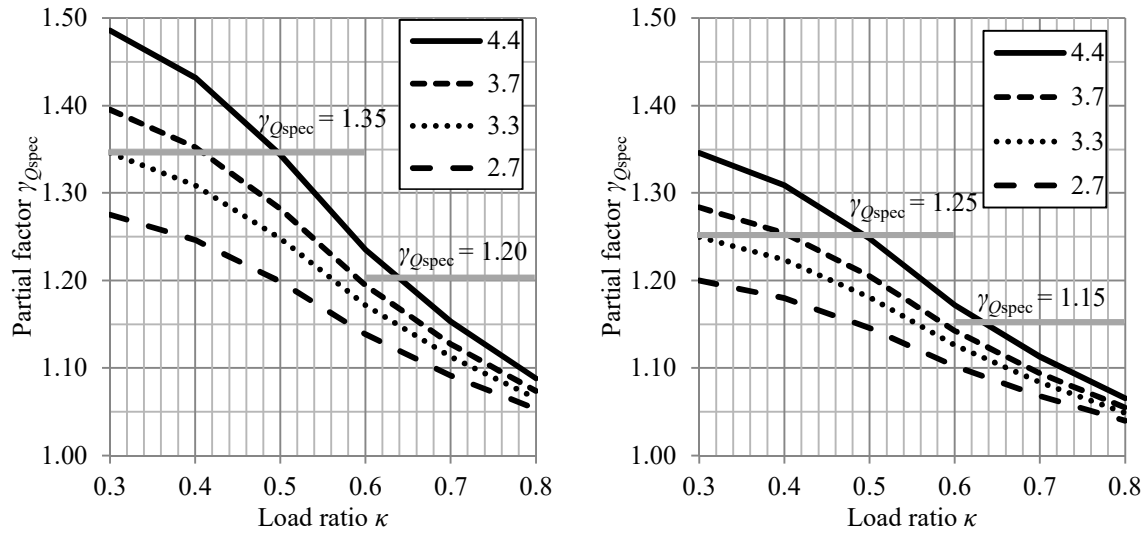


Figure 43: Variation of the partial factor  $\gamma_{Q_{\text{spec}}}$  with the load ratio  $\kappa$  for unrestricted traffic conditions ( $COV_{Q_{\text{spec}}} = 0.12$ , left) and for the controlled crossing ( $COV_{Q_{\text{spec}}} = 0.09$ , right) (Lenner & Sýkora, 2016).

It can be observed that the load ratio has a major impact on the partial factor. As the permanent load becomes dominant the partial factor significantly decreases. The selected target reliability index has a larger influence at low  $\kappa$  values. The influence of both load ratio and target reliability is less apparent for the controlled traffic loading where a lower coefficient of variation is applied.

Considering the annual target reliability index of 3.7 for long-span and 3.3 for medium-span existing bridges and sufficiently smooth profile conditions, the following values of the partial factor can be recommended for the assessment of existing bridge due to special heavy vehicles:

- For main structural members of long-span bridges ( $\kappa > 0.6$ ) -  $\gamma_{Q_{\text{spec}}} \approx 1.20$  for unrestricted traffic conditions and  $\gamma_{Q_{\text{spec}}} \approx 1.15$  for the controlled crossing,
- For short to medium span bridges and local verifications ( $\kappa < 0.6$ ) -  $\gamma_{Q_{\text{spec}}} \approx 1.35$  for unrestricted traffic conditions and  $\gamma_{Q_{\text{spec}}} \approx 1.25$  for the controlled crossing.

However, these simplified recommendations should be considered with caution. The main aim of the study here presented was to propose a framework that can be readily extended to case specific situations. The proposed characteristics of basic variables and partial factors given above were intended for general use and are currently deemed as conservative in most cases.



---

## 7 Summary and Conclusions

The here presented work aims at summarizing authors contribution so far to the field of bridge traffic modelling for the bridge design and bridge assessment. Few key contributions were selected for the backbone of the work and each chapter covers and distinctive topic. At first, the general data-driven approach of developing a load model from available WIM data with static calculations and extreme value theory is introduced as the state-of-art to include some more intricate substances such as mixed traffic and governing form of traffic. Subsequently the introduced procedure is employed to develop a notional load model for design in general terms, with an example application including multiple lane presence factors accounting for traffic occupying multiple lanes on the bridge deck. This covers the field of design from the perspective of the loading and developing of load models based on available data. In the second part of the work, the use of traffic loads for assessment is introduced as the infrastructure evidently needs it – it is ageing and the general, often conservatively chosen design load models are not suitable for the assessment of individual structures. The initial topic investigates the adjustment of partial factors within the semi-probabilistic format and then summarizes a method previously developed for the adjustment of characteristic values of traffic loads based on simply obtainable traffic descriptors. It is often the case that WIM data is not available and hence limited options exist for a more appropriate traffic loads at a specific site. However, the approach offered is based on descriptors such as AADT or percentage of long vehicles, which makes it more suitable for the engineering use. A formwork as well as validation and reliability verification were performed. When the WIM data are available, the example reliability assessment contribution offered two approaches in the reliability verification of existing structures by differently employing the obtained load effects. One case study isolated the load effects while the other considered both the load and the resistance. Finally, the work on the assessment of existing structures investigated the difference between normal traffic, that is including general vehicles crossing a bridge and between special vehicles. These might be quite bit heavier than the legal limits in particular countries, but with a better statistical description of the loads. Hence an approach to calculate the appropriate partial factors for known special loads on bridges was offered.

In conclusion, there is evidence that the assessment is gaining on importance. Even so, developing load models for design is often needed, or at least the resulting intensity must be regularly checked, or new method employed to adjust the status quo. But as the current infrastructure is largely based on existing bridges, the same level care must be taken for a proper structural and reliability treatment to be offered to secure the necessary reliability for a function network while looking at the obvious parameters such as cost. This field is constantly evolving, as new approaches appear the either validate or improve the assumptions of previous researchers leading also to better engineering practices. New vehicles will be surely introduced in future, platooning of vehicles and artificial intelligence will soon play part among others in traffic loading of bridges. Change is inevitable, the only constant is the need for further research.



---

## References

- AASHTO LRFR. (2003). *Guide Manual for Condition Evaluation and Load and Resistance Factor Rating (LRFR) of Highway Bridges*. American Association of State Highway and Transportation Officials.
- Agarwal, A., & Wolkowicz, M. (1976). *Interim report on 1975 commercial vehicle survey*.
- Allaix, D. L. (2007). *Bridge Reliability Analysis with an Up-to-Date Traffic Load Model*. *PhD Thesis*. Politecnico di Torino.
- Allaix, D. L., Botte, W., Diamantidis, D., Engen, M., Faber, M., Hendriks, M., Mancini, G., Prieto, M., Tanner, P., Thöns, S., Weber, M., Holický, M., Linneberg, P., Schnell, J., & Vrouwenvelder, A. (2016). *fib Bulletin 80. Partial factor methods for existing concrete structures* (R. Caspeele, R. Steenberg, & M. Sýkora, Eds.). The International Federation for Structural Concrete. <https://doi.org/10.35789/fib.BULL.0080>
- Anderson, J. R. B. (2006). Review of South African live load models for traffic loading on bridge and culvert structures using Weigh-in-Motion (WIM) data. *MEng Thesis*. University of Cape Town.
- Ang, A., & Tang, W. (1975). *Probability concepts in engineering planning and design*. Wiley.
- ARCHES. (2009). *Assessment and Rehabilitation of Central European Highway Structures - Final activity report: Vol. D 15*.
- Bailey, S. F. (1996). *Basic principles and load models for the structural safety evaluation of existing road bridges*. EPFL.
- Bairán, J.-M., & Casas, J. R. (2018). Safety factor calibration for a new model of shear strength of reinforced concrete building beams and slabs. *Engineering Structures*, *172*, 293–303. <https://doi.org/https://doi.org/10.1016/j.engstruct.2018.06.033>
- Basson, S. (2020). An investigation into the reliability performance of bridges designed according to TMH-7. *MEng thesis*. Stellenbosch University.
- Basson, S., & Lenner, R. (2019). Reliability verification of bridges designed according to TMH-7. *Advances in Engineering Materials, Structures and Systems: Innovations, Mechanics and Applications - Proceedings of the 7th International Conference on Structural Engineering, Mechanics and Computation*, 1865–1870. <https://doi.org/10.1201/9780429426506-322>
- Blomfors, M., Larsson Ivanov, O., Honfi, D., & Engen, M. (2019). Partial safety factors for the anchorage capacity of corroded reinforcement bars in concrete. *Engineering Structures*, *181*, 579–588. <https://doi.org/https://doi.org/10.1016/j.engstruct.2018.12.011>

- Board, T. R., of Sciences Engineering, & Medicine. (2007). *Legal Truck Loads and AASHTO Legal Loads for Posting*. The National Academies Press. <https://doi.org/10.17226/23191>
- Bogath, J., & Bergmeister, K. (1999). Neues Lastmodell für Straßenbrücken. *Bauingenieur*, 74, 270–277.
- Braml, T. (2010). Zur Beurteilung der Zuverlässigkeit von Massivbrücken auf der Grundlage der Ergebnisse von Überprüfungen am Bauwerk. In *Fortschritt-Berichte VDI, Reihe 4, Bauingenieurwesen I, Nr 214* (Vol. 4).
- BRIME. (2001). *Final Report - Deliverable D14* (Issue January 1998). Bridge management in Europe.
- Bruls, A., Calgaro, J.-A., Mathieu, H., & Prat, M. (1996). ENV 1991 Part 3: The main models of traffic loads on road bridges; Background studies. *IABSE Colloquium: Basis of Design and Actions on Structures; Background and Application of Eurocode 1*, 215–228.
- Bruls, A., Croce, P., & Sanpaolesi, L. (1996). Calibration of road load models for road bridges. *IABSE Report, Basis of Design and Action on Structures, Background and Application of Eurocode 1*, 439–453.
- Bruls, A., Croce, P., Sanpaolesi, L., & G, S. (1996). ENV1991 – Part 3: traffic loads on bridges; calibration of load models for road bridges. *Proceedings of IABSE Colloquium on Basis of Design and Actions on Structures*, 439–454.
- Calgaro, J.-A., & Sedlacek, G. (1992). EC1: Traffic Loads on Road Bridges. *IABSE Conference (Davos): Structural Eurocodes*, 81–87.
- CAN/CSA-S6-06. (2006). *Canadian Highway Bridge Design Code*. Canadian Standards Association.
- Cantieni, R. (1992). Dynamic Behavior of Highway Bridges Under the Passage of Heavy Vehicles. *Report 220 EMPA*. Dübendorf.
- Caprani, C. C. (2005). Probabilistic analysis of highway bridge traffic loading. *PhD Thesis*. University College of Dublin.
- Caprani, C. C. (2012). Calibration of a congestion load model for highway bridges using traffic microsimulation. *Structural Engineering International: Journal of the International Association for Bridge and Structural Engineering (IABSE)*, 22(3), 342–348. <https://doi.org/10.2749/101686612X13363869853455>
- Caprani, C. C., González, A., Rattigan, P. H., & O'Brien, E. J. (2012). Assessment dynamic ratio for traffic loading on highway bridges. *Structure and Infrastructure Engineering*, 8(3), 295–304. <https://doi.org/10.1080/15732471003667645>

- 
- Caspeele, R., Steenbergen, R., & Sykora, M. (2016). Partial factor method for existing concrete structures. *fib Bulletin* 80. Germany
- Caspeele, R., Sykora, M., Allaix, D. L., & Steenbergen, R. (2013). The Design Value Method and Adjusted Partial Factor Approach for Existing Structures. *Structural Engineering International*, 23(4), 386–393. <https://doi.org/10.2749/101686613X13627347100194>
- Castillo, E. (1988). *Extreme value theory in engineering*. Academic Press.
- Castillo, E., Solares, C., & Gomez, P. (1996). Probabilities Using Tail Simulated Data. *International Journal of Approximate Reasoning*, 17, 163–189.
- Cervenka, V., Cervenka, J., & Kadlec, L. (2018). Model uncertainties in numerical simulations of reinforced concrete structures. *Structural Concrete*, 19(6), 2004–2016. <https://doi.org/https://doi.org/10.1002/suco.201700287>
- Coles, S. (2001). *An Introduction to Statistical Modelling of Extreme Values*. Springer.
- COST 323. (1998). *Weigh-in-Motion of Road Vehicles* (B. Jacob, E. J. O'Brien, & S. Jehaes, Eds.).
- Crespo-Minguillón, C., & Casas, J. R. (1997). A comprehensive traffic load model for bridge safety checking. *Structural Safety*, 19(4), 339–359. [https://doi.org/10.1016/S0167-4730\(97\)00016-7](https://doi.org/10.1016/S0167-4730(97)00016-7)
- Csagoly, P. F., & Dorton, R. A. (1978). The development of the Ontario highway bridge design code. *Bridge Engineering Conference, 1st*, 1–12.
- Danish Road Directorate. (2004). *Calculation of Load Carrying Capacity for Existing Bridges, Guideline Document*. Transport, Ministry of.
- Dawe, P. (2009). Traffic loading on highway bridges. *Traffic Loading on Highway Bridges, June*. <https://doi.org/10.1680/tlohb.32415>
- de Wet, D. (2010). *Post-Calibration and Quality Management of Weigh-in-Motion Traffic Data* (Issue March). Stellenbosch University.
- EN 1990 (2002). *Basis of structural design*. European Committee for Standardization.
- EN 1991-2 (2003). *Actions on structures - Part 2: Traffic loads on bridges*. CEN.
- EN 1992-1-1 (2004). *Design of Concrete Structures - Part 1-1: General rules for buildings*. CEN.
- EN 1992-2 (2005). *Design of concrete structures - Part 2: Concrete bridges - Design and detailing rules*. CEN.
- EN-1990 (2002). *Eurocode - Basis of structural design*. CEN

- Enright, B. (2010). Simulation of traffic loading on highway bridges. *PhD Thesis*. University College of Dublin.
- Enright, B., Caprani, C. C., & O'Brien, E. J. (2011). Modelling of Highway Bridge Traffic Loading : Some Recent Advances. *Applications of Statistics and Probability in Civil Engineering (ICASP 11)*, 2002, 397–405.
- Enright, B., & O'Brien, E. J. (2011). *Cleaning Weigh-in-Motion Data: Techniques and Recommendations* (Issue January). [http://www.is-wim.org/doc/wim\\_data\\_cleaning\\_ie.pdf](http://www.is-wim.org/doc/wim_data_cleaning_ie.pdf)
- Enright, B., & O'Brien, E. J. (2013). Monte Carlo simulation of extreme traffic loading on short and medium span bridges. *Structure and Infrastructure Engineering*, 9(12), 1267–1282. <https://doi.org/10.1080/15732479.2012.688753>
- Enright, B., O'Brien, E. J., & Leahy, C. (2015). Identifying and modelling permit trucks for bridge loading. *Proceedings of the Institution of Civil Engineers - Bridge Engineering*, 169(4), 235–244. <https://doi.org/10.1680/bren.14.00031>
- fib COM3 TG3.1. (2016). *fib Bulletin 80: Partial factor methods for existing concrete structures* (R. Caspeele, R. Steenbergen, & M. Sykora, Eds.; Issue 80). Fédération internationale du béton.
- Fisher, R. A. (2006). *Statistical methods for research workers*. Genesis Publishing Pvt Ltd.
- Fu, G., & You, J. (2010). Extrapolation for Future Maximum Load Statistics. *Journal of Bridge Engineering*, 16(4), 527–535. [https://doi.org/10.1061/\(ASCE\)BE.1943-5592.0000175](https://doi.org/10.1061/(ASCE)BE.1943-5592.0000175)
- Gonzalez, A. (2012). Vehicle-Bridge Dynamic Interaction Using Finite Element Modelling. *Finite Element Analysis*. <https://doi.org/10.5772/10235>
- González, A., Dowling, J., O'Brien, E. J., & Znidaric, A. (2010). Experimental Determination of Dynamic Allowance for Traffic Loading in Bridges. *Transportation Research Board*.
- González, A., OBrien, E. J., Cantero, D., Li, Y., Dowling, J., & Žnidarič, A. (2010). Critical speed for the dynamics of truck events on bridges with a smooth road surface. *Journal of Sound and Vibration*, 329(11), 2127–2146. <https://doi.org/10.1016/j.jsv.2010.01.002>
- González, A., & Znidaric, A. (2009). *ARCHES D 10 Recommendations on dynamic amplification allowance*. <http://researchrepository.ucd.ie/handle/10197/6238>
- Grave, S. A. (2001). *Modelling of Site-Specific Traffic Loading on Short to Medium Span Bridges*.
- Gulvanessian, H., & Holicky, M. (2005). Eurocodes: Using reliability analysis to combine action effects. *Proceedings of the Institution of Civil Engineers: Structures and Buildings*, 158(4), 243–252. <https://doi.org/10.1680/stbu.2005.158.4.243>

- 
- Guo, D., & Caprani, C. C. (2019). Traffic load patterning on long span bridges: A rational approach. *Structural Safety*, 77(February 2018), 18–29. <https://doi.org/10.1016/j.strusafe.2018.11.003>
- Hanswille, G., & Sedlacek, G. (2007). *Background Report Traffic loads on road bridges Basis of the load models in EN 1991-2 and DIN - Report 101*.
- Harman, D., & Davenport, A. (1976). *The formulation of vehicular loading for design of highway bridges in Ontario*.
- Heywood, R., Gordon, R., & Bouilly, G. (2000). Australia's Bridge Design Load Model: Planning for an Efficient Road Transport Industry. *Transportation Research Record*, 1696(1), 1–7. <https://doi.org/10.3141/1696-36>
- Holický, M. (2009). *Reliability Analysis For Structural Design*. SunMedia.
- Holický, M. (2013). *Introduction to probability and statistics for engineers*. Springer.
- Holický, M., Diamantidis, D., & Sýkora, M. (2018). Reliability levels related to different reference periods and consequence classes. *Beton- Und Stahlbetonbau*, 113, 22–26. <https://doi.org/10.1002/best.201800039>
- Holický, M., & Retief, J. V. (2005). Reliability assessment of alternative Eurocode and South African load combination schemes for structural design. *Journal of the South African Institution of Civil Engineering*, 47(1), 15–20.
- Hwang, E. S., & Nowak, A. S. (1991). Simulation of dynamic load for bridges. *Journal of Structural Engineering*, 117(5), 1413–1434. [https://doi.org/10.1061/\(ASCE\)0733-9445\(1991\)117:5\(1413\)](https://doi.org/10.1061/(ASCE)0733-9445(1991)117:5(1413))
- ISO 2394 (2015a). *General Principles on Reliability for Structures*. ISO
- ISO 13822 (2001). *Basis for design of structures - Assessment of existing structures*. ISO.
- ISO 22111 (2007). *Bases for design of structures - General requirements*.
- Jacob, B., & Feypell-de La Beaumelle, V. (2010). Improving truck safety: Potential of weigh-in-motion technology. *IATSS Research*, 34(1), 9–15. <https://doi.org/10.1016/j.iatssr.2010.06.003>
- JCSS. (2001). Probabilistic Model Codes. In *Joint Committee on Structural Safety working materials*.
- König, G., & Hosser, D. (1982). *The Simplified Level II Method and its Application on the Derivation of Safety Elements for level I*. CEB Bulletin: 147. International Federation for Structural Concrete.
- Kulicki, J., Prucz, Z., Clancy, C., Mertz, D., & Nowak, A. S. (2007). Updating the calibration report for AASHTO LRFD code. *Final Rep. for AASHTO*.

- Leahy, C., O'Brien, E. J., & O'Connor, A. (2015). Traffic Load Effect Forecasting for Bridges. *IABSE Symposium Report*, 105(28), 1–8. <https://doi.org/10.2749/222137815818358231>
- Lenner, R. (2014). Safety Concept and Partial Factors for Military Assessment of Existing Concrete Bridges. *PhD Thesis*. Univeristy of German Armed Forces in Munich.
- Lenner, R., Basson, S. E., Sýkora, M., & van der Spuy, P. F. (2021). Reliability performance of bridges designed according to TMH7 NA load model. *Journal of the South African Institution of Civil Engineering*, 63(1), 25–36. <https://doi.org/10.17159/2309-8775/2021/V63N1A3>
- Lenner, R., & Caprani, C. (2021). Short-to-medium span bridges. In E. OBrien, A. Nowak, & C. Caprani (Eds.), *Bridge Traffic Loading* (1st Edition). CRC Press.
- Lenner, R., de Wet, D. P. G., & Viljoen, C. (2017). Traffic characteristics and bridge loading in South Africa. *Journal of the South African Institution of Civil Engineering*, 59(4), 34–46. <https://doi.org/10.17159/2309-8775/2017/v59n4a4>
- Lenner, R., Keuser, M., & Sýkora, M. (2014). Safety concept and partial factors for bridge assessment under military loading. *Advances in Military Technology*, 9(2), 5–20.
- Lenner, R., & Sýkora, M. (2016). Partial factors for loads due to special vehicles on road bridges. *Engineering Structures*, 106, 137–146. <https://doi.org/10.1016/j.engstruct.2015.10.024>
- Marelli, S., & Sudret, B. (2014). UQLab: A Framework for Uncertainty Quantification in Matlab. *Vulnerability, Uncertainty, and Risk: Quantification, Mitigation, and Management - Proceedings of the 2nd International Conference on Vulnerability and Risk Analysis and Management, ICVRAM 2014 and the 6th International Symposium on Uncertainty Modeling a.* <https://doi.org/10.1061/9780784413609.257>
- Markova, J. (2013). Reliability assessment of traffic load models on road bridges. *Assessment, Upgrading and Refurbishment of Infrastructures*, 253–260.
- Matos, J. C., Moreira, V. N., Valente, I. B., Cruz, P. J. S., Neves, L. C., & Galvão, N. (2019). Probabilistic-based assessment of existing steel-concrete composite bridges – Application to Sousa River Bridge. *Engineering Structures*, 181, 95–110.
- Mei, S., Caprani, C., & Cantero, D. (2023). Dynamic amplification of multi-span simply-supported prestressed concrete girder viaducts subjected to multi-body heavy vehicles. *Structures*, 55, 587–605. <https://doi.org/https://doi.org/10.1016/j.istruc.2023.05.125>
- Meinen, M., & Steenbergen, R. (2018). Reliability levels obtained by Eurocode partial factor design - a discussion on current and future reliability levels. *Heron*, 63(3), 243–301.



- 
- Melhem, M., Caprani, C., Stewart, M., & Zhang, S. (2020). *Bridge Assessment Beyond the AS 5100 Deterministic Methodology*.
- Meyer, M., Lenner, R., & van der Spuy, P. (2019). The Development of a Vehicle-Bridge Interaction Model for South African Traffic. *SEMC in Cape Town*.
- Meyer, M. W., Cantero, D., & Lenner, R. (2021). Dynamics of long multi-trailer heavy vehicles crossing short to medium span length bridges. *Engineering Structures*, 247, 113149. <https://doi.org/10.1016/J.ENGSTRUCT.2021.113149>
- Moccia, F., Yu, Q., Fernández Ruiz, M., & Muttoni, A. (2021). Concrete compressive strength: From material characterization to a structural value. *Structural Concrete*, 22(S1), E634–E654. <https://doi.org/https://doi.org/10.1002/suco.202000211>
- Morales-Napoles, O., & Steenbergen, R. D. J. M. (2014). Analysis of axle and vehicle load properties through Bayesian Networks based on Weigh-in-Motion data. *Reliability Engineering and System Safety*, 125, 153–164. <https://doi.org/10.1016/j.res.2014.01.018>
- Moses, F., & Ghosn, M. (1985). *A comprehensive study of bridge loads and reliability. Final report*.
- Muttoni, A. (2021). *Background document to 4.3.3 and annex A, partial safety factors for materials, cEN/ TC250/ SC2/ WG1/ TG6*.
- NEN8700. (2011). *Nederlands Normalisatie Instituut - Assessment of existing structures in case of reconstruction and disapproval - basic rules*. Nederlands Normalisatie Instituut.
- Newmark, M. M. (1948). Design of I-beam bridges. *American Society of Civil Engineers*, 305–330.
- Nowak, A. S. (1993). Load model for highway bridges. *Structural Safety*, 13(June 1994), 53–66. [https://doi.org/10.1016/0167-4730\(93\)90048-6](https://doi.org/10.1016/0167-4730(93)90048-6)
- Nowak, A. S. (1994). Load model for bridge design code. *Canadian Journal of Civil Engineering*, 21(1), 36–49. <https://doi.org/10.1139/194-004>
- Nowak, A. S. (1996). Calibration of LRFD Bridge Code. *Journal of Structural Engineering*, 121(8), 1245–1251. <https://doi.org/10.1097/HJH.0000000000001207>
- Nowak, A. S., & Rakoczy, P. (2013). WIM-based live load for bridges. *KSCE Journal of Civil Engineering*, 17(3), 568–574. <https://doi.org/10.1007/s12205-013-0602-8>
- O'Brien, E., & Caprani, C. (2005). Headway modelling for traffic load assessment of short to medium span bridges. *The Structural Engineer*, 86(16), 33–36.

- O'Brien, E. J., Bordallo-Ruiz, A., & Enright, B. (2014). Lifetime maximum load effects on short-span bridges subject to growing traffic volumes. *Structural Safety*, *50*, 113–122. <https://doi.org/10.1016/j.strusafe.2014.05.005>
- O'Brien, E. J., & Enright, B. (2011). Modelling same-direction two-lane traffic for bridge loading. *Structural Safety*, *33*(4–5), 296–304. <https://doi.org/10.1016/j.strusafe.2011.04.004>
- O'Brien, E. J., Lipari, A., & Caprani, C. C. (2015). Micro-simulation of single-lane traffic to identify critical loading conditions for long-span bridges. *Engineering Structures*, *94*, 137–148. <https://doi.org/10.1016/j.engstruct.2015.02.019>
- O'Brien, E. J., Schmidt, F., Hajializadeh, D., Zhou, X. Y., Enright, B., Caprani, C. C., Wilson, S., & Sheils, E. (2015). A review of probabilistic methods of assessment of load effects in bridges. *Structural Safety*, *53*, 44–56. <https://doi.org/10.1016/j.strusafe.2015.01.002>
- O'Connor, A., & Enevoldsen, I. (2007). Probability-based bridge assessment. *Proceedings of the Institution of Civil Engineers - Bridge Engineering*, *160*(3), 129–137. <https://doi.org/10.1680/bren.2007.160.3.129>
- O'Connor, A., & Enevoldsen, I. (2009). Probability-based assessment of highway bridges according to the new Danish guideline. *Structure and Infrastructure Engineering*, *5*(2), 157–168. <https://doi.org/10.1080/15732470601022955>
- O'Connor, A., & O'Brien, E. J. (2005). Traffic load modelling and factors influencing the accuracy of predicted extremes. *Canadian Journal of Civil Engineering*, *32*(1), 270–278. <https://doi.org/10.1139/104-092>
- Oosthuizen, A. P. C., Meintjies, C. J., Trumpelmann, V., Peters, D., Ullmann, K. K. A. B., & Oppermann, G. H. P. (1991). TMH7 Part 2: Traffic Loading (1991) Proposed Substitution of Section 2.6. In *CSRA, Department of Transport*.
- Orcesi, A., Diamantidis, D., O'Connor, A., Sýkora, M., Palmisano, F., Boros, V., Caspeepe, R., Chateaneuf, A., Ivankovič, A., Lenner, R., Kušter, M., Nadolski, V., Schmidt, F., Skokandič, D., & van der Spuy, P. (2023). Investigating Partial Factors for the Assessment of Existing Bridges. *Structural Engineering International*.
- Papagiannakis, A. T., Senn, K., & Huang, H. (1996). On-Site Calibration Evaluation Procedures for WIM Systems. *Transportation Research Record*, *1536*(1), 1–11. <https://doi.org/10.1177/0361198196153600101>
- Pérez Sifre, S. (2020). Site specific traffic load factor approach for the assessment of existing bridges (*Phd Thesis*). Stellenbosch University.

- 
- Pérez Sifre, S., & Lenner, R. (2019). Bridge assessment reduction factors based on Monte Carlo routine with copulas. *Engineering Structures*, *198*(August), 109530.
- Pérez Sifre, S., & Lenner, R. (2021). Partial factors and reliability verification for the site load factor approach for the assessment of existing bridges. *Structures*.
- prEN 1992-1-1. (2021). *Design of Concrete Structures - Part 1-1: General rules - rules for buildings, bridges and civil engineering structures*.
- Rackwitz, R. (2000). Optimization - the basis of code-making and reliability verification. *Structural Safety*, *22*(1), 27–60. [https://doi.org/10.1016/S0167-4730\(99\)00037-5](https://doi.org/10.1016/S0167-4730(99)00037-5)
- Retief, J. V., Viljoen, C., & Holický, M. (2019). Standardized basis for assessment of existing structures. *Advances in Engineering Materials, Structures and Systems*, 779–780.
- Sanders, W. W., & Elleby, H. A. (1970). *Distribution of wheel loads on highway bridges*.
- SANS-10160-1. (2009). *Part 1: Basis of structural design*. South African Bureau of Standards.
- Sedlacek, G., Merzenich, G., Paschen, M., Bruls, A., Sanpaolesi, L., Croce, P., Calgaro, J. A., & Pratt, M. (2008). *Background document to EN 1991- Part 2 - Traffic loads for road bridges - and consequences for the design*.
- Sivakumar, B., Moses, F., & Ghosn, M. (2008). Protocols for Collecting and Using Traffic Data in Bridge Design Prepared for NCHRP. In *Protocols for Collecting and Using Traffic Data in Bridge Design* (Issue July 2008). National Academies Press. <https://doi.org/10.17226/14521>
- Soriano, M., Casas, J. R., & Ghosn, M. (2017). Simplified probabilistic model for maximum traffic load from weigh-in-motion data. *Structure and Infrastructure Engineering*, *13*(4), 454–467. <https://doi.org/10.1080/15732479.2016.1164728>
- Srinivas, S., Menon, D., & Meher Prasad, A. (2006). Multivariate Simulation and Multimodal Dependence Modeling of Vehicle Axle Weights with Copulas. *Journal of Transportation Engineering*, *132*(12), 945–955. [https://doi.org/10.1061/\(asce\)0733-947x\(2006\)132:12\(945\)](https://doi.org/10.1061/(asce)0733-947x(2006)132:12(945))
- STANAG 2021. (2006). *Military Load Classification of Bridges, Ferries Rafts and Vehicles: NATO Standardization Agreements*.
- Steenbergen, R. D. J. M., Sýkora, M., Diamantidis, D., Holický, M., & Vrouwenvelder, T. (2015). Economic and human safety reliability levels for existing structures. *Structural Concrete*, *16*(3), 323–332. <https://doi.org/10.1002/suco.201500022>
- Steenbergen, R. D. J. M., & Vrouwenvelder, A. C. W. M. (2010). Safety philosophy for existing structures and partial factors for traffic loads on bridges. *Heron*, *55*(2), 123–140.

- Sykora, M., & Holicky, M. (2012). Target reliability levels for the assessment of existing structures - Case study. *Life-Cycle and Sustainability of Civil Infrastructure Systems - Proceedings of the 3rd International Symposium on Life-Cycle Civil Engineering, IALCCE 2012*, 813–820.
- Sykora, M., Holicky, M., Lenner, R., & Mañas, P. (2014). Target reliability levels for existing bridges considering emergency and crisis situations. *Advances in Military Technology*, 9(1), 45–57.
- Sýkora, M., Holický, M., & Marková, J. (2013). Verification of existing reinforced concrete bridges using the semi-probabilistic approach. *Engineering Structures*, 56, 1419–1426. <https://doi.org/10.1016/j.engstruct.2013.07.015>
- Sykora, M., Holicky, M., Prieto, M., & Tanner, P. (2015). Uncertainties in resistance models for sound and corrosion-damaged RC structures according to EN 1992-1-1. *Materials and Structures*, 48(10), 3415–3430. <https://doi.org/10.1617/s11527-014-0409-1>
- Teichgräber, M., Nowak, M., Köhler, J., & Straub, D. (2018). The effect of traffic load model assumptions on the reliability of road bridges. In *Life Cycle Analysis and Assessment in Civil Engineering: Towards an Integrated Vision* (1st ed.). CRC Press.
- van der Spuy, P. F. (2020). Derivation of a traffic load model for the structural design of highway bridges in South Africa. *PhD Thesis*. Stellenbosch University.
- van der Spuy, P., & Lenner, R. (2019). Towards a New Bridge Live Load Model for South Africa. *Structural Engineering International*, 29(2), 292–298.
- van der Spuy, P., Lenner, R., de Wet, T., & Caprani, C. C. (2019). Multiple lane reduction factors based on multiple lane weigh in motion data. *Structures*, 543–549.
- Vrouwenvelder, A. C. W. M. W. M. (2002). Developments towards full probabilistic design codes. *Structural Safety*, 24(2–4), 417–432. [https://doi.org/10.1016/S0167-4730\(02\)00035-8](https://doi.org/10.1016/S0167-4730(02)00035-8)
- Zhou, J., Shi, X., Caprani, C. C., & Ruan, X. (2018). Multi-lane factor for bridge traffic load from extreme events of coincident lane load effects. *Structural Safety*, 72, 17–29. <https://doi.org/10.1016/j.strusafe.2017.12.002>
- Zhou, X. Y. (2013). *Statistical Analysis of Traffic Loads and Traffic Load Effects on Bridges*.
- Zhou, X. Y., Schmidt, F., & Jacob, B. (2012). Extrapolation of traffic data for development of traffic load models: Assessment of methods used during background works of the Eurocode. *Bridge Maintenance, Safety, Management, Resilience and Sustainability - Proceedings of the Sixth International Conference on Bridge Maintenance, Safety and Management*, 1503–1509.

---

Zhou, X. Y., Schmidt, F., Toutlemonde, F., & Jacob, B. (2016). A mixture peaks over threshold approach for predicting extreme bridge traffic load effects. *Probabilistic Engineering Mechanics*, 43(December), 121–131. <https://doi.org/10.1016/j.probengmech.2015.12.004>

Zokaie, T., Imbsen, R., & Osterkamp, T. (1991). Distribution of Wheel Loads on Highway Bridges. *Transportation Research Record 1290*, 119–126.